SYNTHESIS OF ISOTOPICALLY LABELED SUBSTRATES, LIPID PEROXIDATION PRODUCTS, AND A NOVEL METABOLITE, 2-(AMINOMETHYL)MALONATE, FOR USE IN METABOLIC RESEARCH

By

JEREMY P. HESS

Submitted in partial fulfillment of the requirements for the degree of Doctor of Philosophy

Department of Chemistry

CASE WESTERN RESERVE UNIVERSITY

May 2020

Case Western Reserve University

School of Graduate Studies

We hereby approve the dissertation of

Jeremy P. Hess

Candidate for the degree of **Doctor of Philosophy**

March 30, 2020

Robert Salomon, Ph.D. (Chair)

Gregory P. Tochtrop Ph.D. (Advisor)

Daniel Scherson, Ph.D.

Clemens Burda, Ph.D.

Henri Brunengraber, M.D. Ph.D. (Department of Nutrition)

I dedicate this work to my fiancée Trizi and son Theo.

Table of Contents

List of Figures

List of Schemes

Acknowledgments

First and foremost I would like to extend my deepest gratitude to my advisor Dr. Gregory Tochtrop. His guidance, passion for chemistry, and genuine concern for the futures of all his students has been inspirational throughout my time here. He always found the perfect ways to allow me to grow independently while still encouraging me to push myself further than I thought I could go. I would not be where I am today without him taking me under his wing.

I would like to acknowledge my committee, Dr. Robert Salomon, Dr. Daniel Scherson, Dr. Clemens Burda, and Dr. Henri Brunengraber for their support and advice over the years. I would also like to thank former committee member Emily Pentzer for her previous contributions to my academic career.

There are a number of collaborators who were invaluable to my time here at Case. In particular, the members of the Brunengraber lab with whom a majority of my work was in collaboration. Henri Brunengraber was always a source of support and guidance throughout my time, and working in their lab taught me many of the biological techniques that were vital to my work. It was a privilege to work with Dr. Guofang Zhang and Dr. Kirkland Wilson on the liver perfusion and GCMS analysis of biological assays. I also would like to thank Dr. Charandeep Singh for the late nights spent teaching me the ins and outs of developing LC/MS/MS methods for detecting difficult to assay analytes.

I'd also like to acknowledge all Tochtrop lab members past and present who provided both valuable insight and friendship throughout my time here. First of all, Dr. Chuan Shi played a large part in getting me settled into the lab and teaching me the skills needed to

continue his work on the kinase identification project. Dr. Roozbeh Eskandari was critical for his work on EKODE synthesis as well as his help with the current manuscript. I'd like to thank Dr. Yong Han for his constant support and guidance. The amount of skills from synthesis to instrument maintenance that I have learned from him has been unbelievable. Last but certainly not least, I would like to thank all the current members of the Tochtrop lab for all their advice and companionship over the years. I wouldn't trade our time together for anything.

List of Symbols and Abbreviations

4-HNE- 4-Hydroxynonenal

AABA- α-Aminobutyrate

ALE- Advanced lipoxidation endproducts

AMM- 2-(Aminomethyl)malonate

AOA- Aminooxyacetate

CNS- Central nervous system

DCM- Dichloromethane

DNA- Deoxyribonucleic acid

EKODE- Epoxyketooctadecenoic acid

EtOAc- Ethyl acetate

FPLC- Fast protein liquid chromatography

GABA- γ-Hydroxybutyric acid

GC- Gas Chromatography

GHB- γ-Hydroxybutyrate

GHP-CoAT- γ-Hydroxypentanoyl CoA-transferase

GST- Glutathione S-transferase

LPO- Lipid peroxidation

MID- Mass isotopomer distribution

MS- Mass spectrometry

MS/MS- Tandem mass spectrometry

NAA- *N*-Acetyl aspartate

NFkB- Nuclear factor kappa-light-chain-enhancer of activated B cells

NIST- National institute of standards and technology

NMR- Nuclear magnetic resonance

PUFA- Polyunsaturated fatty acid

RNS- Reactive nitrogen species

ROS- Reactive oxygen species

RT- Room temperature

SDS PAGE- Sodium dodecyl sulfate-polyacrylamide gel electrophoresis

TBDMS- *Tert*-butyldimethylsilyl

TCA- Tricarboxylic acid

THF- Tetrahydrofuran

Synthesis of Isotopically Labeled Substrates, Lipid Peroxidation Products, and a Novel Metabolite, 2-(Aminomethyl)malonate, for Use in Metabolic Research

JEREMY P HESS

Abstract

Stable isotopomers of biological molecules or xenobiotics can be utilized to probe the metabolic pathways with which these compounds are involved. By introducing these labeled substrates into living systems, we can use techniques such as mass spectrometry to track the fates of the isotopically labeled atoms. One set of projects described herein focuses on the synthesis of these substrates for use by collaborating laboratories.

Of particular interest to our lab are biomolecules known as lipid peroxidation (LPO) products. These molecules are formed in increased concentrations during periods of oxidative stress. In the past, our lab has discovered metabolic pathways that allow for catabolism of the ubiquitous LPO product 4-hydroxynonenal. In order to better understand these pathways, we need to identify the enzymes that affect the steps of each pathway. It also stands to reason that there may be other pathways that exist for additional families of LPO products. To this end, I describe work done on the isolation of the kinase involved in 4-HNE metabolism as well as synthesis of epoxyketooctadecenoic acids for use in additional metabolic studies.

The final topic of study involves the confirmation of the identity of a novel metabolite 4-(aminomethyl)malonate. Results from a previous study led us to hypothesize the existence of this molecule. Synthesis of both isotopically unlabeled and labeled analogues of this molecule was completed and utilized to confirm the identity of the molecule. An

in vivo study was conducted where rats were fed β-alanine, the proposed metabolic precursor to this molecule. The tissue specific concentration of AMM formed during periods of high β-alanine was tracked and its effect on neurotransmitters was assessed.

Chapter 1

INTRODUCTION:

BACKGROUND AND SIGNIFICANCE

Chapter 1: Introduction

1.1 History of synthetic chemistry in metabolism

Life as we know it is made possible by two types of chemical pathways flowing opposite of each other. Catabolic pathways break down endogenous and exogenous molecules into smaller, fragments while releasing useful energy. Anabolic pathways utilize the energy and fragments generated by catabolic pathways in order to build all molecules necessary for life to exist. Together, these processes are known as metabolism.[1]

The field of metabolism is highly interdisciplinary, with many modern researchers focusing on the role of genetics, signaling, protein expression, and microbiomes on human metabolism. Most introductory texts on metabolism take a biochemical approach to the topic, focusing on the end results of a metabolic pathway, such as the amount of energy or metabolites generated, as well as which enzymes affect the transformations involved. For instance, one of the most commonly known and studied metabolic pathways is the citric acid cycle.[2] When studying this pathway, most focus on the enzymes involved as well as the efficiency of energy generation of this biochemical pathway. A critical aspect of the field that is often overlooked is the role that organic chemistry and synthesis has and continues to play in the field.

The study of metabolism has evolved from the work of the natural philosophers and physicians. The term itself is derived from the Greek term “metabole”, meaning to change. Since ancient times, it was believed that living creatures had a “vital force” that regulated their bodies and animated matter.[3] This spark divided living and inanimate matter. It was believed that organic compounds produced by living organisms were

created through the use of that force and therefore were incapable of being created by "inorganic" chemical processes.

It was the chemist Friedrich Wohler's synthesis of urea[4] in 1828 that changed the face of the field. The Wohler reaction produced urea, a biological compound first isolated in 1727,[5] from the completely inorganic ammonium cyanate. This event led other chemists to continue to prove that organic matter obeys the same chemical mechanisms as inorganic matter. One of Wohler's students, Hermann Kolbe, continued this trend by producing acetic acid from carbon disulfide in 1845.[6] **Figure 1** shows these important reactions in depth.

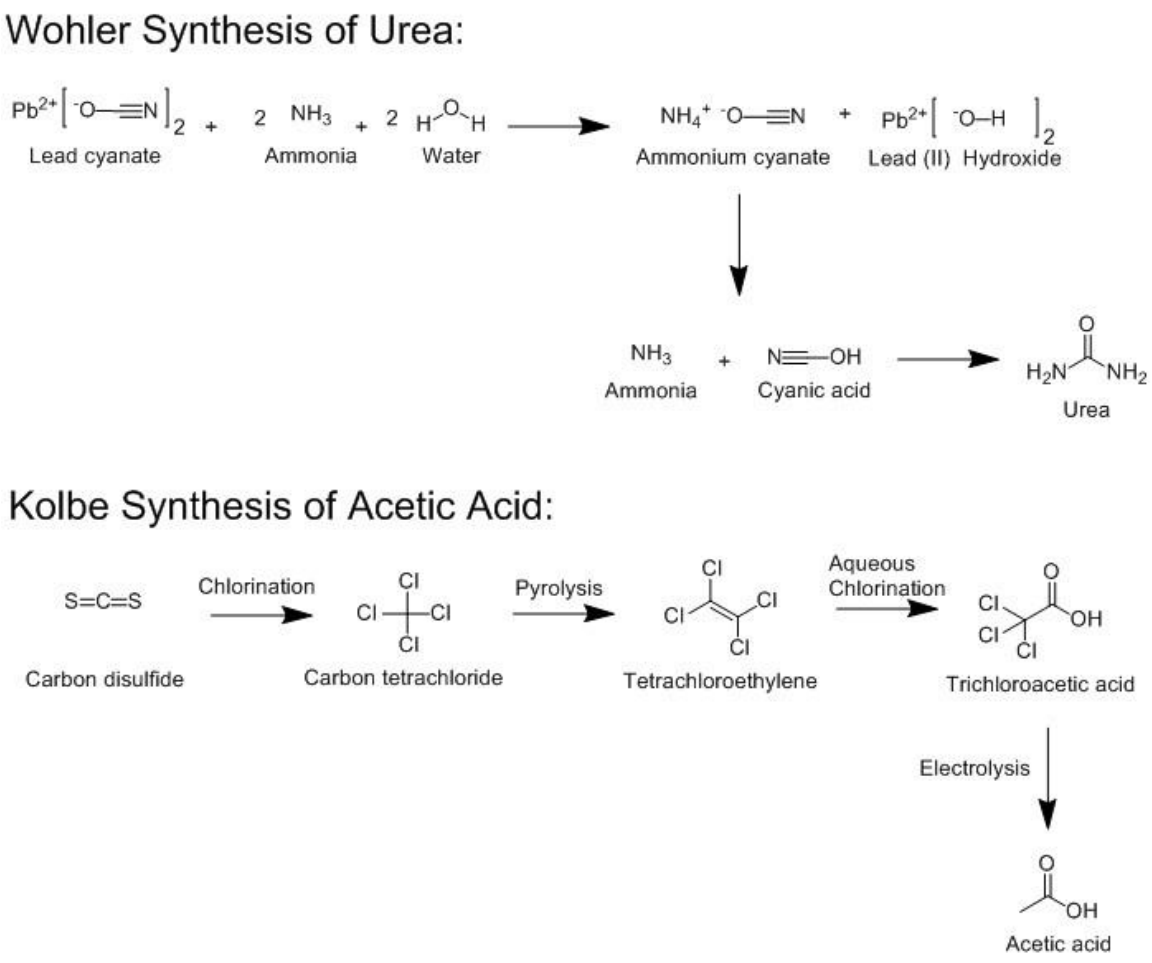

Figure 1: The Wohler synthesis of urea and the Kolbe synthesis of acetic acid

From this point on, the fields of metabolism, nutrition, and pharmacology were permanently intertwined with the work of the synthetic chemist. One chemist whose work led to great strides in the understanding of metabolism was Emil Fischer. His early work on studying caffeine[7] and theobromine, the active constituents of tea, coffee, and cocoa led him to realize that these two compounds were part of the same family of molecules. Later, he added adenine, guanine, and uric acid to this list of common metabolites.[7] He characterized these molecules as all containing a nitrogenous bicyclic compound, the parent of which he named purine. **Figure 2** shows the structures of the molecules he grouped as well as the structure of the parent molecule he hypothesized to exist. It was not until 15 years later that he was able to confirm its existence through synthesis of this molecule from uric acid purified from kidney stones.[8]

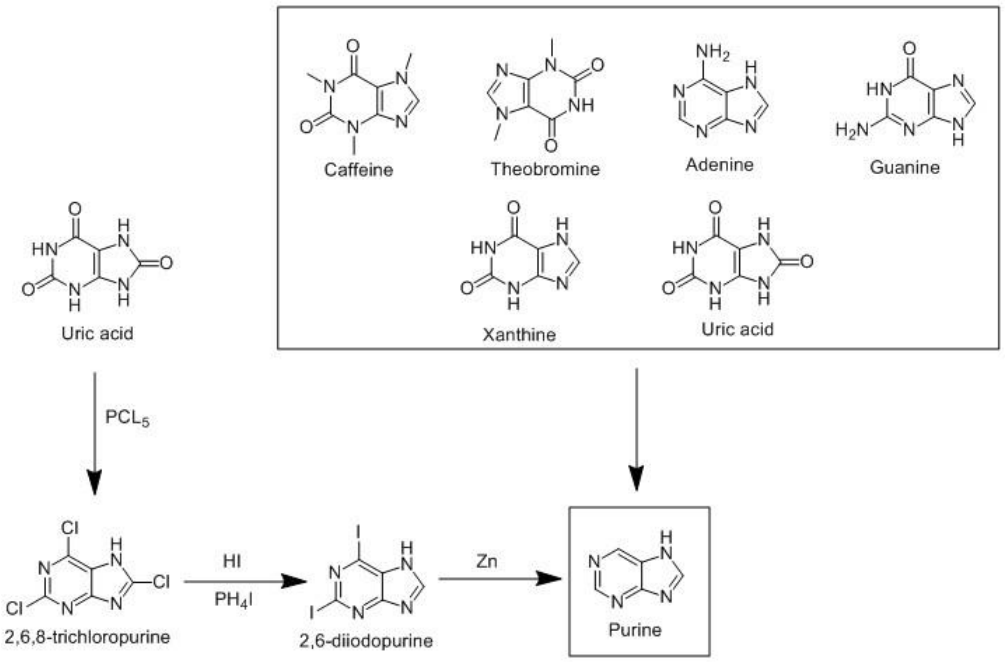

Figure 2: Emil Fischer's hypothesized base structure for purines and later confirmation via synthesis

1.2 Synergistic relationship between synthesis and metabolic research

1.21 Analytical approaches to identifying metabolites

The traditional methods for analyzing human metabolites utilize tools that would be familiar to any chemist. Samples are extracted from tissues,[9,10] fluids,[11–13]or condensation from breath.[14,15] These extracts are typically analyzed via GC/MS or LC/MS in order to separate all metabolites as well as characterize the individual peaks. In mass spectrometry, the fragmentation pattern can be compared to a database such as those kept by the National Institute of Standards and Technology (NIST), massbank, or lipidblast to positively identify well characterized metabolites.[16]

The data obtained via mass spectrometry is a powerful tool that can be utilized for a variety of purposes. Metabolites can be used in a clinical setting as biomarkers of disease.[12,17] Metabolites can be tracked during changes in diet to see how eating patterns affect the biochemistry of an individual.[18–20] Differences in metabolic profiles between soldiers who served in the Gulf War and non-military personal have been used to help elucidate the causes of the Gulf War Disorder.[21] The metabolism and clearance rate of drugs can also be tracked through this method.[22,23]

Occasionally, this data yields new metabolites and novel metabolic pathways. Unknown compound peaks can be isolated via the chromatographic stage and further analyzed through means such as NMR to determine chemical components. Liquid chromatography can be directly coupled with NMR to increase the rate of metabolite identification by eliminating the isolation step.[24] A typical workflow for accurately identifying metabolites that have not been characterized is utilizing the accurate mass and isotope distribution to

find the correct chemical formula.[25] The formula is used to calculate all possible structures and predict the MS/MS fragmentation patterns and NMR spectra. These predictions can be compared to the actual spectra in order to narrow down the possible structures.

1.2.2 Synthesis to confirm the identity of metabolites

The powerful techniques referred to in the previous section can give detailed information about structure and conformation; however, without obtaining a pure standard, it is not possible to confirm the exact structure. Many labs pursue total synthesis projects to confirm the exact confirmation of a biologically active compound. For example, the Evans lab at Harvard synthesized aflastatin A in order to confirm the stereochemistry that other labs had determined via detailed NMR studies.[26] Synthesis is also necessary in cases where the concentration of a natural product is low[27] or when studies are unable to determine the stereochemistry of a moiety.[28,29]

1.2.3 Mass isotopomer research

Determining metabolic pathways from *in vivo* experiments can be complicated due to the large number of compounds that exist within one sample. In addition, if the experiment involves increasing the concentration of an analyte to determine downstream metabolites, it can be difficult to differentiate the concentration that is endogenously formed from that which has been introduced through the experiment. In order to solve this issue, there must be a method that allows the researcher to trace the fate of individual atoms in the compound being studied. One common method to alleviate the issue is the incorporation of isotopic labeling to the target molecule.

Both radioisotopes and stable isotopes have been utilized to help quantify metabolic pathways. Radioisotopes allow for quantification of metabolites by measuring the energy given off by a sample.[30] The amount of energy is directly proportional to the number of radioisotopic atoms in a sample. Common radioisotopes used for this purpose are ^{3}H, ^{14}C, ^{32}P, and ^{125}I.

Due to the inherent hazard of radioisotopes, many researchers prefer to incorporate stable isotopes into their analytes of choice. These analytes are then able to be analyzed by mass spectroscopy where they will have a unique mass compared to the endogenous analyte population.

The mass isotopomer distribution (MID) of all common metabolites can be found. A change in the MID of a compound would suggest that the compound is metabolically linked to your analyte, as the increase in abundance of heavy isotopes implies that the isotopically labeled analyte is either catabolized or anabolized into the compound in question.

Commonly stable isotopomers utilized to isotopically label molecules include ^{2}H, ^{13}C, ^{15}N, and ^{18}O. Synthesizing compounds containing these isotopes is limited by cost and availability of starting materials. The approach needed in order to incorporate isotopic labels in targeted positions requires a different synthetic approach then most normal synthesis schemes.

Throughout this thesis, one common nomenclature that will be utilized is the M# system describing molecules containing 0 to n (denoted by #) stable isotopes. For instance, if a compound contains one ^{13}C carbon, we will refer to this as an M1 compound, no matter

which carbon is labeled. A compound labeled M3 could have any combination of three isotopic labels and has a mass that is three greater than its natural weight. This parlance will be used throughout to discuss both compounds which have been synthesized as well as metabolites discovered through mass spectroscopy.

Stable isotope synthesis and analysis plays a large role in the field of metabolic research. Coupled with mass spectrometry, it is possible to track the fate of individual atoms. This premise has been utilized by the Tochtrop lab in the past to discover entirely new metabolic pathways.[31] It can also give quantitative information about the turnover of metabolites and metabolic flux.

1.2.4 Perfused organ systems

There are a number of methods that can be utilized to study the metabolism of compounds. Some labs choose to utilize liver microsomes[23,32] while others choose to feed or inject solutions into an animal model. The method utilized in our research is the isolated rat liver perfusion technique that was developed by our collaborators in the Brunengraber lab.[33] The isolation of the organ from the model organism allows for testing without the potential metabolic changes caused by anaerobic conditions or anesthetics. The rates of metabolism demonstrated by this technique have been comparable to those determined *in vivo*. The setup required to run an isolated organ perfusion is shown in **Figure 3**.

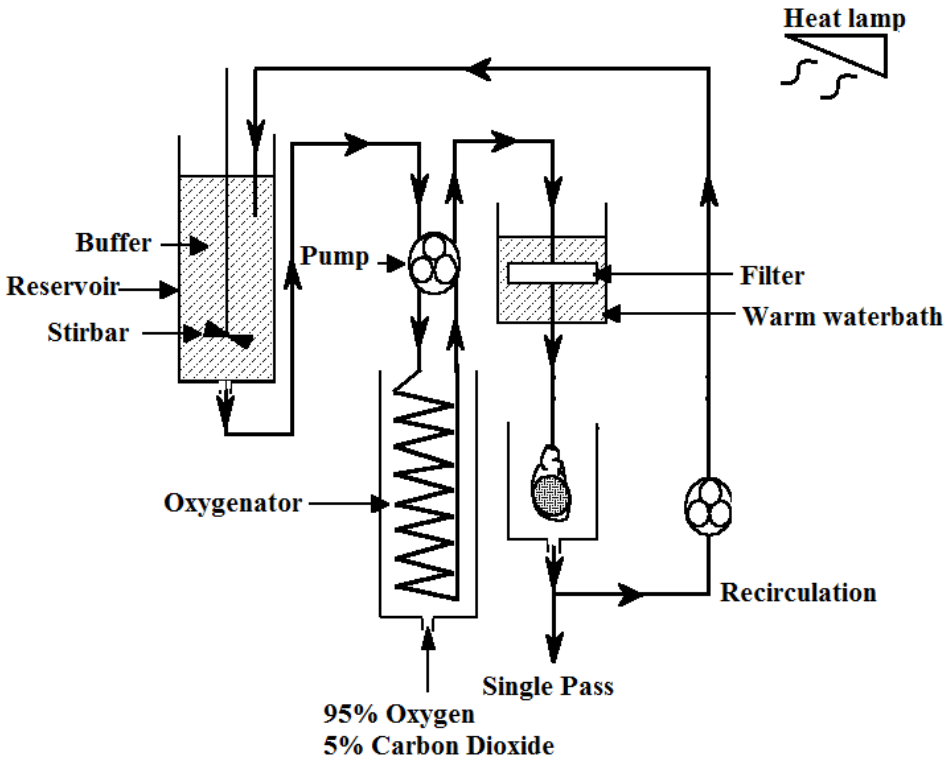

Figure 3: Isolated liver perfusion apparatus

1.3 The synergies between synthesis and metabolism addressed in this thesis

The synthetic techniques and tools described in the previous sections play a critical role throughout my metabolic projects. Progress in each field has a positive synergistic effect on the other. Discoveries of novel metabolites guide synthetic chemists to potential drug scaffolds. Development of analytic and isotopic tools by organic chemists allows for deeper understanding of metabolic pathways.

All research described herein ties back to the overarching goal of utilizing synthesis as a tool to study metabolic pathways. **Chapter 2** describes the synthesis of a number of stable isotope labeled substrates. These substrates were synthesized for use in metabolic

studies run by collaborators. One of the results found utilizing these isotopically labeled molecules led to the development of the project discussed in **Chapter 4**.

Chapter 3 focuses on the catabolic fate of 4-hydroxynonenal, the most common LPO product. It describes previous research done within my lab utilizing isotopic labeling to elucidate the pathways involved in this compounds degradation. My work on this topic involves identifying the enzymes that catalyze this transformation. It also covers another family of LPO products known as epoxyketooctadecenoic acids (EKODEs). The metabolism of this family of molecules is not yet known. My work on this topic covers the synthesis and preparation of EKODEs in order to perform the experiments needed to elucidate the metabolic pathways.

The work covered in **Chapter 4** involves the discovery, synthesis, and confirmation of a novel metabolite, 2-(aminomethyl)malonate (AMM). This compound was first identified while analyzing metabolic pathways that stem from β-alanine. This molecule had no published synthesis and may potentially play a role in neurotransmission. **Figure 4** shows the structures of the molecules described in this section and how they relate to oxidative stress.

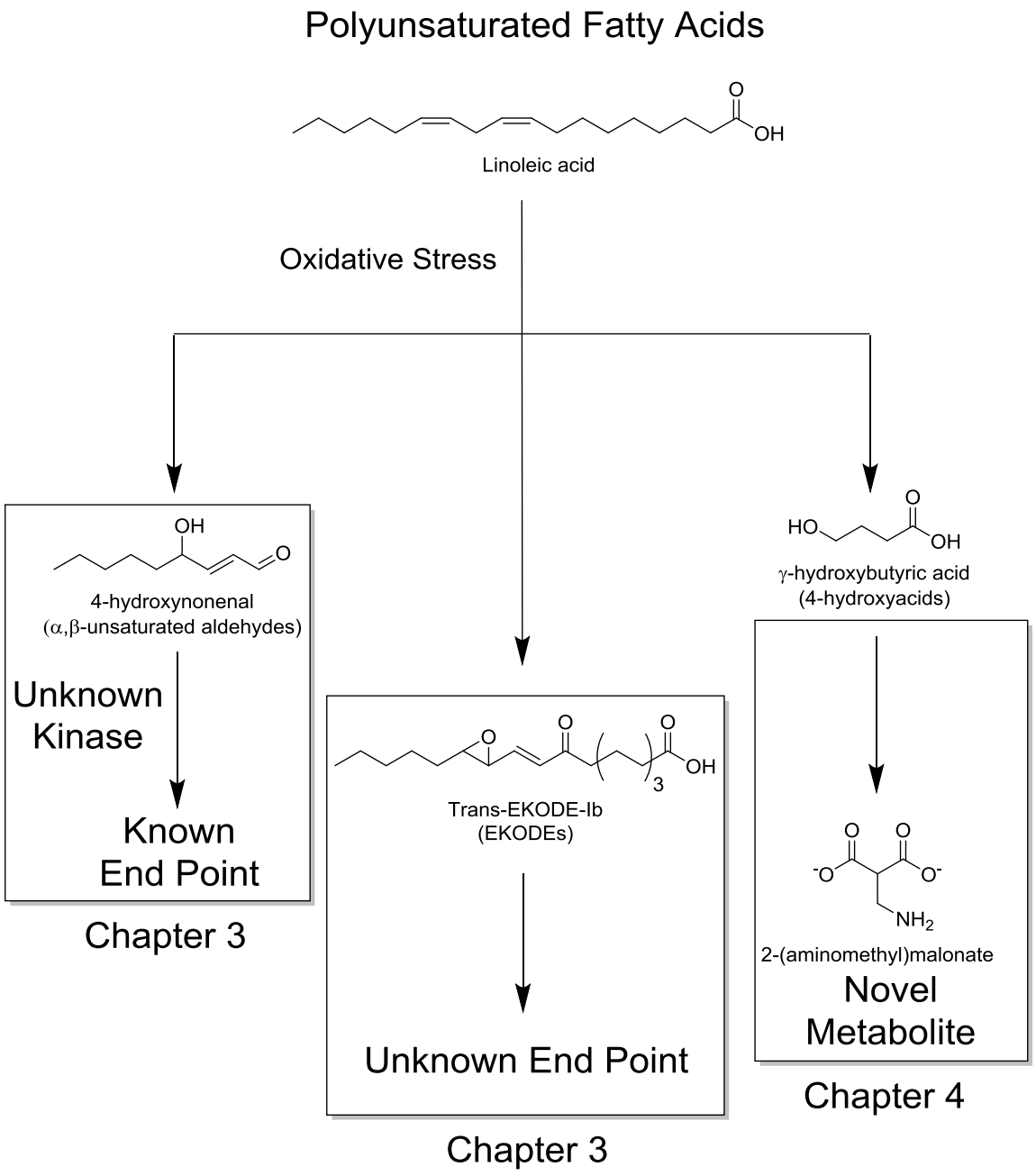

Figure 4: Overview of the focus of each chapter and how they relate to lipid peroxidation

1.4 Oxidative stress

One consequence of oxygen based metabolism is the generation of reactive oxygen species (ROS) and reactive nitrogen species (RNS). These reactive species can be produced both enzymatically as well as nonenzymatically. In the former case, they are utilized by macrophages in order to kill bacteria in a process called the oxidative burst.[34] In the latter case, ROS production can be caused by endogenous and exogenous sources. The leading endogenous cause of ROS generation is leakage of electrons from the electron transport chain proteins in the mitochondrial membrane.[35] This reduction leads to superoxide, which continues to react with nitrogen monoxide to form the RNS peroxinitrite.[36] Exogenous sources include smoke, radiation, and pollution.

ROS and RNS are capable of reacting with a variety of biomolecules to cause damage throughout an organism. The human body has antioxidant defense systems that are utilized to neutralize these reactive molecules before damage can occur. For instance, an enzyme called superoxide dismutase is capable of converting superoxide into hydrogen peroxide.[37] This peroxide is then scavenged by enzymes with high turnovers such as catalase[38] that convert it safely to water and oxygen.

When the concentration of ROS and RNS overwhelm the antioxidant defenses of a system, the organism enters a state called oxidative stress. The buildup of peroxides and radicals in the system damage proteins, lipids, DNA, and can lead to system-wide changes. Many diseases have an oxidative stress component: Alzheimer's,[39–41] cancer,[35,42,43] atherosclerosis,[44–46] and depression.[47]

1.5 Polyunsaturated fatty acids (PUFAs)

Polyunsaturated fatty acids (PUFAs) are components of the majority of lipids in biological systems. They are primarily known as structural components of membranes. In recent years, their significance has increased as studies have demonstrated the ability of PUFAs to function as signaling molecules.[48]

These PUFA molecules consist of fatty acids of varying chain length and degrees of unsaturation. The characterizing trait that all PUFAs share is a series of cis double bonds. This structural motif produces doubly allylic positions that define the reactivity of the molecule. During periods of oxidative stress, the concentration of reactive oxygen species (ROS) overwhelms the body's antioxidant systems. The non-enzymatic ROS can perform radical hydrogen abstraction from the doubly allylic carbon, leaving a stabilized radical that can propagate further reaction.[49] The products of these further reactions are referred to as lipid peroxidation (LPO) products.

1.6 Lipid peroxidation products

Lipid peroxidation products typically take the form of short chain aldehydes and α,β-unsaturated compounds. Examples of these molecules, shown in **Figure 6**, are highly electrophilic and capable of reacting with biological molecules through a number of different means. The reactive aldehydes can form Schiff bases with DNA and protein side chains. The unsaturated carbonyls can form Michael adducts which can further react to form compounds known as advanced lipoxidation endproducts (ALE).

The initial products of lipid peroxidation as well as their decomposition products both play important roles in a number of disease states. Although reactive oxygen and nitrogen

species are the most commonly known and discussed markers of oxidative stress, LPO products can be more dangerous due to their increased stability relative to reactive oxygen and nitrogen species and capability to permeate through membranes. This allows them to undergo adduction to proteins and DNA bases far from their site of generation. These adducts can abrogate natural protein function or promote new behavior such as misfolding. For instance, protein adducts with LPO products such as 4-HNE and acrolein[50] cause misfolding and aggregation in the brain. These effects are commonly seen in cases of dementia, but it is currently unknown whether they are a symptom or if they have a causative role. Peroxidized lipids and their protein adducts have been observed heavily contributing to both heart disease[44–46] and neurological disorders.[40]

Reactive Oxygen Species: Superoxide, Hydrogen peroxide, Hydroxyl radical
Reactive Nitrogen Species: Nitric oxide, Peroxynitrite

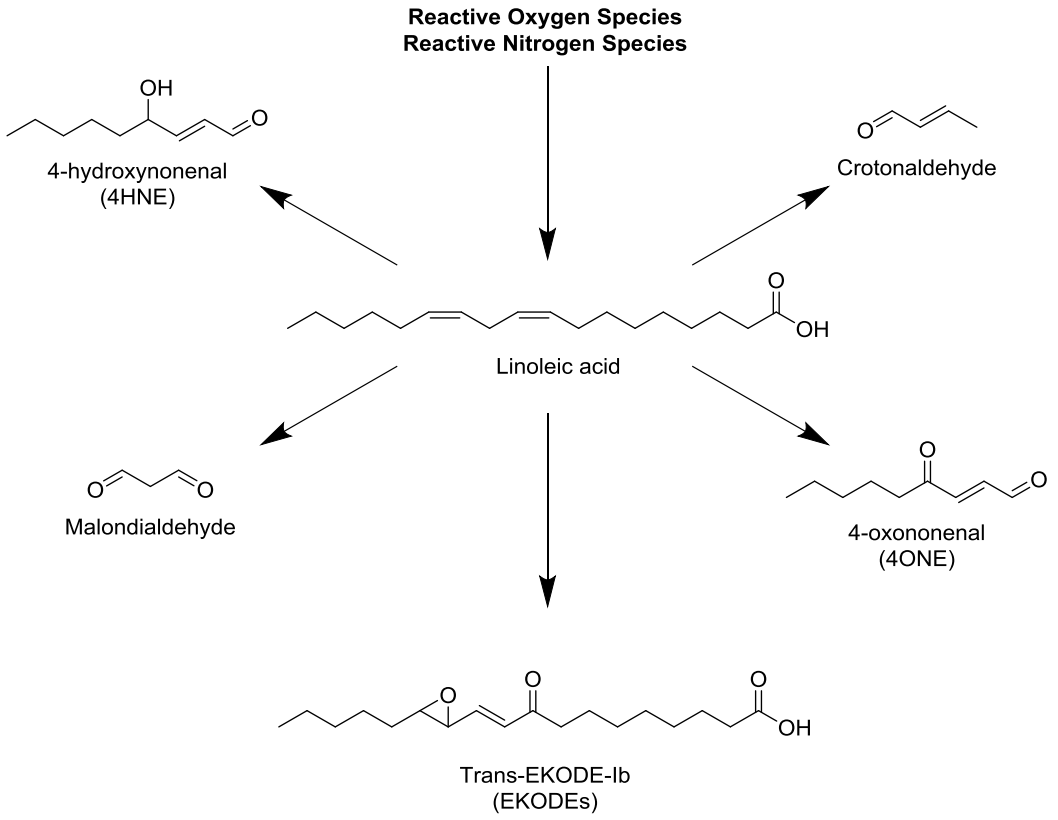

Figure 5: Structures of lipid peroxidation products generated from linoleic acid

1.6.1 Metabolism of 4-hydroxynonenal (4-HNE)

During periods of high oxidative stress, the concentrations of LPO products can increase over 100-fold over their basal concentrations.[51] Common theories in the field suggest that the formation of LPO products is solely a toxic byproduct of increased oxidant activity/decreased antioxidant activity. A quick look at the turnover of a common LPO product derived from linoleic acid, 4-hydroxynonenal (4-HNE), in a healthy organism per day suggests otherwise. A 50 kg mammal can turnover roughly 10 g of 4-HNE in a 24 hour period. This large amount of LPO product produced and catabolized in such a short

period suggests that formation of LPO products may not be merely a symptom of aberrant biological function. The primary hypothesis that we seek to prove is formation of LPO products regularly occur during normal metabolic processes and that organisms are equipped with catabolic pathways to degrade these compounds.[52]

Prior to the Tochtrop lab's work in this field, the predominant established pathway for LPO catabolism was conjugation to glutathione.[53] A study utilizing isotopically labeled 4-HNE demonstrated that there are two major catabolic pathways for 4-hydroxy acids and 4-hydroxy aldehydes.[31] The Tochtrop lab has demonstrated that these two pathways are the predominant catabolic fate of 4-HNE under normal conditions. It is only after increased 4-HNE concentrations that the conjugation pathway occurs.

1.6.2 Metabolism of 4-hydroxy acids

A logical progression from the work done on 4-HNE is to determine whether additional biological 4-hydroxyacids are catabolized via the same pathways. One such molecule is γ-hydroxybutyric acid (GHB), the simplest 4-hydroxyacid and a compound found in human physiology from both endogenous and exogenous sources. Endogenously it is derived from γ-aminobutyric acid (GABA), a major neurotransmitter in the central nervous system.[54] Exogenously, it is used to treat narcolepsy[55] as well as being abused as a drug for recreational purposes.

The accepted catabolic fate of GHB was thought to be conversion to succinic semialdehyde[56] and entrance into the citric acid cycle as succinate. A study completed with isotopically labeled GHB in perfused rat livers not only showed that this route only accounted for 8% of the total catabolic flux of GHB, but also elucidated two novel

pathways where GHB is catabolized to acetyl-CoA and formate through a 3-hydroxypropionate intermediate.[57]

1.7 3-Hydroxypropionate, β-alanine, and the discovery of 2-(aminomethyl)malonate

The importance of 3-hydroxypropionate was also noted by our collaborators in the Brunengraber lab. One focus of their lab is the study of propionic acidemia, an inborn error of metabolism in which an individual is unable to produce functional propionyl-CoA carboxylase.[58] Without this enzyme, the endogenous propionate formed from the metabolism of isoleucine, valine, methionine, threonine, and odd chain fatty acids is unable to be catabolized and will build up in the body. This perturbs the entire metabolic system and the body is forced to compensate by catabolizing through different pathways. In the case of propionic acidemia, this leads to an increase in multiple other biological molecules, one of which is 3-hydroxypropionate.

Metabolic data from both laboratories intersected at the molecule 3-hydroxypropionate. For this reason, a project was designed to discover the catabolic fate of this metabolite. One notable result from the perfusion of rat livers with 3-hydroxypropionate was that a large increase in β-alanine concentration was noted.[59] We theorized that β-alanine was a byproduct caused by transamination of malonic semialdehyde, the intermediate molecule in the pathway that catabolizes 3-hydroxypropionate to acetyl-CoA. When the experiment was repeated utilizing M3 labeled 3-hydroxypropionate, the molecular isotope distribution showed the formation of M3 labeled β-alanine, confirming the hypothesis.

β-Alanine, or 3-aminopropanoic acid, is an uncommon amino acid that is differentiated from its common counterpart alanine by shifting the amino group from the 2-position to the 3-position. Although a small amount of β-alanine is present in the liver and other tissues through the degradation of uracil[60] and the aforementioned formation from 3-hydroxypropionate, the bulk of human β-alanine is obtained through the diet. It is predominantly absorbed as a histidine dipeptide from animal sources.[61] A diet containing meat or fish provides roughly 300 mg of β-alanine per day.

The canonical role of ß-alanine is formation of dipeptides with histidine known as carnosine (β-alanyl-L-histidine) and anserine (β-alanyl-L-methylhistidine). These biomolecules are found in high concentration in muscle tissue and have been demonstrated to act as physiological pH buffers. They can counteract the buildup of lactic acid formed during strenuous exercise. The limiting reagent for the formation of these peptides is β-alanine. Increasing concentrations of plasma β-alanine have been demonstrated to increase carnosine and anserine levels in multiple types of muscle tissue. This has led to an increase of supplementation among athletes and military personnel. The common belief is that by increasing β-alanine, and therefore its dipeptides, they can neutralize lactic acid buildup and therefore push their workouts further than they would be able to otherwise.

Studies have shown that β-alanine supplementation increases the concentration of available carnosine and anserine. However, the increase in pH buffering dipeptides has not shown any notable increase in physical capability or endurance. Despite this, it remains a popular recommendation to bodybuilders. One reported detrimental effect of β-

alanine supplementation is paresthesia, a type of pain that is typically referred to as a "pins and needles" feeling. This effect occurs at high doses and the mechanism by which β-alanine causes this effect is currently unknown. It has been hypothesized that the similarity in chemical structure between common neurotransmitters and β-alanine suggests that it either acts as a neurotransmitter or interferes with neurotransmission.[62]

Our collaborators in the Brunengraber lab conducted a study to determine the reversibility of the pathway of β-alanine formation from 3-hydroxypropionate. During this study, they found an increased concentration of a compound with a mass to charge ratio 44 higher than β-alanine. A +44 *m/z* is typically associated with a carboxylation. The only characterized compound that fits this motif is aspartate, a common amino acid whose structure is similar to β-alanine with a carboxylic acid attached to the 3 position. However, a +44 *m/z* peak with the known fragmentation pattern of aspartate occurs concurrently with our unknown peak. This led us to hypothesize the existence of 2-(aminomethyl)malonate (AMM), a neurotransmitter-like compound that has no published synthesis or characterization. In order to prove the identity of our unknown and determine the role of this molecule in human metabolism, a standard had to be synthesized and compared to the experimental results.

1.8 References

1. Boyle, J. *Molecular biology of the cell, 5th edition by B. Alberts, A. Johnson, J. Lewis, M. Raff, K. Roberts, and P. Walter*. *Biochemistry and Molecular Biology Education* (2008).

2. Baldwin, J. E. & Krebs, H. The evolution of metabolic cycles. *Nature* **291,** 381–382 (1981).

3. Ramberg, P. J. The Death of Vitalism and The Birth of Organic Chemistry: Wohler's Urea Synthesis and the Disciplinary Identity of Organic Chemistry. *Ambix* **47,** 170–195 (2014).

4. Kinne-Saffran, E. & Kinne, R. K. H. Vitalism and synthesis of urea. *Am. J. Nephrol.* **19,** 290–294 (1999).

5. Kurzer, F. & Sanderson, P. M. Urea in the history of organic chemistry: Isolation from natural sources. *J. Chem. Educ.* **33,** 452 (1956).

6. Johnson, J. A. & Rocke, A. J. The Quiet Revolution: Hermann Kolbe and the Science of Organic Chemistry. *Am. Hist. Rev.* **100,** 177 (1995).

7. Fischer, E. Ueber das Caffeïn. *Berichte der Dtsch. Chem. Gesellschaft* **14,** 637–644 (1881).

8. Fischer, E. Ueber das Purin und seine Methylderivate. *Berichte der Dtsch. Chem. Gesellschaft* **31,** 2550–2574 (1898).

9. Zukunft, S. *et al.* High-throughput extraction and quantification method for targeted metabolomics in murine tissues. *Metabolomics* **14,** 18 (2018).

10. Römisch-Margl, W. *et al.* Procedure for tissue sample preparation and metabolite extraction for high-throughput targeted metabolomics. *Metabolomics* **8,** 133–142 (2012).

11. Bruce, S. J. *et al.* Evaluation of a protocol for metabolic profiling studies on human blood plasma by combined ultra-performance liquid chromatography/mass spectrometry: From extraction to data analysis. *Anal. Biochem.* **372,** 237–249 (2008).

12. Luque-Garcia, J. L. & Neubert, T. A. Sample preparation for serum/plasma profiling and biomarker identification by mass spectrometry. *J. Chromatogr. A* **1153,** 259–276 (2007).

13. Lapolla, A., Fedele, D., Seraglia, R. & Traldi, P. The role of mass spectrometry in the study of non-enzymatic protein glycation in diabetes: An update. *Mass Spectrom. Rev.* **25,** 775–797 (2006).

14. Sofia, M. *et al.* Exploring Airway Diseases by NMR-Based Metabonomics: A Review of Application to Exhaled Breath Condensate. *J. Biomed. Biotechnol.* **2011,**

1–7 (2011).

15. Borras, E. *et al.* Detecting opioid metabolites in exhaled breath condensate (EBC). *J. Breath Res.* **13,** 046014 (2019).

16. Kind, T. *et al.* Identification of small molecules using accurate mass MS/MS search. *Mass Spectrom. Rev.* **37,** 513–532 (2018).

17. Moselhy, H. F., Reid, R. G., Yousef, S. & Boyle, S. P. A specific, accurate, and sensitive measure of total plasma malondialdehyde by HPLC. *J. Lipid Res.* **54,** 852–858 (2013).

18. Gu, Q. *et al.* Metabolic profiling of adherence to diet, physical activity and body size recommendations for cancer prevention. *Sci. Rep.* **8,** 16293 (2018).

19. Playdon, M. C. *et al.* Identifying biomarkers of dietary patterns by using metabolomics. *Am. J. Clin. Nutr.* **105,** 450–465 (2017).

20. Robberecht, H., De Bruyne, T. & Hermans, N. Effect of various diets on biomarkers of the metabolic syndrome. *Int. J. Food Sci. Nutr.* **68,** 627–641 (2017).

21. Naviaux, R. *et al.* Metabolic features of Gulf War illness. *PLoS One* **14,** (2019).

22. Kharasch, E. D., Regina, K. J., Blood, J. & Friedel, C. Methadone Pharmacogenetics. *Anesthesiology* **123,** 1142–1153 (2015).

23. De Bruyn, T., Augustijns, P. F. & Annaert, P. P. Hepatic Clearance Prediction of Nine Human Immunodeficiency Virus Protease Inhibitors in Rat. *J. Pharm. Sci.* **105,** 846–853 (2016).

24. Walker, G. S. & O'Connell, T. N. Comparison of LC-NMR and conventional NMR for structure elucidation in drug metabolism studies. *Expert Opin. Drug Metab. Toxicol.* **4,** 1295–1305 (2008).

25. Boiteau, R. *et al.* Structure Elucidation of Unknown Metabolites in Metabolomics by Combined NMR and MS/MS Prediction. *Metabolites* **8,** 8 (2018).

26. Evans, D. A., Trenkle, W. C., Zhang, J. & Burch, J. D. Synthesis and Confirmation of the Absolute Stereochemistry of the (−)-Aflastatin A C 9 −C 27 Degradation Polyol. *Org. Lett.* **7,** 3335–3338 (2005).

27. Furber, M. & Mander, L. N. Synthesis and confirmation of structure of the antheridium-inducing factor from the fern Anemia mexicana. *J. Am. Chem. Soc.* **110,** 4084–4085 (1988).

28. Corey, E. J. & Myers, A. G. Total synthesis of (.+-.)-antheridium-inducing factor (AAn) of the Fern Anemia phyllitidis. Clarification of stereochemistry. *J. Am. Chem. Soc.* **107,** 5574–5576 (1985).

29. Sudhakar Reddy, G., Arjunreddy Mallampudi, N., Lakshmi, J. K. & Mohapatra, D. K. Total Synthesis of Cryptorigidifoliol K: Confirmation of Structure and Absolute

Configuration. *Asian J. Org. Chem.* **7,** 2504–2510 (2018).

30. Kim, S.-H., Kelly, P. B. & Clifford, A. J. Calculating Radiation Exposures during Use of 14 C-Labeled Nutrients, Food Components, and Biopharmaceuticals To Quantify Metabolic Behavior in Humans. *J. Agric. Food Chem.* **58,** 4632–4637 (2010).

31. Sadhukhan, S., Han, Y., Zhang, G. F., Brunengraber, H. & Tochtrop, G. P. Using isotopic tools to dissect and quantitate parallel metabolic pathways. *J. Am. Chem. Soc.* **132,** 6309–6311 (2010).

32. Knights, K. M., Stresser, D. M., Miners, J. O. & Crespi, C. L. In vitro drug metabolism using liver microsomes. *Curr. Protoc. Pharmacol.* (2016).

33. Lincoln, B. C., Rosiers, C. Des & Brunengraber, H. Metabolism of S-3-hydroxybutyrate in the perfused rat liver. *Arch. Biochem. Biophys.* **259,** 149–156 (1987).

34. Slauch, J. M. How does the oxidative burst of macrophages kill bacteria? Still an open question. *Mol. Microbiol.* **80,** 580–583 (2011).

35. Li, X. *et al.* Targeting mitochondrial reactive oxygen species as novel therapy for inflammatory diseases and cancers. *J. Hematol. Oncol.* **6,** 19 (2013).

36. Goldstein, S., Lind, J. & Merényi, G. Chemistry of peroxynitrites as compared to peroxynitrates. *Chemical Reviews* (2005).

37. Fridovich, I. Superoxide Anion Radical ($O^{\cdot-}_2$), Superoxide Dismutases, and Related Matters. *J. Biol. Chem.* **272,** 18515–18517 (1997).

38. Chelikani, P., Fita, I. & Loewen, P. C. Diversity of structures and properties among catalases. *Cell. Mol. Life Sci.* **61,** 192–208 (2004).

39. Sayre, L. M. *et al.* 4-Hydroxynonenal-derived advanced lipid peroxidation end products are increased in Alzheimer's disease. *J. Neurochem.* **68,** 2092–2097 (1997).

40. Su, B. *et al.* Oxidative Stress Signaling in Alzheimers Disease. *Curr. Alzheimer Res.* **5,** 525–532 (2008).

41. Agostinho, P., A. Cunha, R. & Oliveira, C. Neuroinflammation, Oxidative Stress and the Pathogenesis of Alzheimers Disease. *Curr. Pharm. Des.* **16,** 2766–2778 (2010).

42. Reuter, S., Gupta, S. C., Chaturvedi, M. M. & Aggarwal, B. B. Oxidative stress, inflammation, and cancer: How are they linked? *Free Radic. Biol. Med.* **49,** 1603–1616 (2010).

43. Gorrini, C., Harris, I. S. & Mak, T. W. Modulation of oxidative stress as an anticancer strategy. *Nat. Rev. Drug Discov.* **12,** 931–947 (2013).

44. Harrison, D., Griendling, K. K., Landmesser, U., Hornig, B. & Drexler, H. Role of oxidative stress in atherosclerosis. *Am. J. Cardiol.* **91,** 7–11 (2003).

45. Singh, U. & Jialal, I. Oxidative stress and atherosclerosis. *Pathophysiology* **13,** 129–142 (2006).

46. Stocker, R. & Keaney, J. F. Role of Oxidative Modifications in Atherosclerosis. *Physiol. Rev.* **84,** 1381–1478 (2004).

47. Bajpai, A. Oxidative Stress and Major Depression. *J. Clin. DIAGNOSTIC Res.* (2014).

48. Papackova, Z. & Cahova, M. Fatty Acid Signaling: The New Function of Intracellular Lipases. *Int. J. Mol. Sci.* **16,** 3831–3855 (2015).

49. Csala, M. *et al.* On the role of 4-hydroxynonenal in health and disease. *Biochim. Biophys. Acta - Mol. Basis Dis.* **1852,** 826–838 (2015).

50. Qin, Z. *et al.* Effect of 4-Hydroxy-2-nonenal Modification on α-Synuclein Aggregation. *J. Biol. Chem.* **282,** 5862–5870 (2007).

51. Uchida, K. 4-Hydroxy-2-nonenal: a product and mediator of oxidative stress. *Prog. Lipid Res.* **42,** 318–343 (2003).

52. Li, Q. *et al.* 4-Hydroxy-2(E)-nonenal (HNE) catabolism and formation of HNE adducts are modulated by β oxidation of fatty acids in the isolated rat heart. *Free Radic. Biol. Med.* **58,** 35–44 (2013).

53. Alary, J., Guéraud, F. & Cravedi, J.-P. Fate of 4-hydroxynonenal in vivo: disposition and metabolic pathways. *Mol. Aspects Med.* **24,** 177–187 (2003).

54. Mamelak, M. Gammahydroxybutyrate: An endogenous regulator of energy metabolism. *Neurosci. Biobehav. Rev.* **13,** 187–198 (1989).

55. Boscolo-Berto, R. *et al.* Narcolepsy and effectiveness of gamma-hydroxybutyrate (GHB): A systematic review and meta-analysis of randomized controlled trials. *Sleep Med. Rev.* **16,** 431–443 (2012).

56. Kaufman, E. E., Nelson, T., Miller, D. & Stadlan, N. Oxidation of ?-Hydroxybutyrate to Succinic Semialdehyde by a Mitochondrial Pyridine Nucleotide-Independent Enzyme. *J. Neurochem.* **51,** 1079–1084 (1988).

57. Sadhukhan, S., Zhang, G.-F. & Tochtrop, G. P. Modular Isotopomer Synthesis of γ-Hydroxybutyric Acid for a Quantitative Analysis of Metabolic Fates. *ACS Chem. Biol.* **9,** 1706–1711 (2014).

58. Nyhan, W., Barshop, B. & Al-Aqeel, A. in *Atlas of Inherited Metabolic Diseases 3E* 8–18 (CRC Press, 2011).

59. Wilson, K. *et al.* Inter-relations between 3-hydroxypropionate and propionate metabolism in rat liver: relevance to disorders of propionyl-CoA metabolism. *Am.*

J. Physiol. Metab. **313,** E413–E428 (2017).

60. Harris, R. C. *et al.* The absorption of orally supplied β-alanine and its effect on muscle carnosine synthesis in human vastus lateralis. *Amino Acids* **30,** 279–289 (2006).

61. Baguet, A. *et al.* Carnosine loading and washout in human skeletal muscles. *J. Appl. Physiol.* **106,** 837–842 (2009).

62. Tiedje, K. E., Stevens, K., Barnes, S. & Weaver, D. F. β-Alanine as a small molecule neurotransmitter. *Neurochem. Int.* **57,** 177–188 (2010).

CHAPTER 2

RESEARCH STRATEGIES:

SYNTHESIS OF ISOTOPICALLY LABELED SUBSTRATES

2.1 Introduction

Since the development of the mass spectrometer in the early 1900s[1] and subsequent use for the identification of stable isotopes, researchers have been chemically introducing stable isotopes into biological molecules to study the fates of these molecules. One of the initial projects that showed the promise of this type of research utilized deuterated linseed oil to analyze fat metabolism.[2] Deuterated molecules were generated by placing a compound in a deuterium atmosphere with palladium catalyst, allowing for exchange of deuterium for hydrogen.[3] The labeled oil was then fed to mice as part of their diet and the labeling followed through the metabolome. This allowed Schoenheimer and Rittenberg to determine that the bulk of ingested fats were utilized immediately for energy, and the fat that was stored in deposits were eventually used in times of energy deficit.

This new technique proved successful in elucidating metabolism beyond fatty acids. These researchers continued to utilize this technique to publish 14 metabolism papers within a few years.[3–7] The use of similar techniques continued to spread and improve as techniques to concentrate and isolate isotopes of carbon,[8] nitrogen,[9] and oxygen[10] were developed.

2.1.1 Studying metabolic rates in healthy and disease states

One use of stable isotope studies is to elucidate metabolic pathways and rates of molecules production, degradation, or turnover in a typical healthy organism. For instance, one of the earliest studies involved repeated dosing of ^{15}N labeled glycine.[11] Urine samples were collected and the rate of enrichment of ^{15}N labeled urea was monitored. Eventually this enrichment would reach a steady state, reflecting the rate of

protein turnover *in vivo*. These types of whole body measurements have many beneficial qualities such as ease of isotope administration and easy sampling, but lack the ability to distinguish the role of specific metabolite pools or tissue types.[12] In order to further understand these metabolic factors, more invasive sample collection of blood or tissue samples can be performed. When performing such experiments, the timing, temperature, and external conditions must be carefully controlled to ensure that metabolic perturbations are minimized.[13]

When in a disease state, normal metabolism is upended by various metabolic pathways being upregulated or downregulated compared to those found in healthy individuals. Understanding these changes in concentrations of metabolites can help to clarify the cause of underlying symptoms. These observations can also be utilized as a biomarker for tracking disease progression or determining potential therapeutic targets.[14] The various types of human cancers provide a particularly good example of this principle. In order for cancerous tumors to grow, they must exert a high amount of biosynthetic effort and require a large increase in nutrient uptake and energy.[15]

2.1.2 Uniformly labeled vs positionally labeled substrates

The most common types of isotopically labeled substrates are referred to as uniformly labeled. In this type of substrate, all atoms of an element are isotopically labeled. These labeled substrates are typically used to look at system-wide metabolism, labeling all downstream metabolites simultaneously. This can be particularly useful when trying to elucidate unknown metabolic pathways or looking for changes in metabolic rate due to disease state.[16] One commonly used uniformly labeled molecule is $^{13}C_6$-glucose.[17]

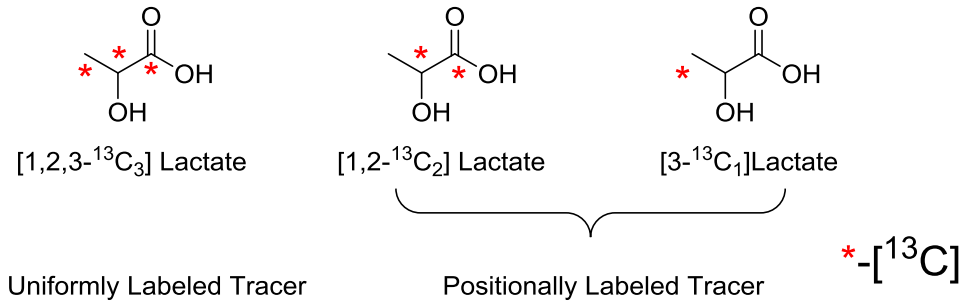

Figure 6: Uniformly labeled substrates vs positionally labeled substrates

The other major category of labeled molecule is the positionally labeled substrate. In this type of molecule, a logical scheme is planned in which only specific atoms of an element are isotopically labeled. The labeling schemes are designed rationally to elucidate additional information. One exemplary study that demonstrates the power of positional labeling was done on human lung tumors. The researchers utilized uniformly labeled glucose in conjunction with positionally labeled lactate to measure the contribution of these molecules to the TCA cycle in the tumor.[18] This was possible due to the labeling scheme of both molecules being chosen in such a way that they would produce a unique labeling scheme for the TCA cycle intermediates. The labeling scheme and the unique labeling pattern of subsequent catabolites are illustrated in **Figure 7.**

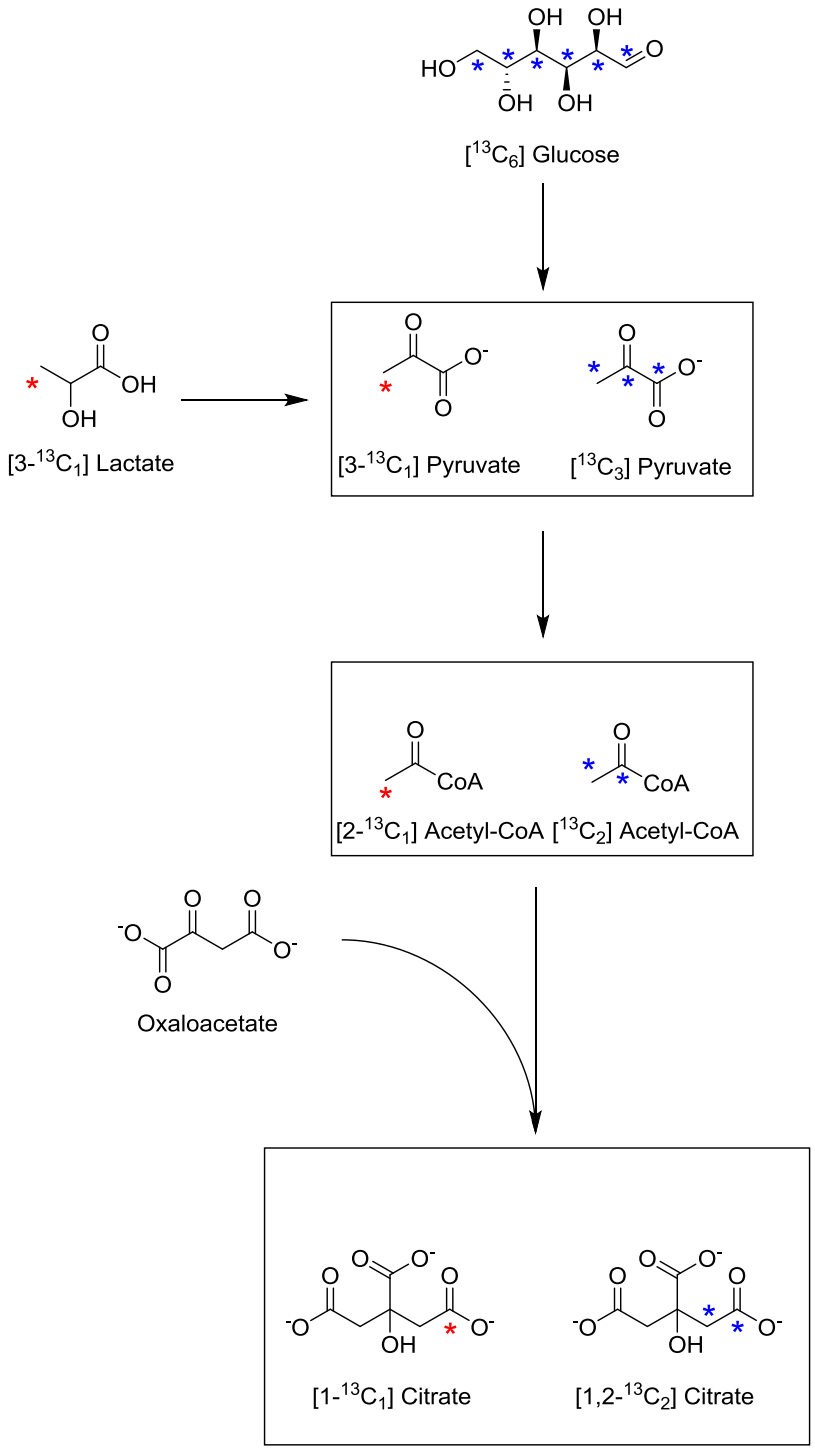

Figure 7: Positionally labeled substrates leading to different labeled metabolites

2.2 Results

2.2.1 Heptanoic acid

An example of how synthetic strategy must change when utilizing stable isotopes is displayed in **Scheme 1**. Our collaborators at the Cleveland Clinic required two different positionally labeled heptanoic acids to measure metabolic flux during isolated limb perfusions. The first was M2 labeled in the 1 and 2 positions. I accomplished this synthesis utilizing the commercially available [$^{13}C_2$] ethyl bromoacetate. This was done by forming the triphenylphosphine ylide and subsequent Wittig reaction with pentanal. The resulting α,β-unsaturated ester **3** was then hydrogenated to afford the saturated ester **4**. This was then hydrolyzed to provide the desired M2 heptanoic acid **5**.

The second isotopologue required for this study was a 5,6,7-labeled M3 heptanoic acid. In order for the previous synthetic scheme to work, the Wittig reagent would need to be unlabeled and reacted with a 3,4,5-[$^{13}C_3$]-labeled pentanal. This labeling scheme for pentanal is not commercially available, so a new synthetic route had to be devised. I began this scheme by reacting commercially available M4 ethyl acetoacetate and unlabeled ethyl bromobutanoate to form **6**. Hydrolysis under basic conditions was followed by reflux with sulfuric acid to remove one of the ^{13}C labeled carbons as carbon dioxide to afford 6-oxoheptanoic acid **7**. The final step was a Huang-Minlon modification[19] of the Wolff-Kishner reduction to provide the M3 labeled heptanoic acid **8**. As has been demonstrated by these two examples, targeting different atoms in a substrate requires entirely different approaches to synthesize the molecules.

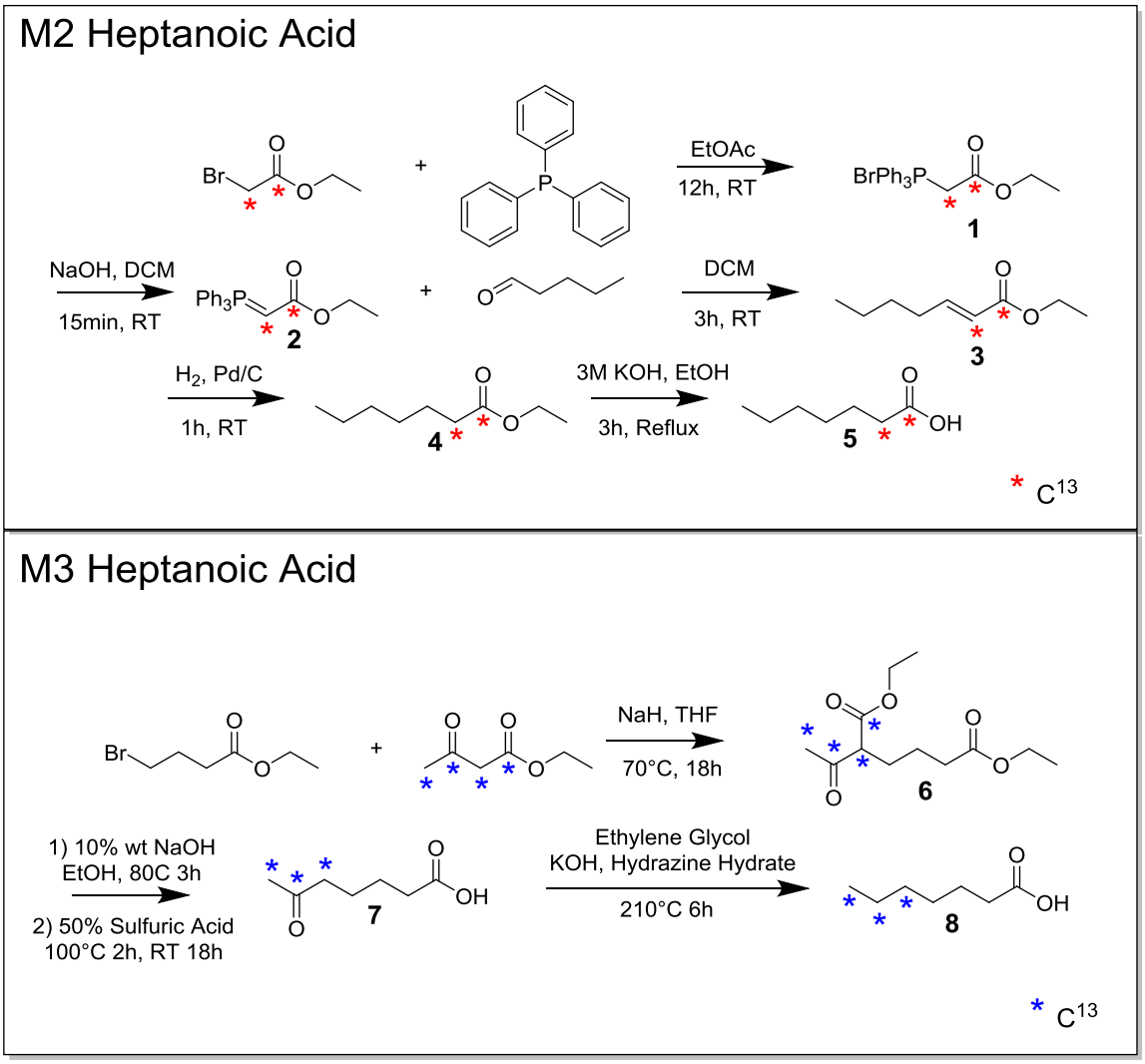

Scheme 1: Synthetic schemes for M2 and M3 heptanoic acid

2.2.2 Succinic semialdehyde

Another example of how synthetic plans must be modified to accommodate stable isotopes is demonstrated by my synthesis of M4 succinic semialdehyde. This work was done in collaboration with the Zhang and Newgard labs at Duke University. Their interests lie in studying insulin secretion and their recent data points to succinic semialdehyde being an insulin secretagogue. In order to discover the mechanism behind

this phenomenon, they need to better understand the metabolic pathways with which succinic semialdehyde is capable of reacting.

To assist with this project, a uniformly ^{13}C labeled isotopologue of succinic semialdehyde is required. The initial approach to synthesizing this molecule involved attempting to join two M2 labeled ethyl bromoacetate molecules together. After a number of unsuccessful attempts, a method was found to start from commercially available $^{13}C_5$-glutamic acid. In order for this reaction to occur, a sodium hypochlorite solution of higher concentration than commercial strength was needed. This was obtained by bubbling chlorine gas through a sodium hydroxide solution. Using this method, succinic semialdehyde was obtained in high purity. It was found that **9** is capable of cyclization to a hemiacetal and the ratio of linear to cyclized was roughly 1 to 1 as noted by NMR.

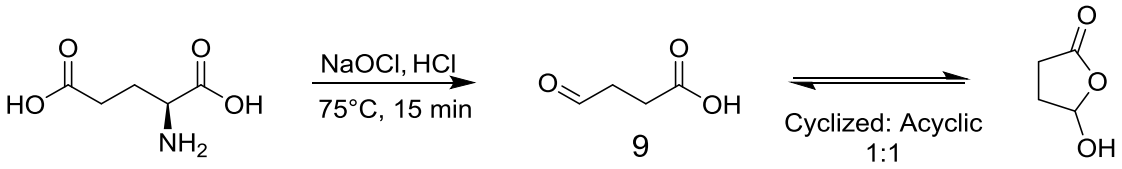

Scheme 2: Synthesis of succinic semialdehyde from glutamic acid

2.2.3 3-Hydroxypropionate

The interest in labeled 3-hydroxypropionate was generated at the intersection of projects done by the Tochtrop and Brunengraber laboratories. The full history of the projects and biological relevance of this molecule can be found in the introduction to **Chapter 4**. In

order to study the metabolism of this compound, it was decided that a number of isotopologues would be useful to distinguish labeling patterns of catabolites.

The first molecule synthesized was a uniformly ^{13}C labeled 3-hydroxypropionate. The method utilized could be utilized to produce three potential isotopologues by simply exchanging labeled starting materials for unlabeled varieties. As seen in a previous synthesis in this chapter, M2 ethyl bromoacetate is a common starting material for many stable isotope syntheses due to its low cost. This [$^{13}C_2$] molecule can be extended to three labeled carbons by substitution reaction using labeled potassium cyanide. The resulting nitrile can be reduced via hydrogenation with platinum oxide. The amine can be converted to an alcohol through a diazonium intermediate by reacting with nitrous acid. Once all the functionalities are in place, all that remains is hydrolysis of the ester. An overview of this synthetic path can be seen in **Scheme 3**.

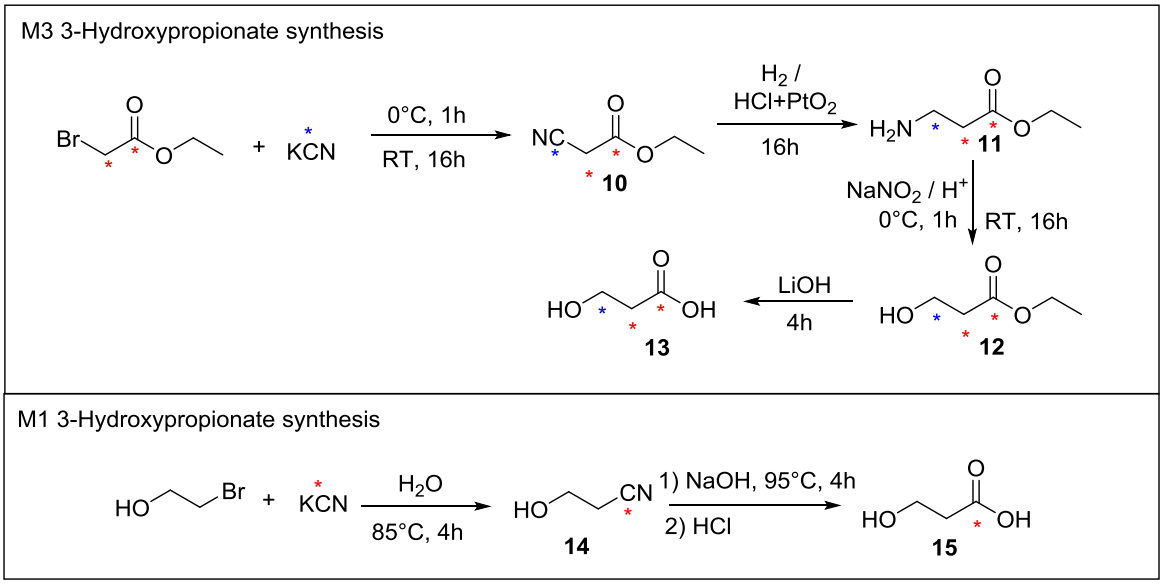

Scheme 3: Synthetic pathways for M3 and M1 3-hydroxypropionate

The positional isomer of greatest interest would be labeled at the 1-position. Although the original synthesis of labeled 3-hydroxypropionate was versatile, M1 1-[$^{13}C_1$]- ethyl bromoacetate is not commercially available. Therefore, a new synthetic scheme was needed. In the M1 synthetic scheme, 2-bromoethanol underwent a substitution reaction with labeled potassium cyanide to form 3-hydroxypropanenitrile **14**. This nitrile could then be hydrolyzed to form the desired labeling pattern of 1-[$^{13}C_1$] 3-hydroxypropionate **15**.

2.3 Conclusions

Throughout this chapter, a number of collaborative projects have been discussed. In all three projects, synthetic schemes for stable isotope labeled substrates were designed and successfully completed. These substrates were sent to the Cleveland Clinic, the Zhang lab at Duke, and the Brunengraber lab in Case Western's Department of Nutrition to assist in metabolic studies.

The results of the 3-hydroxypropionate study were published in the *American Journal of Physiology- Endocrinology and Metabolism*. The results of this study have spawned a number of other investigations, including the work discussed in **Chapter 4**. These results and how they tie into the discovery of 2-(aminomethyl)malonate will be discussed in the introduction to that chapter.

2.4 Experimental protocols

2.4.1 Materials and methods

All reactions were performed in oven-dried glassware under an inert atmosphere. Reagents were purchased from Sigma-Aldrich and used as supplied unless otherwise noted. Isotopically labeled compounds were purchased from Cambridge Isotope Labs. NMR analyses were run on a Bruker **Ascend Avance III HD^{TM}** operating at 500 MHz and 125 MHZ for the ^{1}H and ^{13}C-NMR spectra (at the Department of Chemistry, Case Western Reserve University). The internal references were $CDCl_3$ (δ 7.26), CD_3OD (δ 3.31) for ^{1}H and (δ 77.4), CD_3OD(δ 49.0) for ^{13}C spectra, respectively. NMR data are presented in the following order: chemical shift, peak multiplicity (b = broad, s = singlet, d = doublet, t = triplet, q = quartet, m = multiplet, dd = doublet of doublets, ddd = doublet of doublets of doublets, ddt = doublet of doublet of triplet, dq = doublet of quartets, coupling constant (in Hz).

2.4.2 Synthetic routes

[1,2-$^{13}C_2$](Ethoxycarbonylmethyl)triphenylphosphonium Bromide (1)

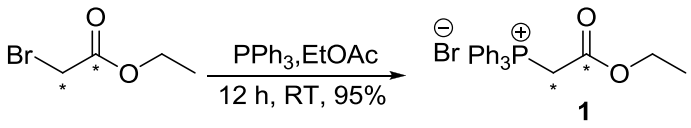

1

Ethyl [1,2-$^{13}C_2$]-2-bromoacetate (2.54 g, 15.03 mmol) in ethyl acetate (10 mL) was slowly added to a solution of triphenylphosphine (4.06 g, 15.47 mmol) in ethyl acetate

(10 mL). The reaction mixture was then stirred at room temperature overnight and the white precipitate filtered off, washed with diethyl ether (3 × 10 mL), and dried under vacuum for 2 h to give **1** (6.06 g, 14.05 mmol, 95% yield): ^{1}H NMR (400 MHz, $CDCl_3$) δ 1.06 (t, *J* = 7.2 Hz, 3H), 4.03 (dq, 2H, *J* = 7.2 Hz, 3.2 Hz), 5.39 (ddd, 2H, $^{1}J_{H\text{-}C}$ = 134.8 Hz, $J_{H\text{-}P}$ = 14 Hz, $^{2}J_{H\text{-}C}$ = 7.6 Hz), 7.66−7.93 (m, 15H); ^{13}C NMR (100 MHz, $CDCl_3$) δ 13.6, 33.4 (dd, $^{1}J_{C\text{-}P}$ = 55.7 Hz, $^{1}J_{C\text{-}C}$ = 58.7 Hz), 62.8, 117.8 (d, $^{1}J_{C\text{-}P}$ = 88.9 Hz), 130.2 (d, $^{3}J_{C\text{-}P}$ = 13.8 Hz), 133.8 (d, $^{2}J_{C\text{-}P}$ = 10.7 Hz), 135.1 (d, $^{4}J_{C\text{-}P}$ = 3.8 Hz), 164.7 (dd, $J_{C\text{-}C}$ = 59.1 Hz, $^{2}J_{C\text{-}P}$ = 3.0 Hz).

[1,2-$^{13}C_2$](Ethoxycarbonylmethylene)triphenylphosphorane (2)

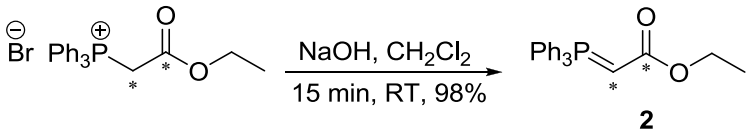

2

A solution of sodium hydroxide (1.0 M, 50 mL) was added to a solution of 2-[1,2-$^{13}C_2$](Ethoxycarbonylmethyl)triphenylphosphonium bromide **1** (6.0 g, 13.91 mmol) in dichloromethane (50 mL) and the reaction mixture stirred vigorously for 15 minute. The organic layer was removed and the aqueous layer extracted with dichloromethane (3 × 15 mL). The combined organic layers were dried over Na_2SO_4 and concentrated under vacuum to give 4.78 g (13.64 mmol, 98% yield) of **2**: ^{1}H NMR (400 MHz, $CDCl_3$) δ 1.06 (br, 3H), 2.9 (br, d, $J_{H\text{-}P}$ ≈120 Hz, 1H,) 3.96 (br,2H), 7.43–7.68 (m, 15H); ^{13}C NMR (100 MHz, $CDCl_3$) δ 15.0, 30.1 (dd, $J_{C\text{-}P}$ = 124.7 Hz, $J_{C\text{-}C}$ = 87.3 Hz), 58.1, 128.0 (d, $^{1}J_{C\text{-}P}$ = 90.6 Hz), 128.9 (d, $^{3}J_{C\text{-}P}$ = 11.4 Hz), 132.1, 133.2 (d, $^{2}J_{C\text{-}P}$ = 9.9 Hz), 171.5 (dd, $J_{C\text{-}C}$ = 87.8 Hz, $^{2}J_{C\text{-}P}$ = 11 Hz).

Ethyl (*E*)-[1,2-$^{13}C_2$]Hep-2-enoate (3)

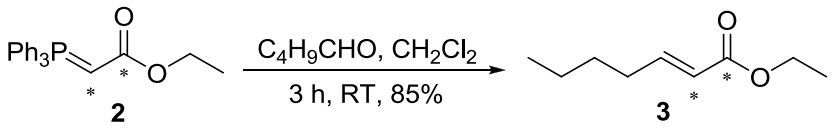

To a solution of valeraldehyde (1.81 mL, 16.96 mmol) in dichloromethane (25 mL) was added 2-[1,2-$^{13}C_2$]-(ethoxycarbonylmethylene)triphenylphosphorane **2** (4.75 g, 13.56 mmol) in dichloromethane (25 mL) and the reaction mixture was stirred for 3 hours. The solvent was evaporated *in vacuo* and the crude product purified by column chromatography over silica (10:1 Hexane: Ethyl Acetate) to give 1.82 g of **3** (11.50 mmol, 85% yield) : ^{1}H NMR (400 MHz, $CDCl_3$) δ 0.91 (t, *J* = 7.2 Hz, 3H), 1.29 (t, *J* = 7.2 Hz ,3H), 1.31-1.46 (m, 4H), 2.17−2.24 (m, 2H), 4.18 (dq, *J* = 7.2 Hz, *J* = 3.2 Hz, 2H), 5.80 (ddm, J = 161.7 Hz, *J* = 15.6 Hz, 1.6 Hz, 1H), 6.91-7.01 (m, 1H); ^{13}C NMR (100 MHz, $CDCl_3$) δ 14.0, 14.5, 22.6 (d, J = 4.6 Hz), 30.3(d, J = 3.4 Hz), 32.1(d, J = 6.6 Hz), 60.3, 121.4(d, J= 75 Hz), 149.6 (d, J = 70.0 Hz), 167.0 (d, J = 74 Hz).

Ethyl (*E*)-[1,2-$^{13}C_2$]Heptanoate (4)

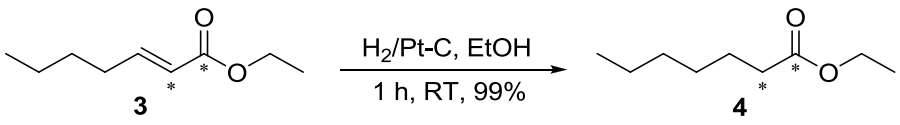

Ethyl (*E*)-[1,2-$^{13}C_2$]Hep-2-enoate **3** (1.80 g, 11.38 mmol) was dissolved in ethanol (25 mL) and mixed with 10% Pt/C under 1 atm of H_2. The mixture was subsequently stirred for 1 h at room temperature, filtered through a pad of celite, the filter cake was washed

with ethanol (10 mL) and the solvent removed *in vacuo* to afford **4** (1.82 g, 11.35 mmol, 99%) obtained was directly used for the next step without any further purification.

[$^{13}C_4$]Diethyl 2-Acetylhexanedioate (6)

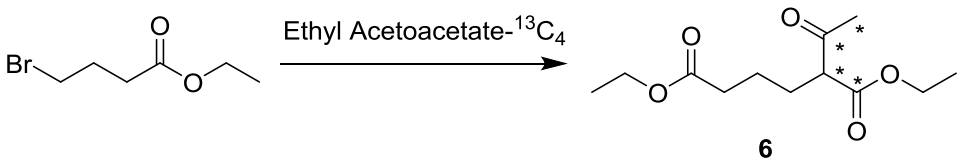

6

To an oven dried 250mL round bottom with stir bar was added 1 g of NaH washed three times with hexane. The NaH was then dissolved in dry THF (25 mL) and cooled to 0 °C. The solution was stirred and a solution of [$^{13}C_3$] ethyl acetoacetate (5 g, 37.9 mmol) in THF (10 mL) was added dropwise over 30 minutes. The solution was then stirred for 15 minutes at room temperature. A solution of ethyl 4-bromobutyrate (7.49 g in 15mL THF, 38.4 mmol) was then added dropwise over 20 minutes. The solution was brought to reflux overnight. Water (10 mL) was added to quench the reaction and the solution was extracted with ethyl ether. The extract was washed with brine, dried with magnesium sulfate, and concentrated under reduced pressure to yield **6** (1.26 g, 5.16 mmol, 13.6%). The product obtained was used immediately in the next step.

[5,6,7 $^{13}C_3$] 6-Oxoheptanoic Acid (7)

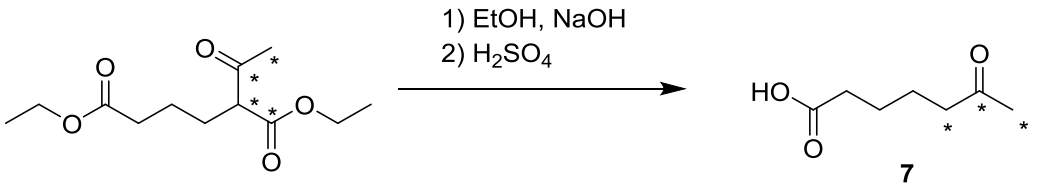

To a 50 mL round bottom with stir bar was added [$^{13}C_4$] diethyl 2-acetylhexanedioate (1.26 g, 5.16 mmol). The oil was dissolved in ethanol (3 mL) and 10% NaOH (3 mL). The solution was refluxed for 3 hours. The solution was cooled to room temperature and 50% sulfuric acid (4 mL) was added. The solution was brought back to reflux for 2 hours, then cooled to ambient temperature and stirred for 16 hours. The compound was extracted with ethyl ether, dried over magnesium sulfate, and concentrated under reduced pressure to afford product **7** (.6 g, 4.17 mmol, 80.7%).

5,6,7 [$^{13}C_3$] Heptanoic Acid (8)

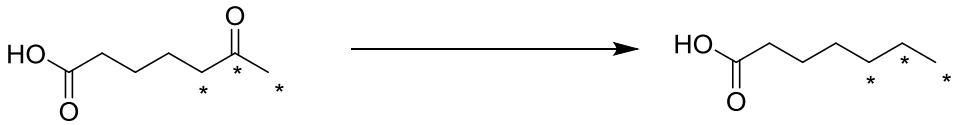

To a 25 mL oven dried round bottom flask with stir bar was added 5,6,7 [$^{13}C_3$] 6-oxoheptanoic acid (0.6 g, 4.17mmol). To this solution was added potassium hydroxide (0.66 g) and hydrazine hydrate (0.5 mL). The resulting mixture was refluxed at 200 °C for 2 hours. After the 2 hour period, the condenser was removed while the solution remained at reflux and volatile compounds were purged with a stream of argon for 3

minutes. The condenser was reassembled and the solution was heated at 210 °C for 16 hours. The reaction was quenched with addition of water and 3M hydrochloric acid to acidify. The solution was extracted with ethyl ether and dried over magnesium sulfate. The product was concentrated under reduced pressure and vacuum distilled (175 °C, 0.5 mmHg) to afford desired product 8.

[$^{13}C_4$] 4-Oxobutanoic Acid (9)

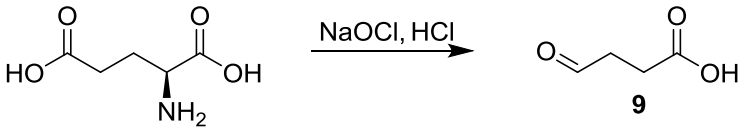

To an oven dried 10 mL round bottom flask equipped with a stir bar was added glutamic acid (0.5 g, 2.9 mmol). The solid was dissolved with the addition of 3 mL of H_2O. To the solution was added 12% NaOCl (3 mL). The pH of the solution was brought to 7 with concentrated HCl before being stirred in a 75 °C sand bath for 15 minutes. The solution was allowed to cool before being brought to pH 3 with concentrated HCl. The solution was then extracted three times with diethyl ether, dried with magnesium sulfate, filtered and concentrated via rotary evaporator to yield **9** (68 mg, 22.7%) as a yellow oil. ^{1}H NMR (500 MHz, chloroform-*d*) δ 2.75 (t, *J* = 6.5 Hz, 1H), 2.69 (t, *J* = 7.1 Hz, 1H), 2.60 (dt, *J* = 14.3, 6.8 Hz, 2H).^{13}C NMR (126 MHz, $CDCl_3$) δ 199.3, 174.1, 28.7, 11.7, 0.0.

1-[^{13}C]- 3-Hydroxypropanenitrile (10)

14

2-Bromoethanol (0.8 g, 6.45 mmol) and ^{13}C- labeled potassium cyanide (0.5 g, 7.57 mmol) were added to water (10 mL) and heated to 85 °C for 4 hours. The reaction then was cooled down. The aqueous phase was extracted by dichloromethane (20 mL x 3) and organic phase was combined and dried by anhydrous sodium sulphate. After removal of the solvent, the product **10** (0.62 g, 86%) was collect as light yellow liquid and used without further purification.^{1}H-NMR ($CDCl_3$, 400 MHz): 3.91 (dt,2H) , 2.62 (dt, 2H). ^{13}C-NMR ($CDCl_3$, 100 MHz): 118.1.

1-[^{13}C $_1$] 4-Hydroxypropionic acid (15)

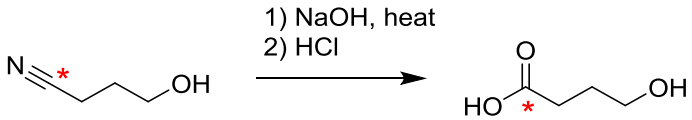

15

1- [^{13}C $_1$] 4-hydroxypropionic acid (0.6 g, 7 mmol) was dissolved in of 40% NaOH (5 mL) solution and then heated to 95 °C for 5 hours. The reaction was monitored by ^{13}C-NMR. After the reaction was completed and cooled to room temperature, 2 M HCl was slowly added at 0 °C until the pH reached 2. Then water was removed under vacuum. The residue was extracted with dry acetone (50 mL x 3). After removal of the acetone, the

product **11** was collected as yellow liquid (0.67g, 82%) ^{1}H-NMR (D_2O, 400 MHz): 3.65 (dt,2H), 2.31 (dt, 2H).^{13}C-NMR (D_2O, 100 MHz): 180.8

[$^{13}C_3$] Ethyl 2-cyanoacetate (10)

Under ice bath, ^{13}C -KCN (2.4 g, 37 mmol) was added in one potion a 20% mixture of acetonitrile in water (100 mL). To which 1,2-[$^{13}C_2$] -ethyl 2-bromoacetate (4.98 g, 30 mmol) was added slowly in 1 hour. The reaction warmed up to room temperature overnight. The mixture was extracted with dichloromethane (100 mL x 3). Organic phase was combined and dried by anhydrous sodium sulphate. After removed the solvent, the product ([$^{13}C_3$]-ethyl 2-cyanoacetate) was collected as yellow liquid (1.81 g, 53%) and used without further purification. ^{1}H-NMR ($CDCl_3$, 400 MHz): 4.28 (dq, 2H), 3.46 (ddd, 2H), 1.33(dt, 3H) ^{13}C-NMR ($CDCl_3$, 100 MHz): 163.1 (d),113.3 (d), 25.0(dd,).

[$^{13}C_3$] Ethyl 3-aminopropionate (11)

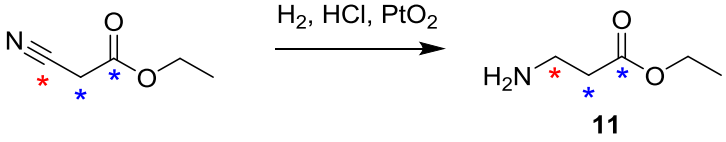

$^{13}C_3$-Ethyl 2-cyanoacetate (1.8 g, 15.5 mmol) was dissolved in ethanol (50 mL) and 4 M HCl (10 mL), to which PtO_2 (130 mg) was added. The reaction was stirring under H_2 balloon for overnight. The color of reaction was changed to from dark solution to clear.

The liquid phase was evaporated under vacuum and the residue was collected as yellow solid **11** (2.2g, 91%) ^{1}H-NMR (D_2O, 400 MHz): 4.10(dq,2H), 3.11 (ddt, 2H), 2.64(ddt, 2H), 1.16(dt, 3H). ^{13}C-NMR (D_2O, 100 MHz): 175.3 (d),37.7 (d), 33.8(dd).

1,2,3-[$^{13}C_3$] Ethyl 3-hydroxypropionate (12)

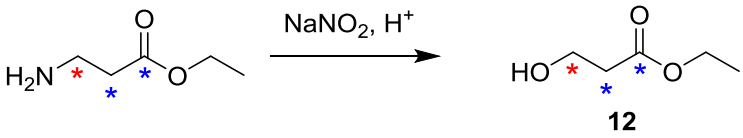

12

1,2,3-[$^{13}C_3$] Ethyl 3-aminopropionate salt (2.2 g, 18.8 mmol) was dissolved in water (10 mL) at 0 °C. Once dissolved, acetic acid was added (4 mL). Sodium nitrite (6 g) was added slowly over 1 hour. The reaction was slowly stirred and warmed to room temperature overnight. The water phase was extracted with dichloromethane (100 mL x 3). Combined organic phase was dried by anhydrous sodium sulphate. After solvent was removed, the product **12** was collected as yellow liquid (1.77g, 90% yield) ^{1}H-NMR (D_2O, 400 MHz): 4.09(dq,2H, -OCH_2), 3.69(ddt, 2H, -$^{13}CH_2OH$), 2.45(ddt, 2H, -$^{13}CH_2$-), 1.15(dt, 3H, - OCH_2CH_3). ^{13}C-NMR (D_2O, 100 MHz): 177.3 (d, ^{13}COO),59.9 (d,^{13} CH_2OH), 39.5(dd, -$^{13}CH_2$-).

1,2,3-[$^{13}C_3$] 3-Hydroxypropionic acid (13)

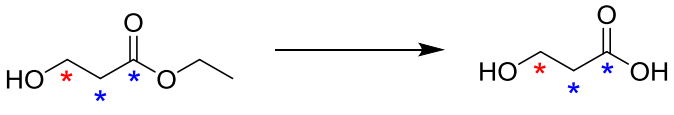

1,2,3-[$^{13}C_3$] Ethyl 3-Hydroxypropionate **12** (1.77 g, X mmol) was dissolved in a 2:1 water/methanol solution (30 mL). LiOH (0.35 g) was added and the reaction was stirred at room temperature for 4 hours. Methanol was removed by rotary evaporator. The aqueous phase was washed with dichloromethane (20 mL x 2), and then acidified with 1 M HCl until the pH read between 1-2. Water was then removed by vacuum and the residue was extracted with dry acetone (100 mL x 3). After removing the solvent, the product **13** was isolated as a yellow liquid, (1.2 g, 88% yield).^{1}H-NMR (D_2O, 400 MHz): 3.65(ddt, 2H), 2.45(ddt, 2H). ^{13}C-NMR (D_2O, 100 MHz): 180.3(d),59.8 (d), 40.2(dd,).

2.5 Acknowledgment

The strategy of the synthesis of 3-hydroxypropionate was originally designed by Dr. Yong Han.

2.6 References

1. Aston, F. W. Bakerian Lecture.— A new mass-spectrograph and the whole number rule. *Proc. R. Soc. London. Ser. A, Contain. Pap. a Math. Phys. Character* **115,** 487–514 (1927).

2. Schoenheimer, R. & Rittenberg, D. Deuterium as an Indicator in the Study of Intermediary Metabolism. III The Role of the Fat Tissues. *J. Biol. Chem.* **111,** 175–181 (1935).

3. Schoenheimer, R. & Rittenberg, D. Deuterium as an indicator in the study of intermediary metabolism. *Science (80-.).* **82,** 156–157x (1935).

4. Schoenheimer, R. & Rittenberg, D. Deuterium as an indicator in the study of intermediary metabolism. VI. Synthesis and destruction of fatty acids in the organism. *J. Biol. Chem.* **114,** 381–396 (1936).

5. Schoenheimer, R. & Rittenberg, D. Deuterium as an indicator in the study of intermediary metabolism XI. Further studies on the biological uptake of deuterium into organic substances, with special reference to fat and cholesterol formation. *J. Biol. Chem.* **121,** 235–253 (1937).

6. Foster, G. ., Schoenheimer, R. & Rittenberg, D. Deuterium as an indicator in the study of intermediary metabolism. XIV. Biological formation of deuteroamino acids. *J. Biol. Chem.* **125,** 13–22 (1938).

7. Foster, G. L., Keston, A. S., Schoenheimer, R. & Rittenberg, D. Deuterium as an indicator in the study of intermediary metabolism XII. The action of proteolytic enzymes on peptides in heavy water. *J. Biol. Chem.* **124,** 159–161 (1938).

8. Nier, A. O. & Gulbransen, E. A. Variations in the Relative Abundance of the Carbon Isotopes. *J. Am. Chem. Soc.* **61,** 697–698 (1939).

9. Urey, H. C., Huffman, J. R., Thode, H. G. & Fox, M. Concentration of N 15 by Chemical Methods. *J. Chem. Phys.* **5,** 856–868 (1937).

10. Urey, H. C., Pegram, G. B. & Huffman, J. R. The Concentration of the Oxygen Isotopes. *J. Chem. Phys.* **4,** 623–623 (1936).

11. Picou, D. & Taylor-Roberts, T. The measurement of total protein synthesis and catabolism and nitrogen turnover in infants in different nutritional states and receiving different amounts of dietary protein. *Clin. Sci.* **36,** 283–96 (1969).

12. Wilkinson, D. J. Historical and contemporary stable isotope tracer approaches to studying mammalian protein metabolism. *Mass Spectrom. Rev.* **37,** 57–80 (2018).

13. Fernández-García, J., Altea-Manzano, P., Pranzini, E. & Fendt, S.-M. Stable Isotopes for Tracing Mammalian-Cell Metabolism In Vivo. *Trends Biochem. Sci.* **45,** 185–201 (2020).

14. Griffin, J. L. Understanding mouse models of disease through metabolomics. *Curr. Opin. Chem. Biol.* **10,** 309–315 (2006).

15. Lane, A. N., Fan, T. W. M. & Higashi, R. M. Stable isotope-assisted metabolomics in cancer research. *IUBMB Life* **60,** 124–129 (2008).

16. Buescher, J. M. *et al.* A roadmap for interpreting 13 C metabolite labeling patterns from cells. *Curr. Opin. Biotechnol.* **34,** 189–201 (2015).

17. Broekaert, D. & Fendt, S.-M. in *Methods in Molecular Biology* 67–82 (2019).

18. Faubert, B. *et al.* Lactate Metabolism in Human Lung Tumors. *Cell* **171,** 358–371 (2017).

19. Huang-Minlon. A Simple Modification of the Wolff-Kishner Reduction. *J. Am. Chem. Soc.* **68,** 2487–2488 (1946).

CHAPTER 3

UNDERSTANDING THE METABOLISM OF LIPID PEROXIDATION PRODUCTS:

4-HYDROXYNONENAL (4-HNE) AND EPOXYKETOOCTADECENOIC ACIDS (EKODEs)

3.1 Introduction

3.1.1 Formation of 4-HNE

As the most studied human LPO product found *in vivo*, it is important to know the origin and fate of 4-hydroxynonenal (4-HNE). One origin of this molecule is the PUFA linoleic acid. Linoleic acid is an essential nutrient[1] for humans and must be obtained in a diet from fatty seeds, oils, and vegetable oils. [2] It is an 18 carbon ω-6 fatty acid with two points of unsaturation. The ω-6 fatty acids are used to biosynthesize arachidonic acid as well as a number of other eicosanoids and signaling molecules that are associated with inflammation and related processes.[3]

Like other PUFAs, the unsaturated bonds of linoleic acid are homoconjugated, i.e., spaced one carbon away from being conjugated. This creates a highly reactive, doubly allylic position that is a prime candidate to react with ROS and RNS. The hydrogen atoms on this doubly allylic position are extremely susceptible to radical hydrogen abstraction. The remaining radical will undergo oxygen addition and oxidation to form lipid hydroperoxides.[4] These hydroperoxides undergo oxidative cleavage to form a family of fragmentation products that contain highly reactive aldehydes and/or α,β-unsaturation such as acrolein, malondialdehyde, and 4-HNE. These highly reactive electrophiles react with biological nucleophiles, leading to cell damage and death.[5]

3.1.2 Role of 4-HNE in Healthy and Disease State Metabolism

Out of all the LPO fragmentation products, 4-HNE is one of the most electrophillic.[6,7] 4-HNE is capable of forming adducts with proteins at any available lysine, histidine, or cysteine residue.[8] The original hypothesis of the field was that LPO product formation

was inherently detrimental to the organism and was an aberrant process that was catabolized through adduction to molecules such as glutathione. However, a basal level of 0.1 to 1.0 μM of 4-HNE is found during normal human physiology. This low concentration has a protective effect by signaling for an upregulation of antioxidant proteins[9] whereas damaging protein adduction occurs at toxic concentrations of 10-50 μM.[10]

Once accumulation of HNE has reached toxic concentrations, adduction will typically occur with proteins involved in inflammation.[11] This is typically done by modifying proteins associated with NFκB expression.[12] Another factor which is altered by 4-HNE modification is apoptosis. Reaction with caspase-3 causes apoptosis in cells with high HNE concentration.[13] However, Michael addition with the p53 protein can cause loss of apoptotic activity[14] and lead to the accumulation of damaged cells.[15] These modifications and effects that occur are summarized in **Figure 8**.

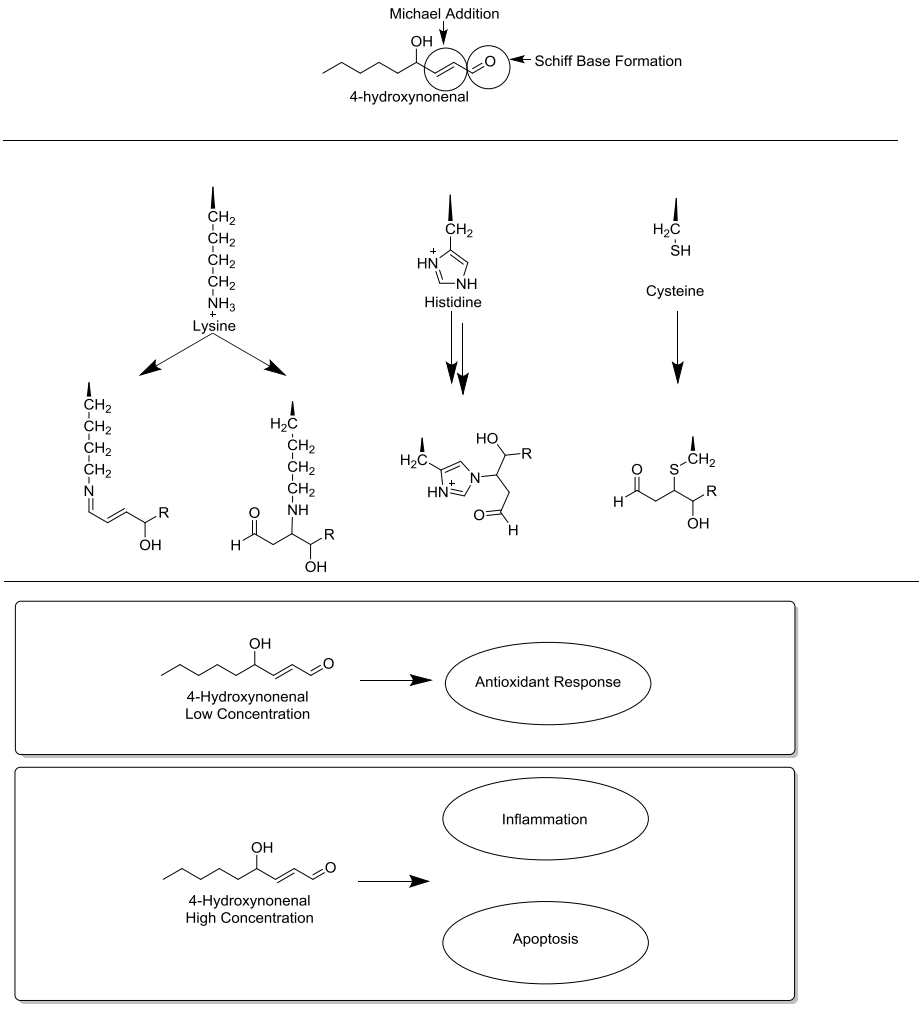

Figure 8: Summary of 4-HNE protein modification

3.1.3 Catabolism of 4-HNE

Prior to the work of the Tochtrop and Brunengraber labs, the pathway for elimination of 4-HNE was thought to be glutathionylation by glutathione S-transferase (GST) and excretion.[16] However, a study utilizing a number of varying stable isotopes of 4-HNE was able to elucidate two separate pathways (**Figure 9**) for catabolism of this LPO product into acetyl-CoA, propanyl-CoA, and formate.[17,18] In one of these pathways, 4-HNE is first catabolized by one round of β-oxidation. It then cleaves one carbon as

formyl-CoA through α-oxidation. The remainder of the catabolism then occurs though β-oxidation. The more novel pathway is a round of β-oxidation followed by a phosphorylation and isomerization of the 4-hydroxy moiety to the 3-position. This then allows full catabolism via β-oxidation. This is evidenced by the presence of propanyl-CoA.

The isomerization pathway is of particular interest to our lab. At the time of publication, the phosphorylation of a 4-hydroxyacyl-CoA and subsequent isomerization to 3-hydroxyacyl-CoA had not been identified in any biological system. Our hypothesized reaction scheme for this pathway is also laid out in **Figure 9**. We believe the first committed step of this pathway lies with an unidentified kinase which phosphorylates the 4-hydroxy moiety of 4-hydroxynonanoyl-CoA. In order to better understand the prevalence and importance of this pathway, we must obtain information on the enzymes which catalyze such a transformation.

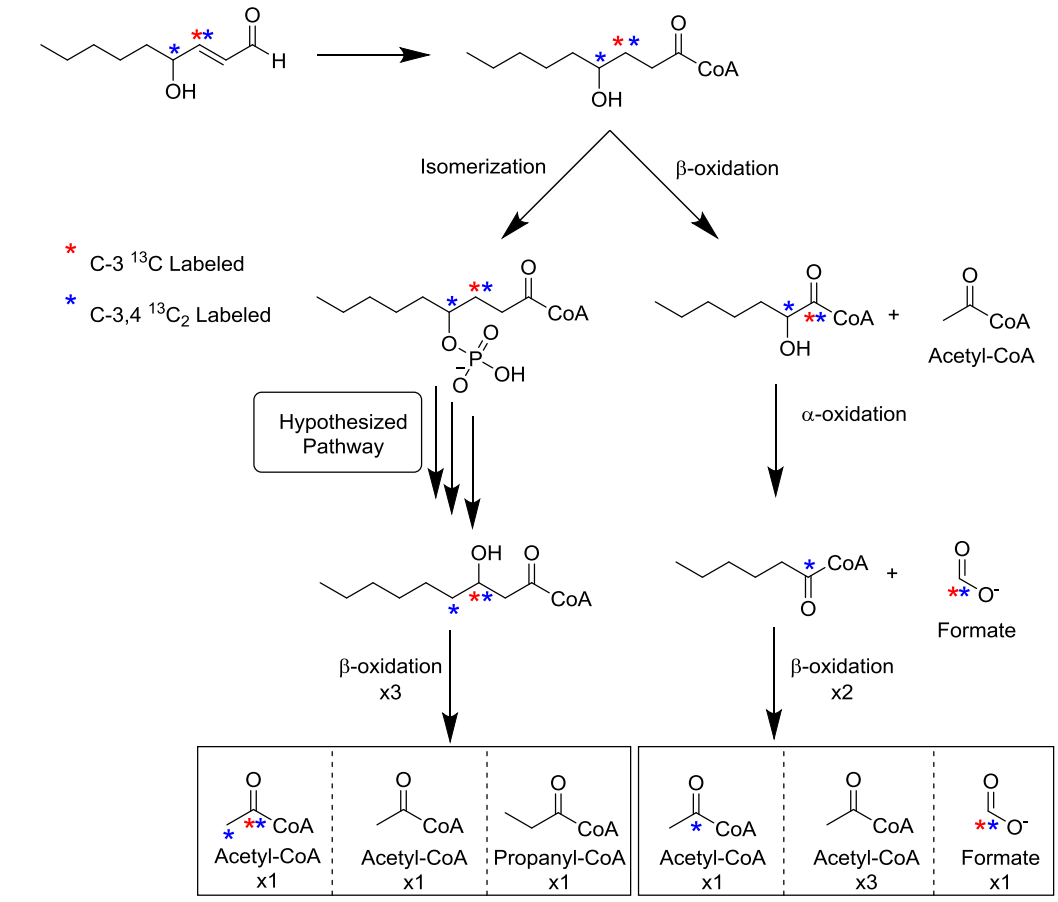

Hypothesized Pathway:

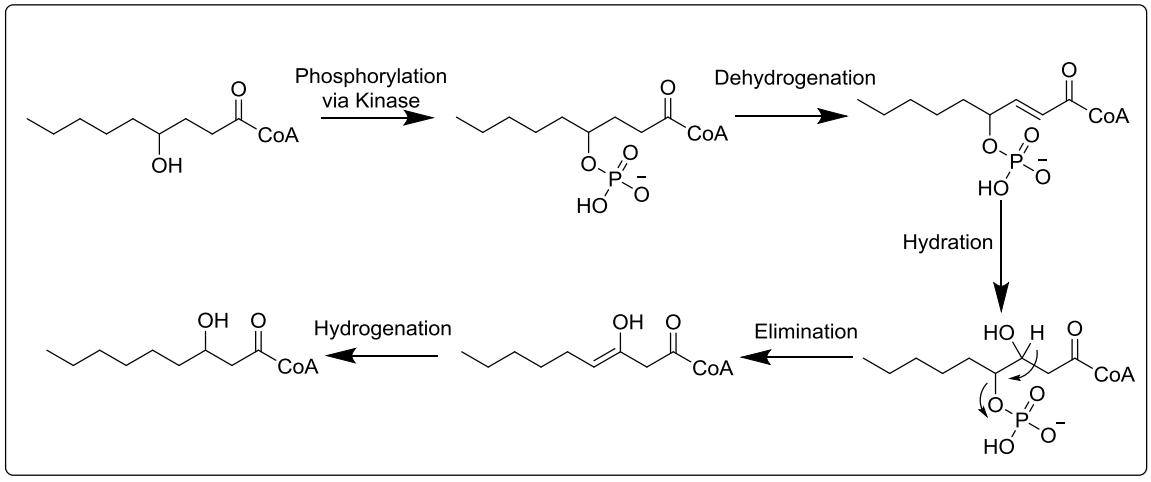

Figure 9: Catabolic pathways of 4-HNE and hypothesized isomerization pathway

3.1.4 Research strategy for further understanding of 4-HNE metabolism

In order to understand the isomerization pathway, we must first isolate and characterize the kinase which catalyzes the first committed step. In order to isolate the enzyme from a bulk protein source, we must first be able to track the activity of the enzyme. Chuan Shi, a former member of the Tochtrop lab, designed an assay that would be able to quantify activity. In order to perform this assay, we will need to synthesize a substrate that would also be phosphorylated by the same kinase while also having little to no presence in biological tissue. Due to the low concentration of endogenous 5-membered fatty acids, we decided to synthesize 4-hydroxypentanoyl-CoA as our substrate. Stable isotope synthesis can be utilized to design a standard whose concentration can be determined with no interference from endogenous molecules. Due to its similarity to the substrate and lack of a hydroxyl moiety, $^{2}H_{9}$-pentanoyl-CoA was chosen to serve as a standard.

This isomerization pathway was originally discovered utilizing rat liver perfusion.[17,18] For protein isolation, we decided to change our bulk protein source to porcine liver. This would decrease the cost and increase the yield of protein while maintaining activity. Once the functional activity assay is in working order, there must be a way to separate the desired kinase from other proteins in a bulk source. To this end, we utilized FPLC separation followed by activity assay to track enzyme activity as we isolated the unidentified kinase from the remaining porcine protein.

3.1.5 EKODEs

In addition to the fragmentation LPO products such as 4-HNE, there exist families of LPO products that retain full chain length. One such family is known as

epoxyketooctadecenoic acids (EKODEs). This family is divided by the position of the ketone (type I/II) and the epoxide (type a/b) (**Figure 10**). In type I EKODEs, the ketone exists as one of the outer functionalities while type II EKODEs feature the ketone in between the two other functionalities. Type a EKODEs have epoxides closer to the carboxylic acid terminal while type b EKODEs have epoxides closer to the aliphatic terminal. These molecules are the predominant products when linoleic acid is oxidized through non-enzymatic means.[19] The ability of these molecules to adduct to protein has been studied by the Sayre lab.[20] Despite this, there are little to no details on the catabolic fate of EKODEs.

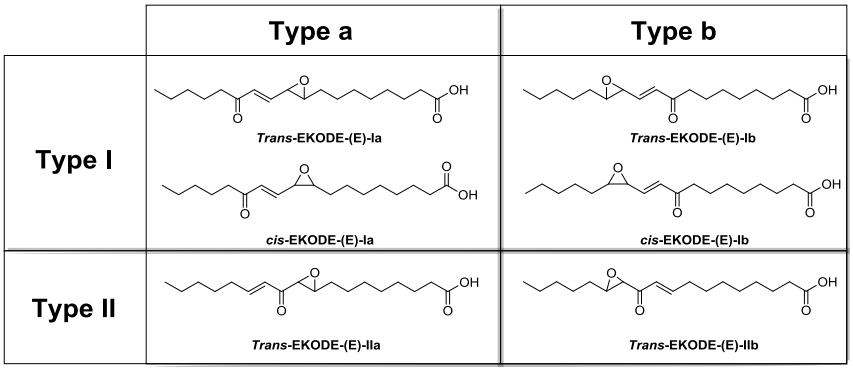

Figure 10: Naming scheme for EKODEs

3.1.6 Research strategy for understanding EKODE metabolism

In order to study the catabolic fate of the EKODE family, these compounds must be synthesized in large quantity utilizing a method that will allow for stable isotope addition. The first target of interest is EKODE-Ib. This is due to the similarity of the structure to that of 4-HNE. This molecule will undergo 4 rounds of β-oxidation, leaving behind an α,β-unsaturated-4,5-epoxyaldehyde. This epoxy group could potentially hydrolyze to the

4-hydroxy moiety. This will then utilize the same enzymes and pathways that were discovered in the study on 4-HNE. Following synthesis of EKODE-Ib, the type II EKODEs would be synthesized in order to utilize a novel bifunctional ylide designed by a former member of the Tochtrop lab.

3.2 Results

3.2.1 Kinase activity assay

A functional activity assay was needed to guide the purification of the putative kinase from bulk protein. An assay to track the phosphorylation of γ-hydroxypentanoyl-CoA was developed by Chuan Shi. In order to run this assay, both γ-hydroxypentanoyl-CoA and $^{2}H_{9}$-pentanoyl-CoA needed to be synthesized. For the former, an enzymatic synthesis was developed. I began preparation with a small volume of pASK- IBA (3+) plasmid containing recombinant γ-hydroxypentanoyl-CoA transferase (GHP-CoAT) DNA (**Figure 11**).[21] I transformed this plasmid into DH5-α cells and utilized a maxiprep procedure to obtain large quantities of the plasmid. Sanger sequencing was used to ensure the plasmid remained viable.

Figure 11: Sanger sequencing results for GHP-CoAT DNA

This plasmid was then transformed into BL21-DE3 cells and grown on chloramphenicol/carbenicillin plates for selection. Colonies from the plates were grown in expression media and each sample was run on SDS-PAGE gel to find the colony with the highest expression. Multiple glycerol stocks of this bacterial strain were created and large scale expression of GHP-CoAT was performed. Purification of the protein on Strep-tacin column provided high purity transferase.

The substrates for this protein are acetyl-CoA and γ-hydroxypentanoic acid. Acetyl-CoA was prepared by nucleophilic attack of acetic anhydride by free coenzyme A.

γ-Hydroxypentanoic acid was prepared via base catalyzed hydrolysis of γ-valerolactone. Incubation of the substrates with GHP-CoAT allowed for transfer of the CoA moiety from acetyl-CoA to GHP-CoA.

In order to synthesize the $^{2}H_{9}$-pentanoic acid standard, I began with $^{2}H_{9}$-valeric acid. Dicyclohexylcarbodiimide coupling was used to make $^{2}H_{9}$-valeric anhydride. This was then attacked by free CoA to produce $^{2}H_{9}$-pentanoic acid.

To ensure the quality of the standard and the substrate, all materials were characterized via LC/MS/MS.

3.2.2 Enzyme isolation

A pig liver freshly obtained from a local farm was homogenized in a Krebs buffer with protease inhibitor cocktail. The soluble portion underwent ammonium sulfate precipitations at 15, 30, 45, and 60%. The total liver homogenate and the 4 precipitates were assayed for activity. The data is summarized in **Figure 12**. The fraction with the highest activity was the 15% ammonium sulfate precipitate and therefore it was the fraction that was chosen for further separation.

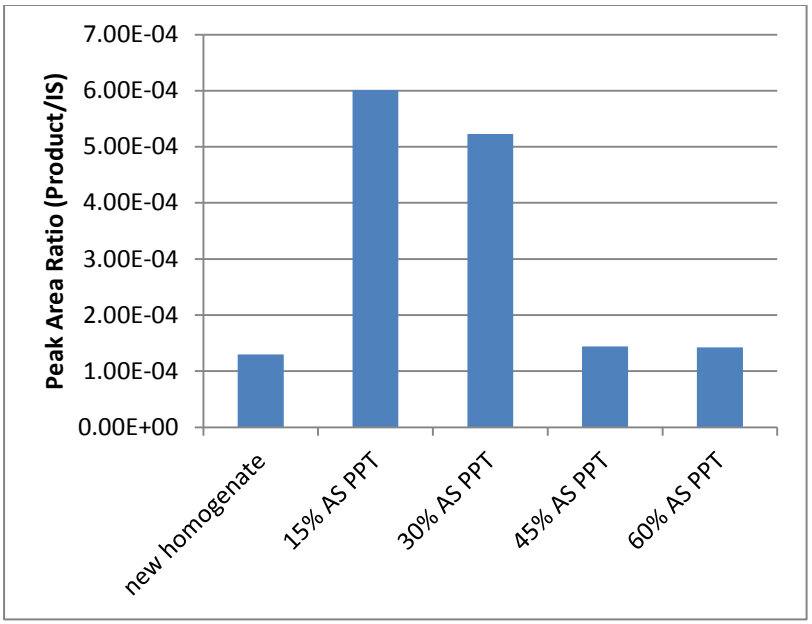

Figure 12: Activity assay of homogenate and precipitates

Protein separation was done on FPLC by successive separations utilizing different columns. First enzymes were separated by hydrophobicity utilizing a phenyl sepharose column. This was followed by a functional separation with a sepharose blue column. The sepharose backbone of this column is bound to a dye known as cibacron blue that binds kinases and dehydrogenases. This functional separation was followed by a Q sepharose based anion exchange column. An example chromatogram from an anion exchange column is shown in **Figure 13**.

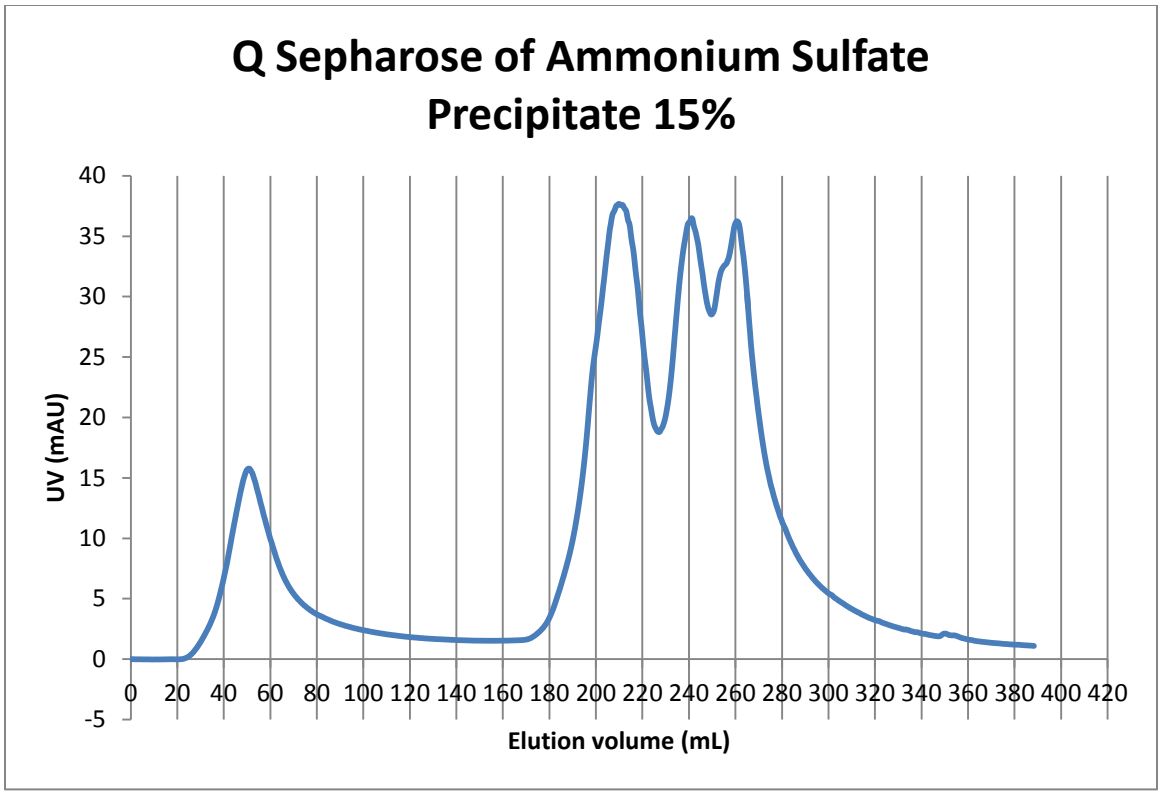

Figure 13: Separation of the 15% ammonium sulfate precipitate with anion exchange chromatography

Prior to checking the results of the final separation, the -80 °C freezer in which all protein and assay reagents were stored malfunctioned and all progress was lost. The time required to synthesize all reagent is significant, and the protein isolation would need to begin from bulk tissue. This led to a decision to focus efforts on the work described in **Chapter 4**.

3.2.3 Synthesis of EKODEs

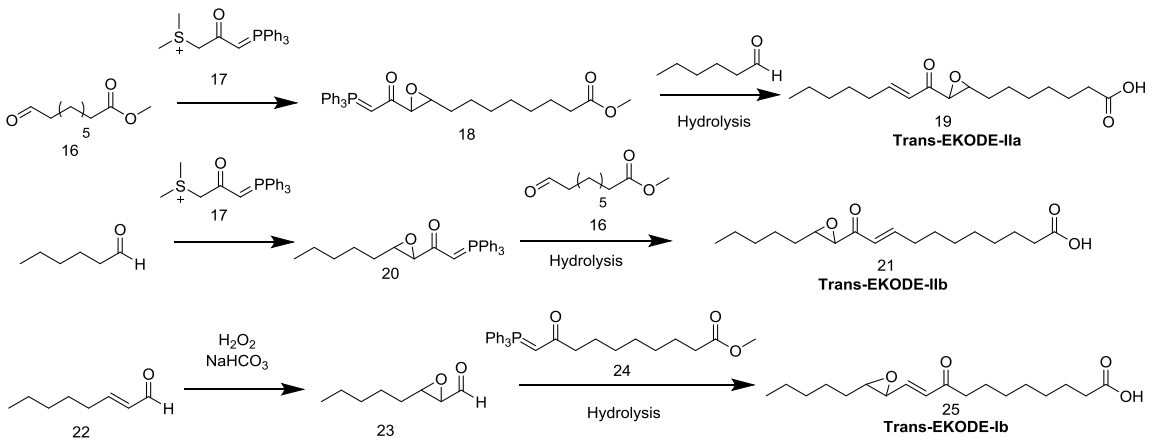

Scheme 4: Synthesis of EKODEs Ib, IIa, and IIb

In order to better understand the metabolism of the EKODE family of LPO products, synthetic standards of these molecules are required for isolated organ perfusion. To this end, I chose to synthesize trans-EKODE-IIa, IIb, and Ib **(Scheme 4).** The rationales for these choices were the following. The trans-EKODE-II series was chosen due to past work completed by Dr. Roozbeh Eskandari in which he developed a bifunctional conjugative ylide for the purpose of generating α,β-unsaturated epoxy ketones. This molecule would allow for rapid assembly of EKODE-IIa and IIb via Johnson-Corey-Chaikovski reaction with the sulfur ylide and Wittig reactions utilizing the phosphorus ylide. The trans-EKODE-Ib was chosen due to the similarity of its functionality to 4-HNE. Metabolism of fatty acids starts with the formation of a CoA ester from the carboxylic acid. This CoA ester undergoes the 4 step process of β-oxidation to shorten the chain by 2 carbons at a time, forming acetyl-CoA. Therefore, it is expected that Ib would begin with 4 rounds of β-oxidation, leaving the 4-epoxy-α,β-unsaturated-CoA ester. This moiety would be similar to the 4-hydroxy-α,β-unsaturated-CoA ester and could reasonably be expected to follow a similar metabolic pathway.

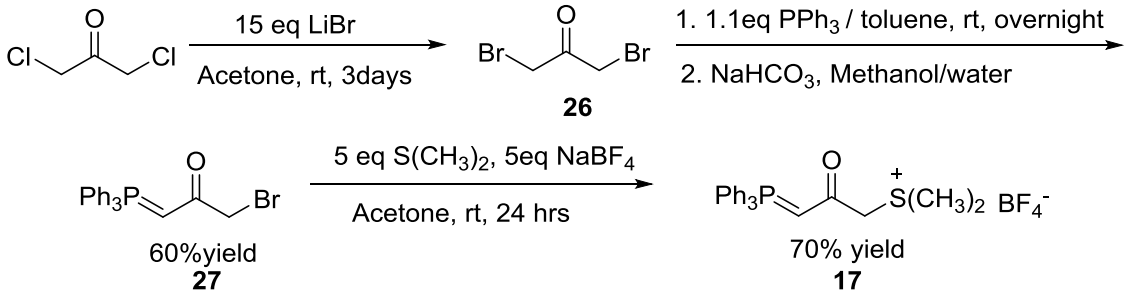

Scheme 5: Synthesis of bifunctional ylide

Scheme 5 shows the detailed synthesis of bifunctional ylide **17**. Commercially available 1,3-dichloroacetone undergoes halogen exchange to 1,3-dibromoacetone **26** when equilibrated in solution containing excess lithium bromide. A single bromine moiety can be exchanged with triphenylphosphine, and workup in basic solution provides the phosphonium ylide **27** in high yield. The final step is to incubate with an excess of dimethyl sulfide and sodium tetrafluoroborate to form the sulfonium ylide salt **17**. This provides the bifunctional sulfur/phosphorus ylide needed for the synthesis of both IIa and IIb. Additional reagents needed to finalize the synthesis are commercially available hexanal and non-commercially available ethyl 9-oxononanoate which must be synthesized as shown in **Scheme 6**.

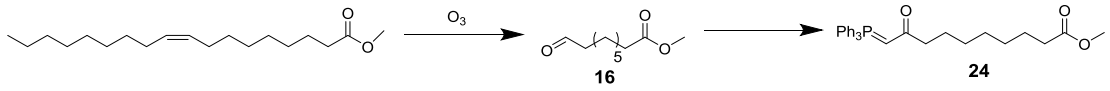

Scheme 6: Synthesis of 9-oxononanoate ester and decanoate ylide

The synthesis of the 9-oxononanoate was completed via ozonolysis of methyl oleate **(Scheme 6)**. A benefit of this method is the nonanoate can be utilized to synthesize decanoate ylide **24** required for the synthesis of EKODE-Ib. This is completed by

converting the aldehyde to an acid chloride and reacting with methyltriphenylphosphonium bromide.

With all required reagents in hand, the three EKODEs were synthesized as shown in **Scheme 4**. EKODE IIa **19** and IIb **21** were synthesized by Johnson-Corey-Chaykovsky reaction and subsequent Wittig reaction. **19** was prepared by first reacting **16** followed by a Wittig utilizing hexanal. **21** was then synthesized by beginning with hexanal and utilizing **16** for the Wittig reaction.

Trans-EKODE-Ib **25** was synthesized starting from

3.3 Conclusion

The first project discussed in this chapter involved the isolation of a kinase involved in the metabolism of 4-HNE. To this end, I was able to express and purify γ-hydroxypentanoyl-CoA transferase and utilize the enzyme to produce the substrate of the kinase activity assay. The synthesis of the $^{2}H_{9}$-pentanoyl-CoA standard was completed and an LC/MS/MS method for separation and analysis of the assay was developed. Protein was isolated from pig liver and separated via fast protein liquid chromatography. Progress on this project was destroyed when all assay reagents and protein was lost when the freezer in which they were stored failed.

In the second project concerning the EKODE family of molecules, EKODE-Ib, IIa, and IIb were synthesized in high enough quantity to serve as substrates for liver perfusion studies.

3.4 Experimental protocols

3.4.1 Materials and methods

See **2.41** for general materials and methods. The bacterial strains for expressing GHB-CoAT were generously provided by Dr. Wolfgang Buckel (Philipps-Universitat, Germany). DH5-α and BL21-DE3 were purchased from New England Biolabs.

Transformation of plasmid containing GHP-CoAT into DH5-α

100 μL of commercially available competent DH5-α cells (New England Biolabs) were aliquot into a chilled Eppendorf tube and thoroughly mixed. To the cells was added 100 ng of pASK-IBA(3+) plasmid containing GHP-CoAT DNA. The tube was mixed by flicking 5 times and chilled on ice for 30 minutes. The sample then underwent heat shock at 42 °C for 10 seconds. The cells were cooled on ice for 5 minutes. 950 μL of SOC media were added to the cells and the tube was placed in a 37 °C shaker for 1 hour at 250 rpm. The resulting cells were plated on selection plates containing 50 mg/L chloramphenicol and 50 mg/L carbenicillin and grown for 18 hours at 37 °C. A picked colony was grown in 200 mL of lb broth containing the previously mentioned antibiotic. The solution was grown overnight and centrifuged to provide a pellet for maxiprep. The resulting purified plasmid was analyzed via Sanger sequencing.

Transformation into BL21-DE3

50 μl of commercially available competent BL21-DE3 cells (New England Biolabs) were aliquot into a chilled Eppendorf tube and thoroughly stirred with a pipet tip. To the cells was added 100 ng of pASK-IBA(3+) plasmid containing GHP-CoAT DNA. The tube

was mixed by flicking 5 times and chilled on ice for 30 minutes. The sample then underwent heat shock at 42 °C for 10 seconds. The cells were cooled on ice for 5 minutes. 950 μl of SOC media were added to the cells and the tube was placed in a 37 °C shaker for 1 hour at 250 rpm. The resulting cells were plated on selection plates containing 50 mg/L chloramphenicol and 50 mg/L carbenicillin and grown for 18 hours at 37 °C.

Individual colonies grown from the selection plate were streaked onto separate plates to form a stock of each colony. A number of sterile tubes containing 10 mL of standard-I medium (15.6 g peptone, 2.8 g yeast extract, 5.6 g NaCl, 1 g dextrose, 1 L distilled water) were inoculated with bacteria from the different streak plates. Each sample was grown at 37 °C with shaking until the OD_{578} reached 0.5-0.6. At this time, a 1 mL sample of the culture was centrifuged and the resulting pellet was frozen for future analysis. The remaining culture was induced with 0.9 μL of anhydrotetracycline solution (2 mg/ mL). The culture was grown at room temperature for an additional 4 hours with an additional 1 mL sample of the culture taken and centrifuged at 2 hours. OD_{578} was monitored to ensure continued growth. Following the 4 hour incubation, the culture was centrifuged in 1 mL portions the pellets used for SDS gel analysis. The pre-induction, 2 hour, and 4 hour pellets were resuspended in 50 μL of Laemmli buffer and heated to 100 °C for 15 minutes. Samples were run on SDS gel and compared to find the clone with the highest expression for further purification.

Expression of GHB-CoAT

A 1 L flask of standard-I medium (15.6 g peptone, 2.8 g yeast extract, 5.6 g NaCl, 1 g dextrose, 1 L distilled water) was inoculated with a single colony of the GHP-CoAT

containing BL21 CodonPlus(DE3)-RIL *E. coli* identified in the previous step. The culture was grown for 16 hours to an OD_{578} of 2.02. A 1 mL sample of the culture was taken and pelleted for future analysis. Protein expression was induced with 100 μL of anhydrotetracycline (2 mg/ mL) solution for a total concentration of 400 μg per liter. The culture was grown at room temperature for an additional 4 hours with a sample taken for optical density at 2 hours (2.08) and 4 hours (2.11). This sample was spun down and the pellet collected for future analysis. Following the 4 hours incubation period, the liter culture was centrifuged at 16000 rpm for 15 minutes. The supernatant was discarded and the pellet was resuspended in 30 mL of wash buffer (100 mM Tris-Cl, 150 mM NaCl, 1 EDTA). The resuspended protein was subjected to sonication probe (setting 10, 5 x 3 minutes with 2 minute cooling in between) while submerged in an ice bath. The previous centrifugation step was repeated and the supernatant was loaded onto a Strep-tactin column (IBA-Lifesciences) pre-equilibrated with wash buffer. Following loading of the sample, the column was washed with 25 mL of wash buffer and the eluent was collected in 5 mL portions. The desired protein was then eluted out by switching to an elution buffer containing 2.5 mM desthiobiotin. 15 mL of elution buffer were eluted and collected in volumes of 3 mL, 9 mL, and 3 mL. The column was then regenerated utilizing a buffer containing 2-[4-hydroxy-benzeneazo]benzoic acid in order to displace the desthiobiotin. 200 μL of the wash and elution fractions were added to 100 μL of 2x Laemmli sample buffer and heated to 100 °C for 15 minutes. These samples were loaded onto an SDS gel for analysis.

3.4.2 Synthetic routes

γ-Hydroxypentanoic acid

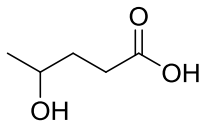

Due to the rapid formation of the lactone, γ -hydroxypentanoic acid must be prepared via base catalyzed hydrolysis from the commercially available γ -valerolactone. To a 10 mL solution of 0.1M NaOH was added 95 μL of γ-valerolactone (0.879 mmol). The mixture was heated to 60 °C for 3 hours and then cooled to room temperature. The solution was used without purification for the synthesis of the CoA salt.

Acetyl-CoA

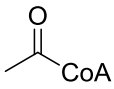

Acetyl-CoA was prepared chemically by nucleophilic attack of the anhydride. CoA trilithium salt (20 mg, 25.5 μmol) was added to a 10 mL round bottom flask. The salt was dissolved in 0.1 M $KHCO_3$ buffer (2 mL) and stirred at 4 °C. Acetic anhydride (40 μl) weas added to the solution and the mixture was stirred for 15 minutes at 4 °C. This solution was then used to synthesize GHP-CoA.

y-Hydroxypentanoyl-CoA

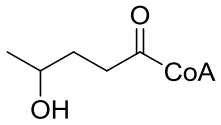

To the previous solution of acetyl-CoA was added 2 mL of KH_2PO_4 solution (125 mM, pH 7) and 2 mL of the GHP mixture from **2.45**. The solution was adjusted to pH 7 and 400 μL of GHP-CoAT from **3.44** was added and the solution was incubated at room temperature for 45 minutes. Following incubation, the solution was aliquoted into 500 μL portions and frozen at -80 °C. One aliquot was directly injected on an LCQ Deca ion trap MS/MS to find the ratio of GHP-CoA to Acetyl-CoA.

$^2H_9$-Pentanoic anhydride

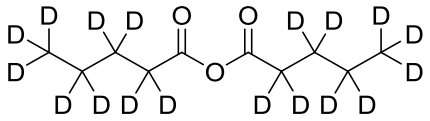

A 150 mL round bottom flask was charged with $^2H_9$-valeric acid (2.32 g, 20 mmol, 2 equiv) and diethyl ether (65 mL). To this stirring solution was added DCC (2.06 g, 10 mmol, 1 equiv). Reaction is occurring when white precipitation is noted. After 5 hours at room temperature, the solution was filtered and any residual ether was removed from the precipitate.

$^{2}H_9$-Pentanoyl-CoA

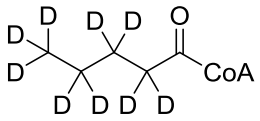

Free coenzyme A (12 mg) was dissolved in a solution of 0.1 M $KHCO_3$ (2 mL) and transferred to a 5 mL plastic falcon tube. 50 μL (~55 mg) of $^{2}H_9$-pentanoic anhydride was added to the solution and the reaction was vortexed at 4 °C. After reacting for 30 minutes at low temperature, the pH of the solution was brought to 2 using HCl. The crude product was purified via preparatory liquid chromatography and stored at -80 °C until use.

1,3-Dibromopropan-2-one (26)

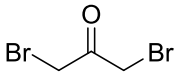

26

1,3-Dibromopropan-2-one **26** was prepared via a modified method adapted from literature.[22] An oven-dried 2 L round-bottomed equipped with a stir bar was charged with 1,3-dichloro-2-propanone (25 g, 196 mmol) in acetone (750 mL). Powdered lithium bromide (150 g, 1.73 mol) was added in 25 g portions via powder funnel. The reaction mixture was stirred at ambient temperature for 48 hours. Additional lithium bromide (100 g, 1.15 mol) and 250 mL acetone were added and stirred for an additional 24 hours. Evaporation of the solvent gave a white solid. The solid was dissolved in cold water (1 L) and transferred to a 2 L separatory funnel. The solution was extracted with methylene chloride (3 × 500 mL), and the combined organic phases were dried with anhydrous magnesium sulfate, filtered via vacuum filtration, and concentrated under reduced

pressure to give 42.1 g (99% crude yield) of the 1,3-dibromopropan-2-one as yellow syrup. Analysis of the crude by ^{1}H NMR indicates conversion was > 90%. Identity and purity of the product were confirmed by ^{1}H NMR. ^{1}H NMR (400 MHz, $CDCl_3$) δ 4.13; ^{13}C NMR (100 MHz, $CDCl_3$) δ 31.18, 194.13.

1-bromo-3-(triphenylphosphoranylidene)propan-2-one (27)

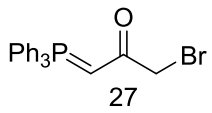

27

1-bromo-3-(triphenylphosphoranylidene)propan-2-one **27** was prepared via a modified method adapted from a literature synthesis of a 1-chloro analogue.[23] To an oven-dried 500- mL, two-necked round-bottomed flask containing a magnetic stirring bar equipped with an equalizing dropping funnel and an argon inlet was added triphenylphosphine (49.8 g, 190 mmol) in toluene (125 mL). The solution of crude 1,3-dibromopropan-2-one (41.0 g, 190 mmol) in toluene (125 mL) was added through the dropping funnel. Stirring continued overnight at ambient temperature. The white precipitate formed during the reaction was collected by filtration, washed with toluene, and concentrated under reduced pressure. To a stirred solution of dried precipitate in 60% aqueous methanol (800 mL) was added powdered sodium bicarbonate (42 g, 0.5 mol). Stirring continued for extra 30 minutes and more water (200 mL) was added to the mixture. After being stirred for another 30 minutes, the solid was collected by filtration and washed thoroughly with water. The solid was transferred to a 2 L separatory funnel charged with 1 L of cold water. The aqueous phase was extracted with methylene chloride (3 × 500 mL), and the

combined organic phases dried with anhydrous sodium sulfate and concentrated under reduced pressure to give 62.6 g (83% crude yield) of the 1-bromo-3-(triphenylphosphoranylidene)propan-2-one as white solid. Analysis of the crude by ^{1}H NMR indicates conversion was > 60% (contaminated with 1-chloro-3-(triphenylphosphoranylidene)propan-2-one). Identity and purity of the product were confirmed by ^{1}H and ^{13}C NMR. ^{1}H NMR (400 MHz, $CDCl_3$) δ 3.91 (d, 2H, $^{4}J_{HP}$ = 1.6), 4.26 (d, 1H, $^{2}J_{HP}$ = 24.0), 7.42-7.70 (15H,m) ; ^{13}C NMR (100 MHz, $CDCl_3$) δ 35.77 (d, $^{3}J_{CP}$ = 17.4 Hz), 52.67 (d, $^{1}J_{CP}$ = 109.0 Hz), 125.95 (d, $^{1}J_{CP}$ = 56 Hz, C-1'), 129.22 (d, $^{3}J_{CP}$ = 12.3 Hz, C-3') 132.65 (d, $^{4}J_{CP}$ = 2.8 Hz, C-4') 133.36 (d, $^{2}J_{CP}$ = 10.2 Hz, C-2'), 184.99 (d, $^{2}J_{CP}$ = 4.3 Hz)

Dimethyl(2-oxo-3-(triphenylphosphoranylidene)propyl)sulfonium tetrafluoroborate (17)

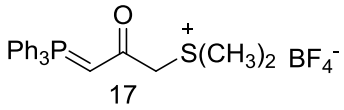

17

Dimethyl(2-oxo-3-(triphenylphosphoranylidene)propyl)sulfonium tetrafluoroborate was synthesized utilizing a procedure adapted from the synthesis of the bromide salt.[24] To an oven-dried 1 L, round-bottomed flask equipped with a magnetic stirring bar was added sodium tetrafluoroborate (27.5 g, 0.25 mol), methyl sulfide (15.5 g, 0.25 mol) , 1-bromo-3-(triphenylphosphoranylidene)propan-2-one (19.86 g, 50 mmol) and acetone (500 mL). The reaction mixture was stirred at room temperature for 48 hours. The resulting heterogeneous mixture was filtered via vacuum filtration. The solvent was removed from the filtrate via rotary evaporator. The resulting solid was purified by column

chromatography (DCM: MeOH/ 95:5) afforded 17.95 g (77% yield) of bifunctional conjunctive ylide as white solid. Identity and purity of the product were confirmed by ^{1}H and ^{13}C NMR. ^{1}H NMR (400 MHz, $CDCl_3$) δ 2.91 (s,6H), 4.16 (d, 1H, $^{2}J_{HP}$ = 21.2 Hz), 4.42 (s, 2H), 7.47-7.64 (15H,m) ; ^{13}C NMR (100 MHz, $CDCl_3$) δ 25.01, 52.43 (d, $^{3}J_{CP}$ = 20.5 Hz), 56.71 (d, $^{1}J_{CP}$ = 104 Hz), 125.20 (d, $^{1}J_{CP}$ = 90.8 Hz, C-1'), 129.45 (d, $^{3}J_{CP}$ = 12.4 Hz, C-3'), 133.09 (bs, C-4'), 133.21 (d, $^{2}J_{CP}$ = 10.3 Hz, C-2'), 177.06 (d, $^{2}J_{CP}$ = 4.0 Hz)

Methyl 9-oxononanoate (16)

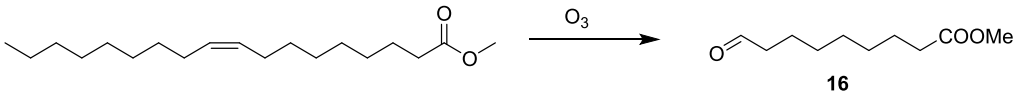

16

Methyl 9-oxononanoate was prepared via a method adapted from literature.[25] An oven-dried 0.5 L, two-necked, round-bottomed flask equipped with a stir bar was loaded with methyl oleate **1** (20.8 g, 70 mmol) in dichloromethane (250 mL), and methanol (100 mL). The flask was cooled to −78 °C in a container of dry ice and ozone was bubbled through the solution using a Pasteur pipet until a dark blue color appeared and persisted through several minutes. The solution was purged with argon gas until the color had dissipated and then the cold bath was removed. The ozonide was decomposed by adding glacial acetic acid (25 mL) in one portion, followed by powdered Zn (9 g, 0.14 mol) in small portions to control heat evolution. The mixture was stirred for half an hour and filtered through Celite to remove any unreacted zinc. Water (100 mL) was added to the solution in order to inhibit acetal formation. The solution was concentrated to roughly one-half initial volume *in vacuo* and slowly added to a saturated solution aqueous $NaHCO_3$ (150 mL). The mixture was extracted three times with CH_2Cl_2 (3 x 200 mL). The organic phases were dried over sodium sulfate and concentrated via rotary evaporator. The crude

product was distilled to produce nonanal (bp 41^{o}C, 0.6 Torr) and 9.82 (75% yield) of methyl 9-oxononanoate **2** as a colorless oil. (bp 103 ^{o}C/ 1 Torr) as a colorless oil. (lit. bp^{25} 105-108 ^{o}C/1 Torr)(*Caution: Ozone is highly toxic and can react explosively with numerous oxidizable materials.*) Identity and purity of the product were confirmed by ^{1}H NMR. ^{1}H NMR (400 MHz, $CDCl_3$) δ 1.28-1.36 (m, 6H) 1.58-1.66 (m, 4H), 2.42 (td, 2H, J = 7.2, 2.0 Hz), 3.66 (s, 3H), 9.76 (t, 3H, J = 2.0 Hz).

Methyl 9-oxo-10-(triphenyl-l5-phosphanylidene)decanoate (24)

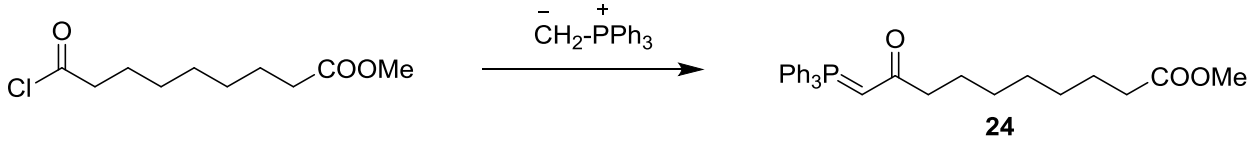

24

Methyl 9-oxo-10-(triphenyl-l5-phosphanylidene)decanoate (24) was prepared as described by Sayre et. al.[19] An oven-dried 100-mL two-necked round-bottomed flask equipped with a magnetic stirring bar was sealed under argon with two rubber septa, one of which contains a needle adapter to an argon-inlet. The flask was charged with methyltriphenyl-phosphonium bromide (3.66 g, 10.26 mmol) in THF (20 mL). The solution was cooled in a dry ice-acetone bath at -78 °C. Then *n*-butyllithium (2.20 mL, 2.33 M in hexane, 10.26 mmol) was added causing a red color to develop. The reaction mixture was continued stirring for 1 hour, whereupon methyl 9-chloro-9-oxononanoate (1.13 g, 5.13 mmol) was added dropwise slowly *via* syringe, the mixture was then allowed to stir at ambient temperature for 1 hour. The reaction mixture was quenched with aqueous saturated NH_4Cl (10 mL) and THF was removed by rotary evaporator. This resulted in viscous oil. The oil was extracted with EtOAc (3 × 20 mL) and washed with

NaOH (2 N, 100 mL).The combined organic phases were dried with anhydrous magnesium sulfate and concentrated under reduced pressure to afford methyl 9-oxo-10-(triphenyl-l5-phosphanylidene)decanoate **10** as a brown oil (2.5 g, 53%). This product was used as crude for next step in Wittig reaction.

Methyl 8-(3-(2-(triphenyl-l5-phosphaneylidene)acetyl)oxiran-2-yl)octanoate (18)

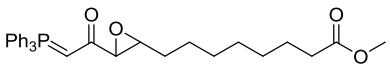

18

An oven-dried two neck round-bottom flask was equipped with a stirbar and sealed under argon. The flask was cooled to −30 °C in a dry ice-ethanol bath. To the flask was added sodium hydride (80 mg, 2 mmol, 60% in mineral oil), methyl 9-oxononanoate **16** (0.37 g, 2 mmol), bifunctional ylide **17** (0.93 g, 2 mmol), and acetonitrile (30 mL). The resulting solution was stirred for 3 hours while allowed to warm to room temperature. Following the reaction period, the mixture was neutralized with saturated NH_4Cl (20 mL). The aqueous solution was extracted with ethyl acetate (3 × 20 mL) and dried with anhydrous sodium sulfate. Evaporating the solvent resulted in a crude oil that was purified with column chromatography (DCM/MeOH 98:2) to afford **18** as yellow oil (561 mg, 56% yield). Identity and purity of the product were confirmed by ^{1}H and ^{13}C NMR. ^{1}H NMR (400 MHz, $CDCl_3$) δ 1.20-1.79 (m, 12H), 2.28 (t, 2H, J = 7.6 Hz), 3.05 (bm, 1H), 3.14 (t, 1H, J = 2 Hz), 3.65 (s, 3H), 3.94 (d, 1H, $^{2}J_{HP}$ = 25.6 Hz), 7.41-7.71 (m, 15H); ^{13}C NMR (100MHz, $CDCl_3$) δ 25.03, 26.11, 29.18, 29.26, 29.30, 32.23, 34.19, 48.26 (d, 1H, $^{1}J_{CP}$ = 98 Hz), 51.58, 59.90, 60.04(d, J = 17 Hz), 126.56 (d, $^{1}J_{CP}$ = 91 Hz, C-1'), 129.05 (d, $^{3}J_{CP}$

= 12.3 Hz, C-3'), 132.40 (d, $^4J_{CP}$ = 2.7 Hz, C-4'), 133.17 (d, $^2J_{CP}$ = 10.3 Hz, C-2'), 174.40, 188.11 (d, $^2J_{CP}$ = 4.0 Hz).

1-(3-Pentyloxiran-2-yl)-2-(triphenyl-l5-phosphaneylidene)ethan-1-one (20)

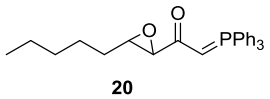

20

The Johnson-Corey-Chaykovsky reaction to produce **20** was performed as described for compound **18** with the exception of replacing aldehyde **16** for commercially available hexanal. Product was isolated as yellow oil (650 mg, 78% yield). ^{1}H NMR (500 MHz, $CDCl_3$) δ 0.88 (t, 3H, J = 6.5 Hz), 1.22-1.82 (m, 8H), 3.05 (bm, 1H), 3.13 (t, 1H, J = 2.0 Hz), 3.94 (d, 1H, $^2J_{HP}$= 24 Hz), 7.35-7.73 (m, 15H) , ^{13}C NMR (125 MHz, $CDCl_3$) δ14.24, 22.80, 25.95, 31.82, 32.35, 48.86 (d, $^1J_{CP}$ = 110 Hz) , 60.07, 60.17 (d, J = 16.6 Hz), 126.36 (d, $^1J_{CP}$ = 90.6 Hz, C-1'), 129.15 (d, $^3J_{CP}$ = 12.3 Hz, C-3'), 132.49 (d, $^4J_{CP}$ = 2.8 Hz, C-4'), 133.31 (d, $^2J_{CP}$ = 10.2 Hz, C-2'), 188.31 (d, $^2J_{CP}$ = 3.5 Hz).

(E)-7-(3-(Oct-2-enoyl)oxiran-2-yl)heptanoic acid (19)

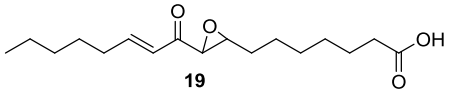

19

An oven-dried round bottom flask was equipped with a stirbar and charged with product **18** (500 mg, 1 mmol) dissolved in toluene (10 mL). To this solution was added commercially available hexanal (100 mg, 1 mmol). The mixture was brought to reflux and left to stir at reflux overnight. The solution was then cooled to room temperature and toluene was removed via rotary evaporator. Intermediate was purified via column chromatography (Hexane/Et_2O 85:15). A portion of the intermediate (31 mg, .1 mmol)

was added to a 25 mL round-bottom flask with stirbar. The intermediate was dissolved in acetone (1 mL) and phosphate buffer (pH 7, 5 mL, 0.2M). To the stirring solution was added lipase from porcine pancreas, type II (220 mg, Sigma Aldrich). The mixture was stirred at room temperature for 4 hours before filtering the enzyme through a pad of Celite. The Celite cake was rinsed with EtOAc (15 mL) and the organic phase was separated from the aqueous phase. The organic phase was dried under reduced pressure and purified by column chromatography (Hexane/ethyl acetate 1:1) to afford **19** as a light yellow oil (142 mg, 91.6% yield). ^{1}H NMR (500 MHz, $CDCl_3$) δ 0.89 (t, 3H, J = 7.0 Hz), 1.21-1.74 (m, 18H), 2.17-2.24 (m, 2H), 2.34 (t, 2H, J = 7.0 Hz), 3.04 (ddd, 1H, J = 6.0, 5.0, 2.0 Hz), 3.33 (d, 1H, J = 2.0 Hz), 6.23 (dt, 1H, J = 15.5, 1.5 Hz), 7.07 (1H, dt, J = 15.5, 7.0 Hz); ^{13}C NMR (125 MHz, $CDCl_3$) δ 14.27, 22.73, 24.91, 26.08, 27.94, 29.20, 29.36, 29.38, 31.68, 32.11, 33.06, 34.25, 58.66, 59.33, 124.26, 151.06, 179.81. 196.08

(E)-11-Oxo-11-(3-pentyloxiran-2-yl)undec-9-enoic acid (21)

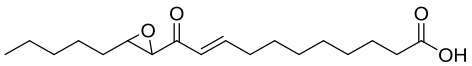

21

The Wittig reaction and enzymatic hydrolysis to produce **21** was performed as described for compound **19** with the exception of replacing product **18** for synthesized product **20**. Product was isolated as yellow oil (125 mg, 80% yield). ^{1}H NMR (400 MHz, $CDCl_3$) δ 0.88 (t, 3H, J = 7.2 Hz), 1.17-1.67 (m, 18H), 2.21 (dq, 2H, J = 6.8, 1.6 Hz), 2.33 (t, 2H, J = 7.6 Hz), 3.05 (ddd, 1H, J = 6.0, 5.0, 2.0 Hz), 3.34 (d, 1H, J = 2.0 Hz), 6.25 (dt, 1H, J = 15.5, 1.5 Hz), 7.06 (1H, dt, J = 15.5, 7.0 Hz); ^{13}C NMR (100 MHz, $CDCl_3$) δ 14.28,

22.84, 24.93, 25.83, 28.20, 29.22, 29.30 (2C), 31.77, 32.14, 33.04, 34.20, 58.74, 59.40, 124.32, 150.76, 179.44, 196.09.

3-Pentyloxirane-2-carbaldehyde (23)

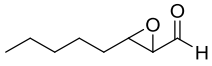

23

3-Pentyloxirane-2-carbaldehyde (23) was prepared as described by Sayre et. al.[19] To an oven-dried round bottom flask with stirbar was added commercially available E-oct-2-enal (714 mg, 5.66 mmol) in methanol (15 mL). The reaction was cooled to 0°C in an ice bath and $NaHCO_3$ (570 mg, 6.78 mmol) was added. H_2O_2 (1.7 mL, 16.7 mmol, 30% solution) was added dropwise over a period of 5 minutes. The mixture was stirred at room temperature for 1.5 hours. The heterogeneous mixture was cooled via ice bath and excess peroxide was neutralized with saterated sodium thiosulfate (2 mL dropwise). The organic solvent was removed under reduced pressure and the aqueous phase was extracted with ethyl acetate (3 × 10 mL). The ethyl acetate was dried with magnesium sulfate and concentrated. The product was purified by column chromatography (hexane/Et_2O 3:1) to afford **23** (510 mg, 63%) as yellow oil. ^1H NMR (400 MHz, $CDCl_3$) δ 0.89 (t, 3H, J = 7.2 Hz), 1.27-1.70 (m, 8H), 3.13 (dd, 1H, J = 6.4, 2.0 Hz), 3.21-3.24 (m, 1H), 9.01 (d, 1H, J = 6.4 Hz).

(E)-9-oxo-11-(3-pentyloxiran-2-yl)undec-10-enoic acid (25)

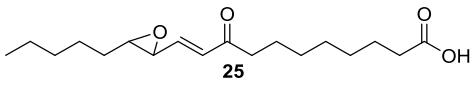

25

The Wittig reaction and enzymatic hydrolysis to produce **25** was performed as described for compound **19** with the exception of utilizing **23** as the aldehyde and **18** as the Wittig reagent. Product was isolated as yellow solid (270 mg, 87% yield). ^{1}H NMR (500 MHz, $CDCl_3$) δ 0.89 (t, 3H, J = 7.0 Hz), 1.24-1.67 (m, 18H), 2.34 (t, 2H, J = 7.5 Hz), 2.53 (td, 1H, J = 7.0, 2.0 Hz), 2.91 (td, 1H, J = 7.0, 2.0 Hz), 3.21 (dd, 1H, J = 7.0, 2.0 Hz), 6.42(d, 1H, J = 15.5 Hz), 7.06(dd, 1H, J = 16.0, 7.0 Hz); ^{13}C NMR (125 MHz, $CDCl_3$) δ 14.40, 22.87, 24.23, 24.92, 25.83, 29.16, 29.31(2C), 31.85, 32.23, 34.14, 40.86, 57.02, 62.00, 131.17, 142.93, 179.18, 200.04.

3.5 Acknowledgement

The assay utilized for the isolation of the 4-hydroxyacyl-CoA kinase was originally designed by Dr. Chuan Shi. The bifunctional ylide and use in synthesis of EKODEs designed by Dr. Roozbeh Eskandari. Manuscript for EKODE work by R. Eskandari and J. Hess in preparation.

3.6 References

1. Burr, GO. Burr, M. On the nature and role of the fatty acids essential in nutrition. *Biol. Chem.* **86,** 587–621 (1930).

2. Deckelbaum, R. J. & Torrejon, C. The Omega-3 Fatty Acid Nutritional Landscape: Health Benefits and Sources. *J. Nutr.* **142,** 587S–591S (2012).

3. Zhou, L. & Nilsson, A. Sources of eicosanoid precursor fatty acid pools in tissues. *J. Lipid Res.* **42,** 1521–42 (2001).

4. Halliwell, B. & Chirico, S. Lipid peroxidation: its mechanism, measurement, and significance. *Am. J. Clin. Nutr.* **57,** 715S–725S (1993).

5. Sayre, L. M., Lin, D., Yuan, Q., Zhu, X. & Tang, X. Protein Adducts Generated from Products of Lipid Oxidation: Focus on HNE and ONE. *Drug Metab. Rev.* **38,** 651–675 (2006).

6. Łuczaj, W., Gęgotek, A. & Skrzydlewska, E. Antioxidants and HNE in redox homeostasis. *Free Radic. Biol. Med.* **111,** 87–101 (2017).

7. Anavi, S., Ni, Z., Tirosh, O. & Fedorova, M. Steatosis-induced proteins adducts with lipid peroxidation products and nuclear electrophilic stress in hepatocytes. *Redox Biol.* **4,** 158–168 (2015).

8. Barrera, G. *et al.* Role of 4-Hydroxynonenal-Protein Adducts in Human Diseases. *Antioxid. Redox Signal.* **22,** 1681–1702 (2015).

9. Valko, M. *et al.* Free radicals and antioxidants in normal physiological functions and human disease. *Int. J. Biochem. Cell Biol.* **39,** 44–84 (2007).

10. Singh, S. P. *et al.* Mutagenic Effects of 4-Hydroxynonenal Triacetate, a Chemically Protected Form of the Lipid Peroxidation Product 4-Hydroxynonenal, as Assayed in L5178Y/ Tk + / – Mouse Lymphoma Cells. *J. Pharmacol. Exp. Ther.* **313,** 855–861 (2005).

11. Skrzydlewska, Elżbieta; Agnieszka, G. Biological effect of protein modifications by lipid peroxidation products. *Chem. Phys. Lipids* **221,** 46–52 (2019).

12. Ji, C., Kozak, K. R. & Marnett, L. J. IκB Kinase, a Molecular Target for Inhibition by 4-Hydroxy-2-nonenal. *J. Biol. Chem.* **276,** 18223–18228 (2001).

13. Mali, V. R. & Palaniyandi, S. S. Regulation and therapeutic strategies of 4-hydroxy-2-nonenal metabolism in heart disease. *Free Radic. Res.* **48,** 251–263 (2014).

14. Buizza, L. *et al.* Conformational altered p53 affects neuronal function: relevance for the response to toxic insult and growth-associated protein 43 expression. *Cell Death Dis.* **4,** e484–e484 (2013).

15. Kruiswijk, F., Labuschagne, C. F. & Vousden, K. H. p53 in survival, death and metabolic health: a lifeguard with a licence to kill. *Nat. Rev. Mol. Cell Biol.* **16,** 393–405 (2015).

16. Ishikawa, T., Esterbauer, H. & Sies, H. Role of cardiac glutathione transferase and of the glutathione S-conjugate export system in biotransformation of 4-hydroxynonenal in the heart. *J. Biol. Chem.* **261,** 1576–81 (1986).

17. Zhang, G.-F. *et al.* Catabolism of 4-Hydroxyacids and 4-Hydroxynonenal via 4-Hydroxy-4-phosphoacyl-CoAs. *J. Biol. Chem.* **284,** 33521–33534 (2009).

18. Sadhukhan, S., Han, Y., Zhang, G. F., Brunengraber, H. & Tochtrop, G. P. Using isotopic tools to dissect and quantitate parallel metabolic pathways. *J. Am. Chem. Soc.* **132,** 6309–6311 (2010).

19. Lin, D., Zhang, J. & Sayre, L. M. Synthesis of six epoxyketooctadecenoic acid (EKODE) isomers, their generation from nonenzymatic oxidation of linoleic acid, and their reactivity with imidazole nucleophiles. *J. Org. Chem.* **72,** 9471–9480 (2007).

20. Zhu, X., Tang, X., Anderson, V. E. & Sayre, L. M. Mass Spectrometric Characterization of Protein Modification by the Products of Nonenzymatic Oxidation of Linoleic Acid. *Chem. Res. Toxicol.* **22,** 1386–1397 (2009).

21. Macieira, S., Zhang, J., Velarde, M., Buckel, W. & Messerschmidt, A. Crystal structure of 4-hydroxybutyrate CoA-transferase from Clostridium aminobutyricum. *Biol. Chem.* **390,** (2009).

22. Catch, J. R., Elliott, D. F., Hey, D. H. & Jones, E. R. H. 66. Halogenated ketones. Part I. The bromination of acetone and methyl ethyl ketone. *J. Chem. Soc.* 272–275 (1948).

23. Hudson, R. F. & Chopard, P. A. The Preparation of Chloromethyl Vinyl Ketones. *J. Org. Chem.* **28,** 2446–2447 (1963).

24. Serrano, E. *et al.* Experimental and computational study of the bonding properties of mixed bis-ylides of phosphorus and sulfur. *Inorg. Chem.* **48,** 6823–6834 (2009).

25. Sun, M., Deng, Y., Batyreva, E., Sha, W. & Salomon, R. G. Novel bioactive phospholipids: Practical total syntheses of products from the oxidation of arachidonic and linoleic esters of 2-lysophosphatidylcholine. *J. Org. Chem.* **67,** 3575–3584 (2002).

CHAPTER 4

SYNTHESIS AND ANALYSIS OF 2-(AMINOMETHYL)MALONATE: A NOVEL β–ALANINE DERIVED METABOLITE

4.1 Introduction

4.1.1 Metabolism of 4-hydroxyacids

The discovery of 2-(aminomethyl)malonate began as an intersection of two projects from the Tochtrop and Brunengraber laboratories. The Tochtrop lab's work on 4-hydroxyacids[1,2] fostered an interest in understanding the metabolism of γ-hydroxybutyrate,[3,4] (GHB) the simplest 4-hydroxyacid. This molecule is of particular interest due not only to its potential for therapeutic uses as treatment for both narcolepsy[5] and alcoholism,[6] but also due to the notoriety it has gained due to its role as an elicit molecule termed the "date rape drug".

The accepted catabolic fate of GHB was conversion to succinic semialdehyde and entrance into the citric acid cycle.[7–9] A study completed with isotopically labeled GHB not only showed that this route only accounted for 8% of the total catabolic flux of GHB, but also elucidated two novel pathways where GHB is catabolized to acetyl-CoA and formate through a 3-hydroxypropionate intermediate.[3]

4.1.2 Metabolism of 3-hydroxypropionate

The importance of 3-hydroxypropionate was also noted by our collaborators in the Brunengraber lab. One focus of their lab is the study of propionic acidemia, an inborn error of metabolism in which an individual is unable to produce functional propionyl-CoA carboxylase. Without this enzyme, the endogenous propionyl-CoA formed from the metabolism of isoleucine, valine, methionine, threonine, and odd chain fatty acids is unable to be catabolized and will build up in the body.[10] This perturbs the entire metabolic system and the body is forced to compensate by catabolizing through different

pathways. In the case of propionic acidemia, this leads to an increase in multiple other biological molecules, one of which is 3-hydroxypropionate.[11]

Metabolic data from both laboratories intersected at the molecule 3-hydroxypropionate. For this reason, a project was designed to discover the catabolic fate of this metabolite. One notable result from the perfusion of a rat liver with 3-hydroxypropionate was that a large increase in β-alanine concentration was noted.[12] We theorized that β-alanine was a byproduct caused by transamination of malonic semialdehyde, the intermediate molecule in the pathway that catabolizes 3-hydroxypropionate to acetyl-CoA. When the experiment was repeated utilizing M3 labeled 3-hydroxypropionate, the molecular isotope distribution showed a heavy increase in M3 labeled β-alanine, confirming the hypothesis.

4.1.3 Metabolism of β-alanine

β-Alanine, or 3-aminopropanoic acid, is an uncommon amino acid that is differentiated from its common counterpart alanine by shifting the amino group from the 2-position to the 3-position. Although a small amount of β-alanine is made available in the liver through the degradation of uracil[13] and the aforementioned formation from 3-hydroxypropionate, the bulk of human β-alanine is obtained through diet. It is predominantly absorbed as carnosine from animal sources.[14] A diet containing meat or fish provides roughly 300 mg of β-alanine per day.

The canonical role of β-alanine is formation of dipeptides with histidine known as carnosine (β-alanyl-l-histidine) and anserine (β-alanyl-l-methylhistidine). These

biomolecules are found in high concentration in muscle tissue and have been demonstrated to act as physiological pH buffers.[15] They can counteract the buildup of lactic acid formed during strenuous exercise. The limiting reagent for the formation of these peptides is β-alanine. Increasing concentration of plasma β-alanine has been demonstrated to increase carnosine and anserine levels in multiple types of muscle tissue.[13] This has led to an increase of supplementation among athletes and military personnel. The common belief is that by increasing β-alanine, and therefore its dipeptides, they can neutralize lactic acid buildup and therefore push their workouts further than they would be able to otherwise.

Studies have shown that β-alanine supplementation increases the concentration of available carnosine and anserine. However, the increase in pH buffering dipeptides has not shown any notable increase in physical capability or endurance. Despite this, it remains a popular recommendation to bodybuilders. One reported detrimental effect of β-alanine supplementation is paresthesia, a type of pain that is typically referred to as a "pins and needles" feeling.[16,17] This effect occurs at high doses and the mechanism by which β-alanine causes this effect is currently unknown. It has been hypothesized that the similarity in chemical structure between common neurotransmitters and β-alanine suggests that it either acts as a neurotransmitter or interferes with neurotransmission.

Our collaborators in the Brunengraber lab conducted a study to determine the reversibility of the pathway of β-alanine formation from 3-hydroxypropionate. During this study, they found an increased concentration of an unknown compound with a mass to charge ratio 44 higher than β-alanine. A +44 *m/z* is typically associated with

carboxylation. The only characterized compound that fits this motif is aspartate, a common amino acid whose structure is similar to β-alanine with a carboxylic acid attached to the 3 position. However, a +44 *m/z* peak with the known fragmentation pattern of aspartate occurs concurrently with the unknown peak. This led them to hypothesize the existence of 2-(aminomethyl)malonate (AMM), a neurotransmitter-like compound that has no published synthesis or characterization.

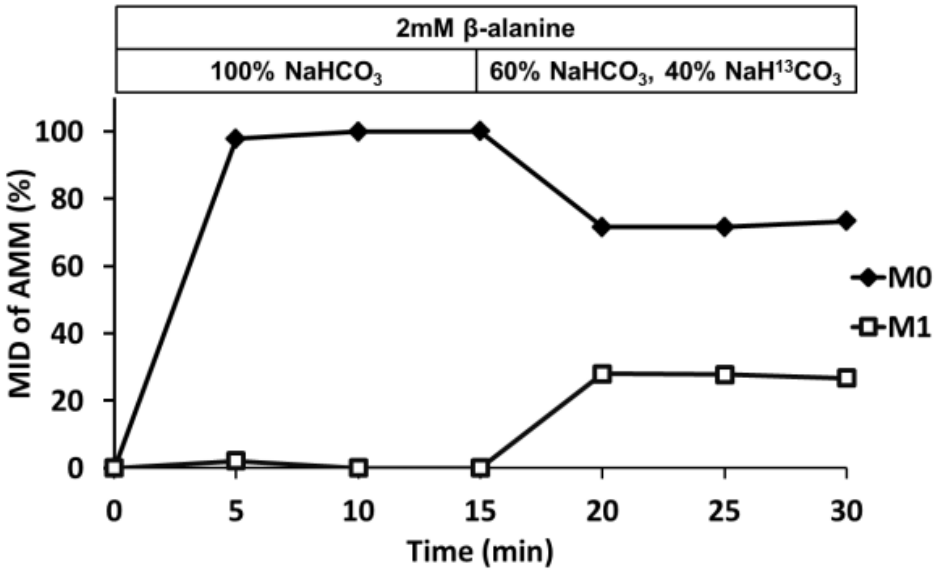

Figure 14: Dependence of AMM isotope distribution on carbonate source*

In order to prove that this molecule is formed from carboxylation of β-alanine, we tracked the concentration of this molecule when β-alanine was perfused in a buffer containing unlabeled $NaHCO_3$ **(Figure 14)**. After 15 minutes had passed, the perfusion buffer was swapped with one containing 30% ^{13}C labeled $NaHCO_3$. Almost immediately, the molecule produced from β-alanine was found at 30% [$^{13}C_1$] labeled. This demonstrates that the molecule in question is formed from the carboxylation of β-alanine.

In order to prove the identity of our unknown and determine the role of this molecule in human metabolism, a standard must be synthesized and compared to the experimental results.

4.2 Experimental results

4.2.1 Synthesis of AMM

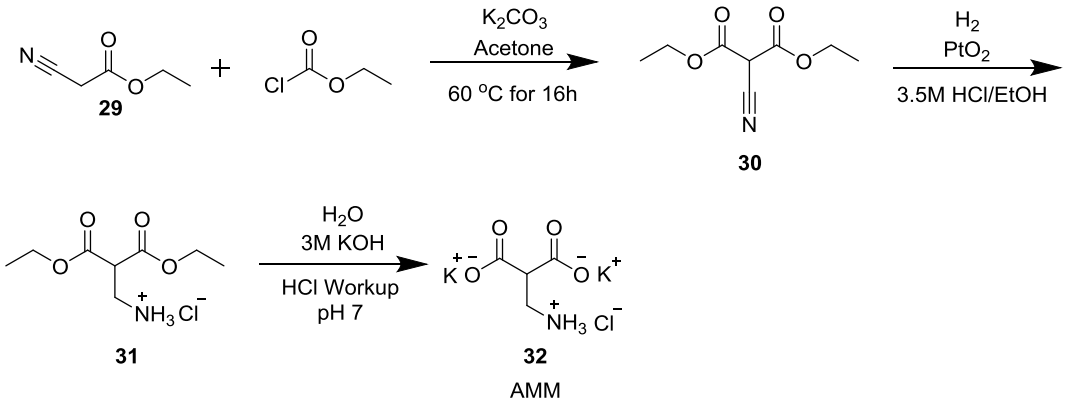

Scheme 7: Synthesis of 2-(aminomethyl)malonate

2-(Aminomethyl)malonate was synthesized starting from commercially available ethyl cyanoacetate. The ethyl cyanoacetate was reacted with ethyl chloroformate to form diethyl 2-cyanomalonate. One benefit of this reaction is that it can be easily purified by vacuum distillation. This allows for rapid preparation of large quantities of the stable intermediate.

The hydrogenation step was attempted with a variety of conditions. The most common hydrogenation catalyst is 10% by weight Pd/C at 1 atm of pressure. No reaction was noted under these conditions. Increasing these conditions up to 250 psi H_2 still showed no

yield. Many other palladium and platinum based catalysts were utilized to no effect. The only condition found that allowed for hydrogenation of the nitrile was PtO_2 in 3.5 M HCl/EtOH. The reaction was completed in a Parr vessel at 250 psi H_2.

The final hydrolysis step proved to be more difficult than imagined. In a similar manner to many malonates, the molecule is prone to decarboxylation under a number of conditions. Many attempts to isolate the final product led to only β-alanine remaining in solution. Utilizing a high vacuum to remove solvent led to spontaneous decarboxylation. However, it was found that crashing the salt out of the aqueous solution with acetone provided the desired product with 49% overall yield as a white solid.

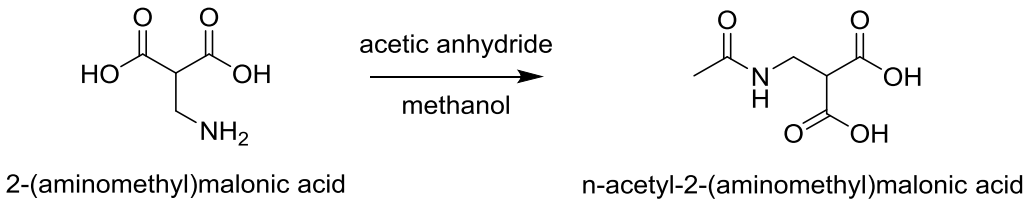

Scheme 8: Synthesis of *N*-acetyl-2-(aminomethyl)malonate

One important role of aspartate in human physiology is incorporation in the brain as N-acetylaspartatic acid (NAA). This molecule is the second most prevalent compound in the adult human brain. Therefore, it seems probable that AMM may also exist *in vivo* as an acetylated derivative. To prepare for investigating this possibility, N-acetyl (aminomethyl)malonate was also prepared from AMM and acetic anhydride **(Scheme 8)**.

4.2.2 Synthesis of isotopically labeled AMM

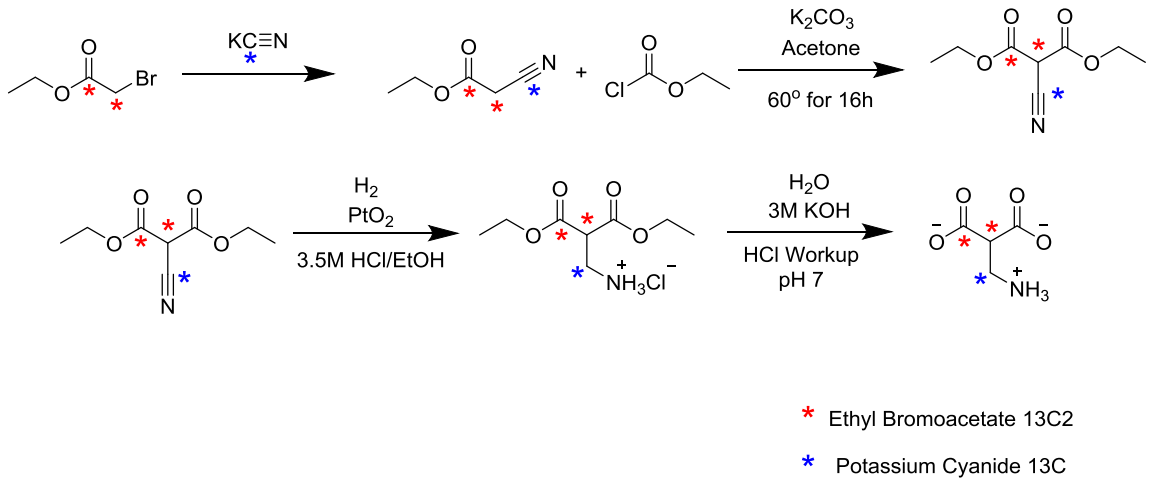

Scheme 9: Synthesis of isotopically labeled M1, M2, M3 2-(aminomethyl)malonate

A synthetic scheme was devised that would incorporate one to three ^{13}C atoms per molecule of AMM. This is accomplished by beginning with ethyl bromoacetate and synthesizing the ethyl cyanoacetate needed for the first reaction. By using labeled potassium cyanide and/or labeled ethyl bromoacetate, one can generate ethyl cyanoacetate with up to three ^{13}C atoms **(Scheme 9)**. The ability to vary the labeling scheme could prove useful for later studies to determine the metabolism of AMM.

4.2.3 LC/MS/MS characterization of AMM and separation from aspartate

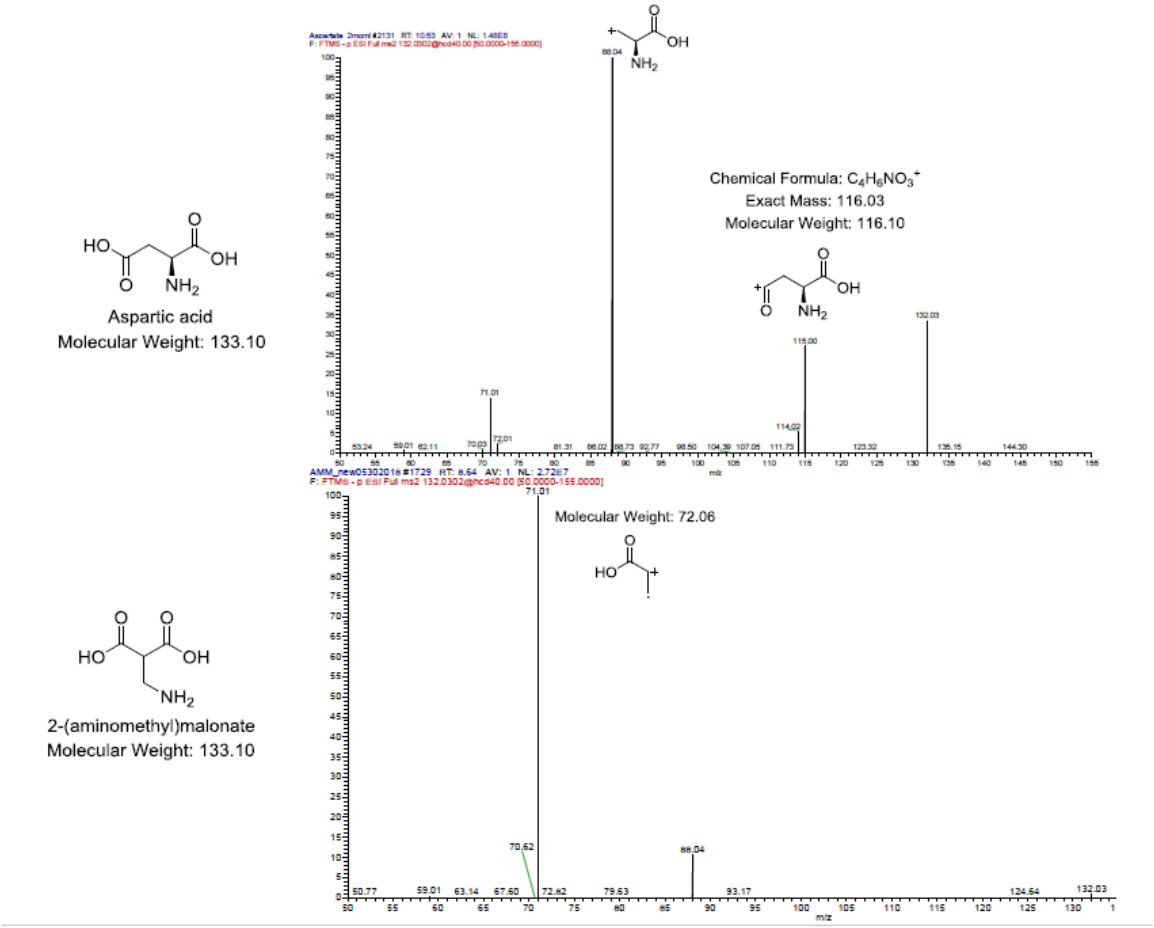

Figure 15: Tandem mass spectroscopy of aspartate and AMM

Tandem mass spectroscopy of the synthesized AMM was done to both characterize the molecule as well as prove the differences between AMM and its isomer aspartate **(Figure 15)**. Using a zwitterionic column, these two similar isomers were able to be separated by liquid chromatography. What was found is a great difference in fragmentation pattern between the two that could be utilized to both differentiate the molecules and help find an enhanced method of quantifying the concentration of AMM.

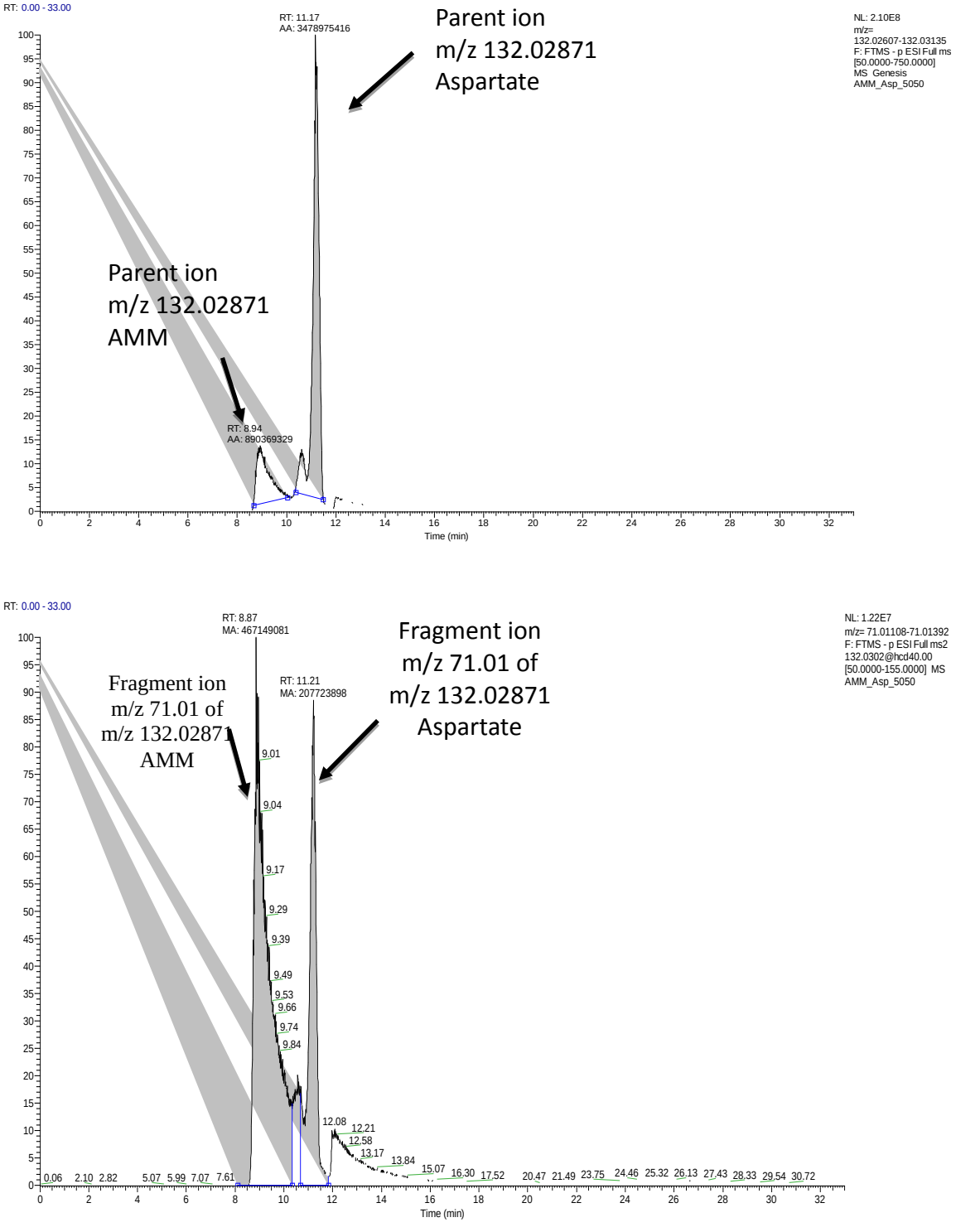

Figure 16: Use of tandem mass spectroscopy to increase AMM signal

The major difference in fragmentation pattern between AMM and aspartate relies on the 71.01 *m/z* fragment. This fragment is the major ion formed from the ionization of AMM, while only constituting a minor amount of aspartate. By running tandem mass spectrometry, the AMM signal can be enhanced more than the aspartate signal by directly monitoring for this 71.01 fragment **(Figure 16)**.

4.2.4 Confirmation of identity of AMM and N-acetyl AMM

In order to confirm that AMM matches the hypothetical peak found in the original assays, we must run the synthetic AMM through the same conditions utilized in the assay and ensure that the retention time and fragmentation pattern match. The synthesized AMM was prepared for assay by GC/MS by suspending the dried powder in TBDMSCl and heating at 70 °C for 45 minutes. This causes the carboxylic acids to form silyl esters. Following injection into the GCMS, the retention time and labeling pattern of the compound were found to match those of the +44*m/z* unknown **(Figure 17)**. AMM is distinct from aspartate, its isomer, through both retention time and fragmentation.

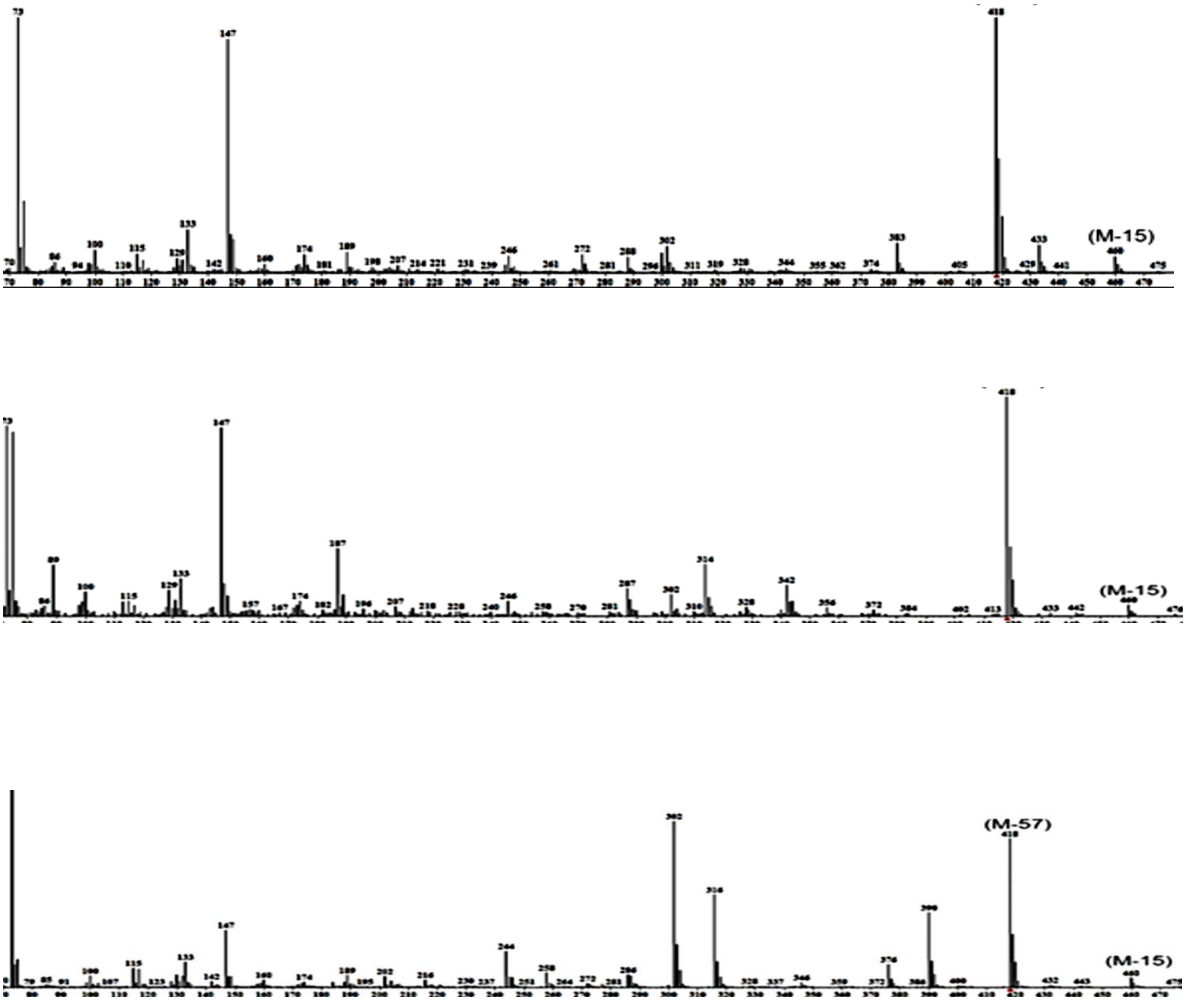

Figure 17: Mass spectra of unknown +44 *m/z* ion, synthesized AMM, and aspartate

The same protocol was utilized to check the integrity of the synthesized N-acetyl AMM. Much like the non-acetylated version, N-acetyl AMM is differentiable from N-acetyl aspartate by both retention time as well as fragmentation pattern **(Figure 18)**.

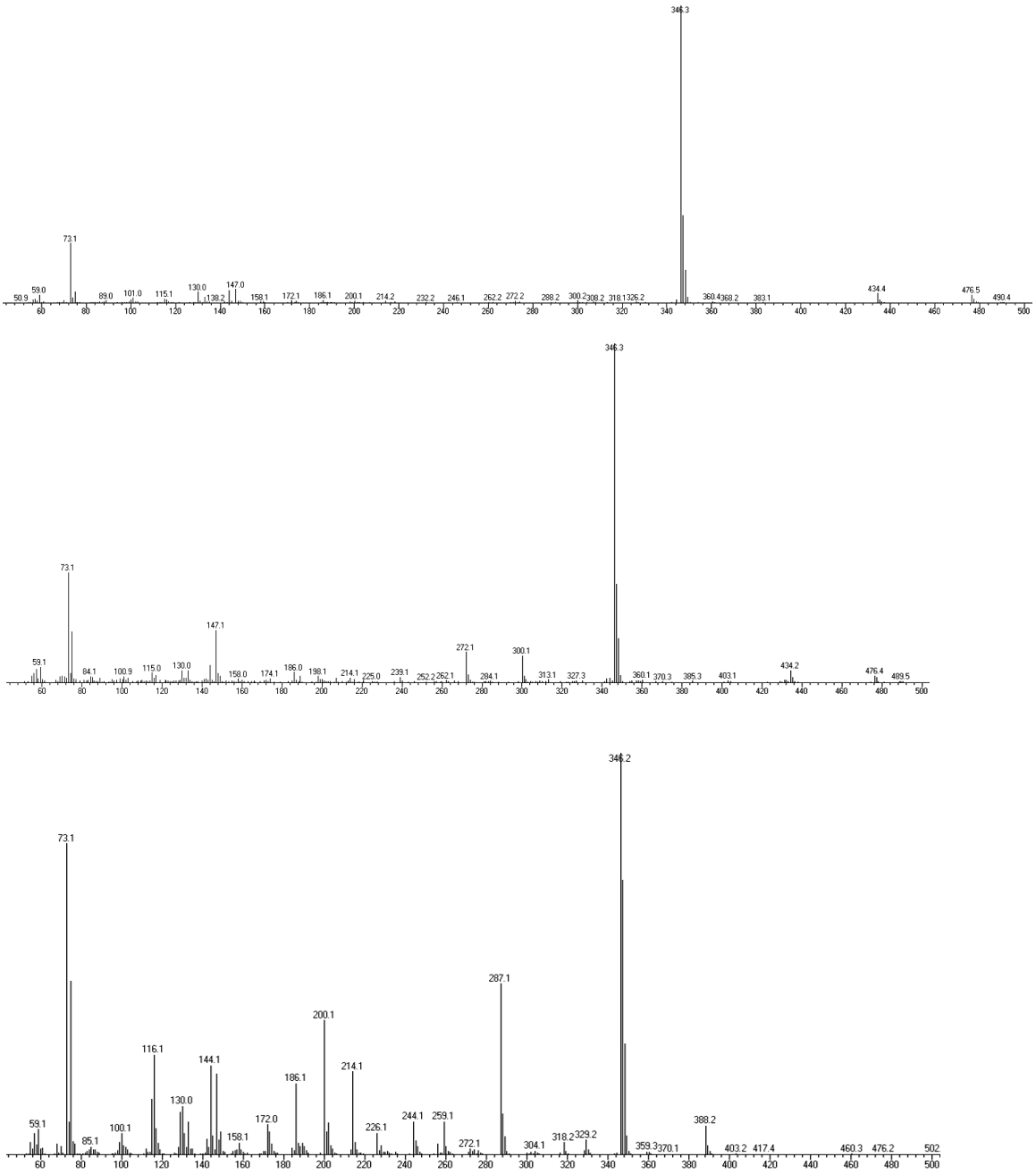

Figure 18: Mass spectra of hypothetical N-acetyl AMM, synthesized N-acetyl AMM, and N-acetyl aspartate

4.2.5 *in vivo* study

With synthetic AMM confirming the identity of our unknown compound, we set out to design and in vivo experiment that would show a correlation between β-alanine levels and formation of AMM. We also wanted to use these experiments to discover whether AMM is a localized metabolite or found ubiquitously throughout the body. We proposed two methods to affect an *in vivo* accumulation of β-alanine, stomach gavage with β-alanine to simulate the upper tolerable dose taken by human athletes as well as an intraperitonial injection of aminooxyacetate (AOA), a transaminase inhibitor that inhibits conversion of β-alanine to malonic semialdehyde. The two different methods for increasing β-alanine concentration led us to define 4 experimental groups of rats as shown in **Figure 19**. Each arrow on the timeline represents one rat sacrificed at that time.

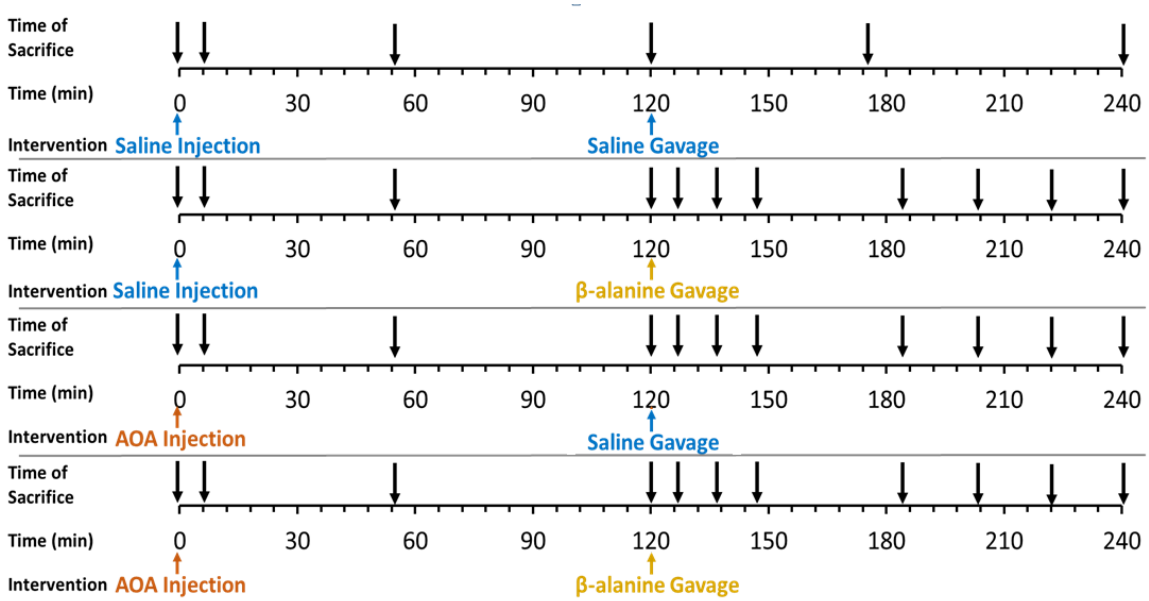

Figure 19: Visual representation of the timeline of 4 groups of *in vivo* experiments. The times of sacrifice of the rats are indicated by black arrows. The rats sacrificed from 0 to 120 min in group 1 serve as controls for the rats sacrificed from 125 to 240 min in group 2. The rats sacrificed from 0 to 120 min in group 3 serve as controls for the rats sacrificed from 125 to 240 min in group 4. Blue arrows denote saline (control) treatment. Yellow arrows denote b-alanine oral gavage. Orange arrows denote IP injection of aminooxyacetate.

In order to understand the role an increase in β-alanine concentration has on the concentration of AMM, we must first look at the effectiveness of our β-alanine loading techniques (**Figure 20**). The control rats that were injected and gavaged with saline show no change in β-alanine baseline throughout the experiment. The second group of rats that underwent an intraperitoneal injection of AOA at the start of the experiment showed increases of β-alanine in plasma and liver tissue but no change in muscle or brain concentration. Direct stomach gavage of β-alanine showed large uptake in all tissue types, and addition of AOA was found to enhance this effect.

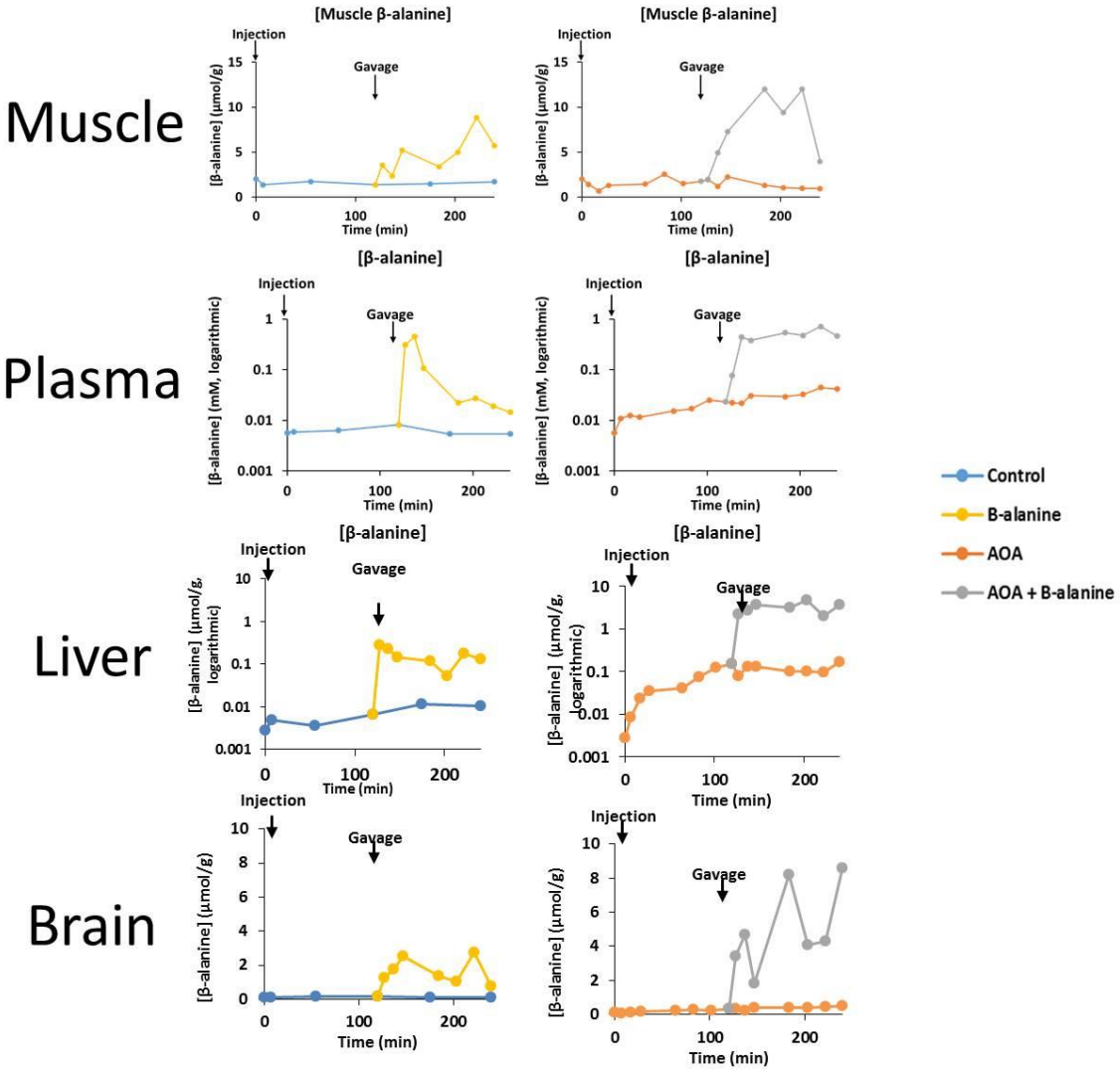

Figure 20: Tissue specific concentration of β-alanine
Each colored point on a graph denotes a concentration (in μmol/g) of β-alanine found at that time point. Experiments are separated into rows based on tissue type. Columns are separated by whether or not the experiment begins with a saline injection (left) or AOA injection (right). Blue line signifies control experiment with saline injection and gavage. Yellow line denotes β-alanine gavage. Orange line denotes AOA injection and saline gavage. Grey line denotes AOA injection and β-alanine gavage.

When pure standards of AMM (containing no β-alanine, per NMR analysis) were assayed by GC-MS, we observed a peak of β-alanine derivative derived from the partial degradation of the AMM derivative on the column. Thus, concentrations of AMM are somewhat underestimated and are reported as relative concentrations to the amount of internal standard 4-hydroxy-[$^{2}H_{6}$] butyrate used.

The change in AMM concentration was found to correlate well to the tissue specific concentration of β-alanine as seen in **Figure 21**. The control group did not experience any increase in AMM. The only tissue that demonstrated an increase in AMM through IP injection of AOA alone was the liver. Stomach gavage of β-alanine caused a spike in AMM formation with addition of pre-injection of AOA potentiating this effect. One important note about this data is that the relative concentrations of AMM are more than twice as high in brain tissue samples as any other tissue type. This lends credence to the hypothesis that AMM or its acetylated version may play a role in the central nervous system affects suffered by those who take β-alanine supplements recreationally.

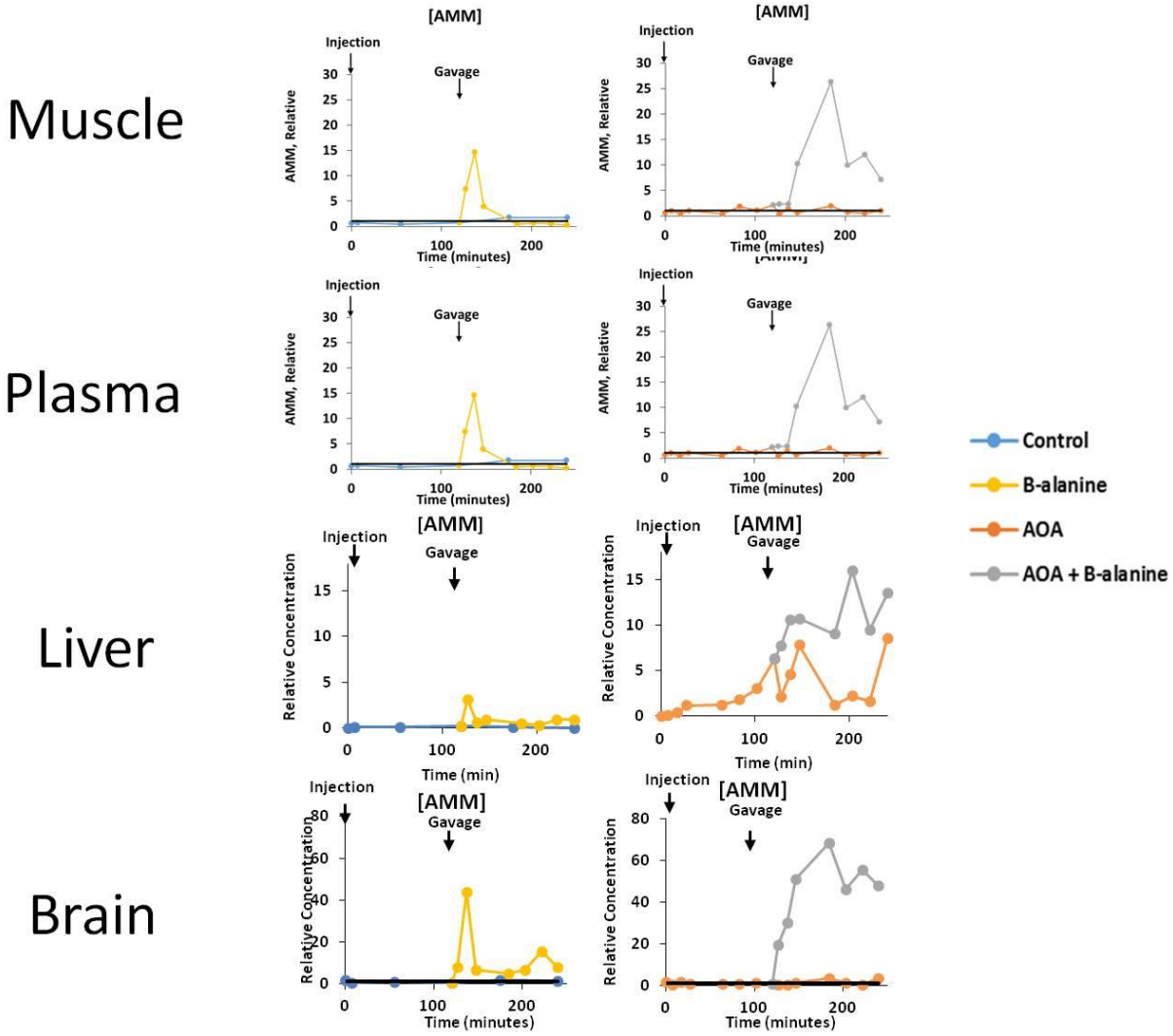

Figure 21: Tissue specific concentration of AMM
Each colored point on a graph denotes a concentration (relative to internal standard) of AMM found at that time point. Experiments are separated into rows based on tissue type. Columns are separated by whether or not the experiment begins with a saline injection (left) or AOA injection (right). Blue line signifies control experiment with saline injection and gavage. Yellow line denotes β-alanine gavage. Orange line denotes AOA injection and saline gavage. Grey line denotes AOA injection and β-alanine gavage.

In order to identify any changes to the neurochemical balance of the brain that the increases of brain β-alanine and AMM may affect, the brain samples were assayed for changes in concentration to major neurotransmitters as well as N-acetyl AMM. After gavage with β-alanine, all assayed neurotransmitters show significantly increased concentration (**Figure 22**). AOA enhanced this effect for α-aminobutyrate (AABA), γ-aminobutyrate (GABA), and N-acetyl-AMM.

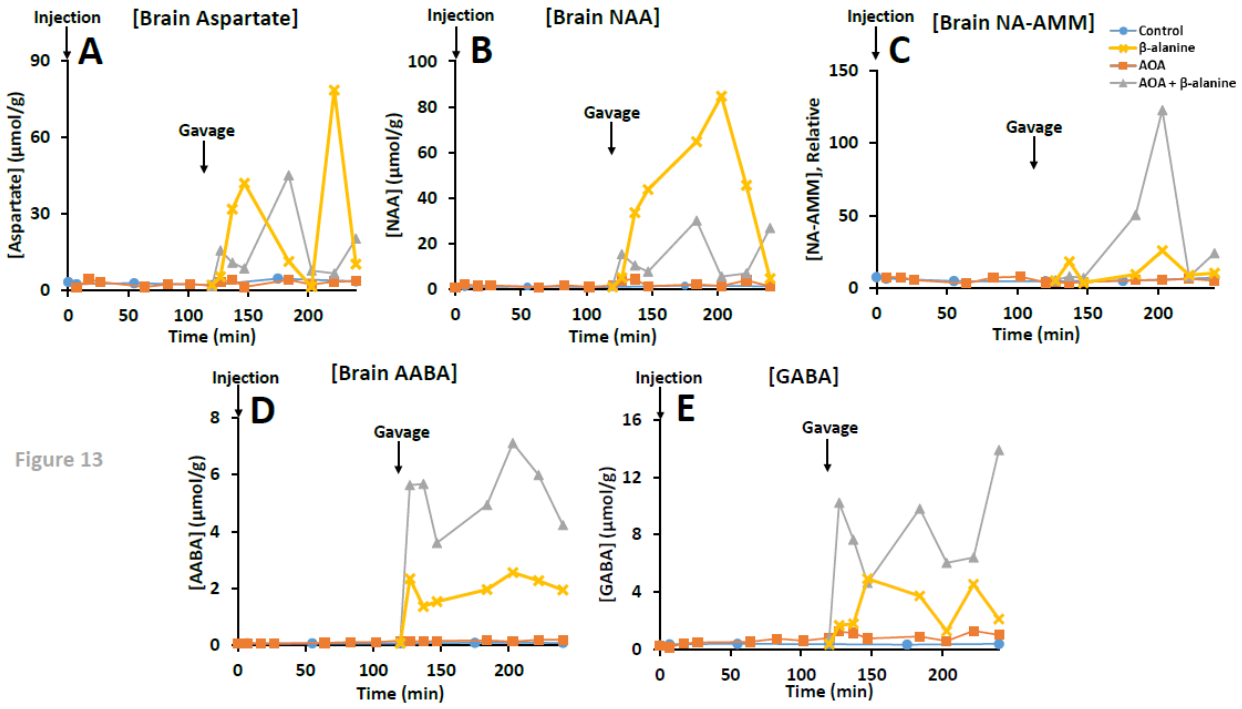

Figure 13

Figure 22: Concentration of aspartate, N-acetyl aspartate, N-acetyl AMM, α-aminobutyric acid, and γ-aminobutyric acid

Each colored point on a graph denotes a concentration (in µmol/g) of neurotransmitter found at that time point. Each graph presents data for a different neurotransmitter as denoted by title. Blue line signifies control experiment with saline injection and gavage. Yellow line denotes β-alanine gavage. Orange line denotes AOA injection and saline gavage. Grey line denotes AOA injection and β-alanine gavage.

4.3 Conclusion

The overall arc of this project is a perfect microcosm of how synthesis and in particular stable isotope synthesis serve as powerful tools in the study of metabolism. What began as a question generated from studying the metabolism of 3-hydroxypropionate led to the identification and confirmation of a new metabolite present *in vivo*. Using stable isotopes, it was confirmed that this molecule was formed from the carboxylation of β-alanine. Confirmation of the hypothesized structure was made possible through synthesis.

The significance of this discovery is multifaceted. On its own, the discovery of this metabolite opens a large number of potential projects to elucidate the metabolic pathways and roles of AMM in both healthy and disease states. Both AMM and N-acetyl AMM were found to be formed in highest concentrations in brain tissue and have structures similar to other canonical neurotransmitters. In addition, β-alanine was also found to increase the concentration of the neurotransmitters AABA, GABA, and N-acetyl aspartate. This great perturbation of chemical balance in the CNS provides physiological evidence for the possible cause of paresthesia in athletes who supplement with a high load of β-alanine.

4.4 Experimental protocols

4.4.1 Materials and methods

For general materials and methods, see section 2.4.1.

Perfused liver experiments

All animal experiments were approved by the IACUC Committee of Case Western Reserve University and performed by Dr. Guofang Zhang, Dr. Henri Brunengraber, Dr. Kirkland Wilson, and Jeremy Hess. Male Sprague-Dawley rats (Envigo) were fed with Prolab Isopro RMH 3000 irradiated chow containing 13 ppm of calcium pantothenate. Livers from overnight-fasted rats (160-180 g) were perfused for 60 minutes with recirculating bicarbonate buffer containing 4% dialyzed, fatty acid-free, bovine serum albumin (fraction V, fatty acid-poor, GenDEPOT) and 4 mM glucose. In some experiments, the buffer also contained 2 mM ß-[^{15}N, $^{13}C_3$]-alanine. Samples of perfusate were taken at regular intervals and quick-frozen. At the end of all perfusion experiments, the livers were quick-frozen and kept in liquid N_2 until analyses.

***in vivo* experiments**

In vivo experiments carried out by Dr. Henri Brunengraber and Dr. Kirkland Wilson. Four groups of overnight-fasted rats were injected intraperitoneally at zero time with either 0.6 mL saline (groups 1 and 2) or 10 mg AOA/kg (groups 3 and 4). At 120 minutes, they were gavaged with 1 mL saline/kg (groups 1 and 3), or 450 µmol ß-alanine/kg in the same volume of saline (groups 2 and 4).

The rats were sacrificed by decapitation one at a time, giving time points between 0 to 240 minutes. Liver, brain, heart, quadriceps muscle were quick-frozen. Blood was

centrifuged and plasma quick-frozen.

Analytical procedures

The labeling patterns and tissue specific concentrations were assayed by GC-MS and LC-MS/MS as described previously.[12] The concentrations of α-aminobutyrate, GABA, aspartate, N-acetylaspartate, AMM, N-acetyl-AMM were assayed as *tert*-butyldimethylsilyl derivatives.[12] Measured mass isotopomer distributions were corrected for natural enrichment and expressed as mol percentages.

LC/MS/MS quantification of AMM from biological samples

The identification of synthetic AMM and its distinction from aspartate were conducted using a ZIC-HILIC Full scan/PRM LC-MS/MS method. The instrument used for this assay was UPLC (Vanquish, Thermo Scientific, Bellefonte, PA, USA) connected to a Q-exactive HF mass spectrometer (Thermo Scientific, Bellefonte, PA, USA). 5 µl of each solution was injected onto a SeQuant ZIC-HILIC column (150 x 2.1 mm, 3.5 µm, 100 Å, Merck, Darmstadt, Germany) attached to a precolumn SeQuant ZIC-HILIC (20 x 2.1 mm, 3.5 µm, 100 Å) leading to the HESI source of the mass spectrometer. Separation was performed using solvent A (100% LC-MS grade water + 0.1% formic acid v/v) and solvent B (100 % acetonitrile + 0.08% formic acid v/v). A gradient of solvent B (80% to 35% B in 28 minutes), was followed by re-equilibration to 80% B for 3 minutes. A constant flow of 150 µl/minute was maintained and column oven was cooled at 20 °C. The mass spectrometer was operated in negative ionization mode. The flow from UPLS was directed to the HESI probe with the following settings: spray voltage 2.5 kV, capillary temperature 250 °C, sheath gas 40%, auxillary gas 10%, probe heater temperature 300 °C and S-lense RF level 50. The mass spectrometer was operated in high

resolution mode with full scan MS1 and PRM MS2 of parent with *m/z* 132.03. Full scans were recorded at 120,000 mass resolution with a scan range from *m/z* 70-1050, automatic gain control target was 3e6 and maximum injection time was 100 ms. The MS2 parallel reaction monitoring were recorded only for $[M-H]^-$ ion with *m/z* 132.03 with 0.5 *m/z* mass window, at a mass resolution of 30,000, AGC target 2e5, normalized collision energy of 40%. Nitrogen was used as a collision gas.

4.4.2 Synthetic routes

Diethyl cyanopropanedioate (30)

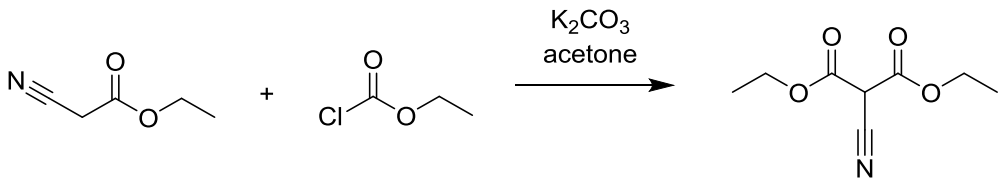

30

Diethyl cyanopropanedioate was prepared from commercially available ethyl chloroformate and ethyl cyanoacetate. In a 250 mL round bottom flask equipped with stir bar, 5.7 mL (1 equiv, 53.56 mmol) of ethyl cyanoacetate was added to a stirring mixture of 24 grams of *redi-dri* anhydrous potassium carbonate and 70 mL of dry acetone. The solution was stirred for 5 minutes, after which 10.2 mL (2 equiv, 106.68 mmol) of ethyl chloroformate was added. The reaction mixture was brought to reflux and stirred for 24 hours. The reaction was quenched with 100 mL H_2O and concentrated via rotovap. An additional 50 mL of H_2O was added and the resulting solution was extracted with dichloromethane. Following the extraction, 30 mL of HCl was added and a second extraction was then completed utilizing ether. The ether layers were combined, dried

using magnesium sulfate, and concentrated via rotovap. The resulting red oil was vacuum distilled (0.5 mmHg, 108 °C) to afford the product as clear oil. (5.86 g, 31.64 mmol, 59%) ^{1}H NMR (500MHz, $CDCl_3$): major tautomer: 4.48 (s, 1H), 4.36 (q, J=5, 4H), 1.37 (t, J=5, 6H) minor tautomer: 4.48 (s, 1H), 4.43(q, J=5, 4H), 1.42 (t, J=, 6H). ^{13}C NMR (500MHz, $CDCl_3$): δ: 160.72, 111.68, 62.60, 44.62, 13.58

Diethyl 2-(aminomethyl)propanedioate (31)

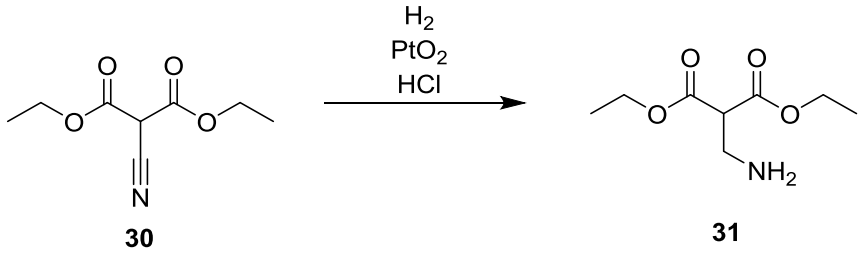

30 **31**

Diethyl 2-(aminomethyl)propanedioate was prepared through hydrogenation of **30**. To a 10 mL round bottom flask with stir bar was added product **30 (**1 g, 5.1 mmol). 4 mL of 3.5 M HCl in EtOH was added, followed by 0.1 g of platinum oxide. The round bottom was placed in a bomb and sealed. The bomb was brought under vacuum then flushed with hydrogen three times. The bomb was charged to 250 atm of H_2 and the reaction was stirred for 60 hours. The resulting heterogeneous mixture was filtered through a cotton plug and concentrated to obtain solid product. The product was rinsed with acetone and filtered to produce 0.925 g (4.89 mmol, 96%) of **31** as a white powder. ^{1}H NMR (500MHz, D_2O): δ4.21 (t, J=5Hz, 4H), 3.45 (s, 2H), 1.20 (t, J=5Hz, 6H). ^{13}C NMR (500MHz, D_2O): δ 168.11, 63.65, 48.98, 36.96, 13.06.

2-(aminomethyl)propanedioic acid (32)

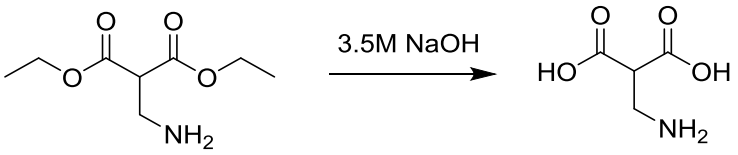

31 **32**

Product **32** was prepared from **31** via base catalyzed hydrolysis. A 10 mL round bottom flask was prepared with 0.20 g (1.05 mmol) of product **31**. The solid was then dissolved in 2.5 mL of 3.5 M aq. NaOH. The solution was stirred at room temperature for 60 hours. The pH was then adjusted to 7 with 3.5 M HCl in EtOH. The product was then precipitated and filtered out of solution by addition of acetone (0.12 g, 0.9 mmol, 85.7%). ^{1}H NMR (500MHz, D_2O): δ 3.36 (s, 2H). ^{13}C NMR (500MHz, H_2O/D_2O): δ 175.14, 53.16, 47.83.

1,2,3-[$^{13}C_3$] Ethyl 2-cyanoacetate

To a 100 mL round bottom flask was added potassium [$^{13}C_1$] cyanide (1.23 g, 18.88 mmol) and 1 M sodium hydroxide (20 ml). This solution was stirred until dissolved. To the reaction was added ethyl [$^{13}C_2$] bromoacetate (2.32 mL, 20mmol). Reaction was stirred at 100 °c for 3 hours. The solution was then cooled to 0 °c and acidified with HCl (1.5 mL). Solvent was then removed under reduced pressure to isolate the intermediate carboxylic acid as a solid. The crystals were suspended in ethanol (50 mL) and filtered through a fritted glass funnel. The filtrate was moved to a 150 mL round bottom along with sulfuric acid (1 mL). The solution was refluxed 16 hours in order to esterify the product. Excess ethanol was removed under reduced pressure and the resulting oil was diluted with cold saturated sodium bicarbonate (50 mL). The product was extracted with

ethyl acetate, dried with magnesium sulfate, and concentrated under reduced pressure to obtain the product as yellow oil. (1.38 g, 1.18 mmol, 63%).^{1}H NMR (500 MHz, Chloroform-*d*) δ 4.30 (qd, *J* = 7.2, 3.2 Hz, 2H), 3.61 (dd, *J* = 10.1, 8.2 Hz, 1H), 3.33 (dd, *J* = 10.1, 8.2 Hz, 1H), 1.35 (t, *J* = 7.2 Hz, 3H). ^{13}C NMR (126 MHz, Chloroform-*d*) δ 162.86 (dd, *J* = 61.3, 3.4 Hz), 113.02 (dd, *J* = 62.9, 3.4 Hz), 41.68 (t, *J* = 59.3 Hz), 24.75 (dd, *J* = 62.9, 61.2 Hz).

1,2,3-[$^{13}C_3$] 2-(Aminomethyl)propanedioic acid

1,2,3-[$^{13}C_3$] 2-(Aminomethyl)propanedioic acid was synthesized via the same method as unlabeled 2(aminomethyl)propanedioic acid with the exception of utilizing 1,2,3-[$^{13}C_3$] Ethyl 2-cyanoacetate as a starting reagent. Reactions proceed the same as described in **30-32** and synthesis was confirmed by GCMS.

4.5 Acknowledgement

Animal experiments carried out in Dr. Henri Brunengraber's lab. (Department of Nutrition, Case Western Reserve University. *In vivo* study data was collected by Dr. Kirkland Wilson. LC/MS/MS methods developed with the assistance of Dr. Charandeep Singh.

4.6 References

1. Zhang, G.-F. *et al.* Catabolism of 4-Hydroxyacids and 4-Hydroxynonenal via 4-Hydroxy-4-phosphoacyl-CoAs. *J. Biol. Chem.* **284,** 33521–33534 (2009).

2. Sadhukhan, S., Han, Y., Zhang, G. F., Brunengraber, H. & Tochtrop, G. P. Using isotopic tools to dissect and quantitate parallel metabolic pathways. *J. Am. Chem. Soc.* **132,** 6309–6311 (2010).

3. Zhang, G.-F. *et al.* Metabolism of γ-hydroxybutyrate in perfused rat livers. *Biochem. J.* **444,** 333–341 (2012).

4. Sadhukhan, S., Zhang, G.-F. & Tochtrop, G. P. Modular Isotopomer Synthesis of γ-Hydroxybutyric Acid for a Quantitative Analysis of Metabolic Fates. *ACS Chem. Biol.* **9,** 1706–1711 (2014).

5. Boscolo-Berto, R. *et al.* Narcolepsy and effectiveness of gamma-hydroxybutyrate (GHB): A systematic review and meta-analysis of randomized controlled trials. *Sleep Med. Rev.* **16,** 431–443 (2012).

6. Caputo, F., Vignoli, T., Maremmani, I., Bernardi, M. & Zoli, G. Gamma Hydroxybutyric Acid (GHB) for the Treatment of Alcohol Dependence: A Review. *Int. J. Environ. Res. Public Health* **6,** 1917–1929 (2009).

7. Kaufman, E. E., Nelson, T., Miller, D. & Stadlan, N. Oxidation of ?-Hydroxybutyrate to Succinic Semialdehyde by a Mitochondrial Pyridine Nucleotide-Independent Enzyme. *J. Neurochem.* **51,** 1079–1084 (1988).

8. Kaufman, E. E. & Nelson, T. An overview of ?-hydroxybutyrate catabolism: The role of the cytosolic NADP+-dependent oxidoreductase EC 1.1.1.19 and of a mitochondrial hydroxyacid-oxoacid transhydrogenase in the initial, rate-limiting step in this pathway. *Neurochem. Res.* **16,** 965–974 (1991).

9. Wong, C. G. T., Chan, K. F. Y., Gibson, K. M. & Snead, O. C. ??-Hydroxybutyric Acid. *Toxicol. Rev.* **23,** 3–20 (2004).

10. Roe, C. R., Sweetman, L., Roe, D. S., David, F. & Brunengraber, H. Treatment of cardiomyopathy and rhabdomyolysis in long-chain fat oxidation disorders using an anaplerotic odd-chain triglyceride. *J. Clin. Invest.* **110,** 259–269 (2002).

11. Ando, T., Rasmussen, K., Nyhan, W. L. & Hull, D. 3-Hydroxypropionate: Significance of -Oxidation of Propionate in Patients with Propionic Acidemia and Methylmalonic Acidemia. *Proc. Natl. Acad. Sci.* **69,** 2807–2811 (1972).

12. Wilson, K. *et al.* Inter-relations between 3-hydroxypropionate and propionate metabolism in rat liver: relevance to disorders of propionyl-CoA metabolism. *Am. J. Physiol. Metab.* **313,** E413–E428 (2017).

13. Harris, R. C. *et al.* The absorption of orally supplied β-alanine and its effect on

muscle carnosine synthesis in human vastus lateralis. *Amino Acids* **30,** 279–289 (2006).

14. Baguet, A. *et al.* Carnosine loading and washout in human skeletal muscles. *J. Appl. Physiol.* **106,** 837–842 (2009).

15. Blancquaert, L., Everaert, I. & Derave, W. Beta-alanine supplementation, muscle carnosine and exercise performance. *Curr. Opin. Clin. Nutr. Metab. Care* **18,** 63–70 (2015).

16. Bellinger, P. M. & Minahan, C. L. Performance effects of acute β -alanine induced paresthesia in competitive cyclists. *Eur. J. Sport Sci.* **16,** 88–95 (2016).

17. Décombaz, J., Beaumont, M., Vuichoud, J., Bouisset, F. & Stellingwerff, T. Effect of slow-release β-alanine tablets on absorption kinetics and paresthesia. *Amino Acids* **43,** 67–76 (2012).

CHAPTER 5

SUMMARY AND FUTURE WORKS

5.1 Summary

The long history of collaboration between synthetic chemistry and metabolic research was discussed in **Chapter 1**. This chapter began with descriptions of some of the earliest synthesis of biological molecules and continued on to describe modern methods utilized to probe metabolic pathways. Techniques crucial to the research described within such as organ perfusion and isotopic labeling was elucidated. Finally, an introduction into lipid metabolism and formation of LPO products was presented.

Chapter 2 introduced the topic of uniformly isotopically labeled substrates and partially isotope labeled substrates. The advantages of each type of labeled substrates are discussed in the context of being utilized to study both healthy and disease state metabolism. The work described in this chapter features collaborative projects that utilize labeled substrates that I have synthesized over the past few years. The syntheses of these molecules were all completed successfully and the results of the 3-hydroxypropionate substrate led directly to the work described in **Chapter 4**.

The work explored throughout **Chapter 3** directly relates to the metabolism of lipid peroxidation (LPO) products. The first project involves elucidation of the enzyme that catalyzes the first committed step of the novel 4-hydroxynonenal pathway discovered previously in our lab. To this end, a functional assay that monitors the phosphorylation of 4-hydroxy-acyl-CoA moieties was prepared and utilized to separate protein from bulk pig liver. The second project of chapter three involved the synthesis of a number of EKODE molecules. These molecules will serve as substrates for future liver perfusion studies.

Chapter 4 covered the discovery, synthesis, and characterization of 2-(aminomethyl)malonate. This molecule is a potential neurotransmitter that is formed *in vivo* during periods of high β-alanine concentration. An experiment was carried out to determine the tissue specific formation of AMM.

5.2 Future works: Lipid peroxidation products

A new approach was designed after an article was published on a set of proteins capable of catabolizing levulinic acid in pseudomonas putida[1]. One step of this catabolic transformation is a phosphorylation of a 4-hydroxy-CoA followed by isomerization to the three-position. This is the only other example of this type of metabolic pathway found in the literature. According to the Pfleger group, two proteins, referred to as IvaA and IvaB, are required for this step of the pathway.. I have run a BLAST search for mammalian homologues of these proteins and results point to ACAD10 bearing high similarity to the first of these proteins.

This leads to two approaches that may prove useful in elucidating the identity of the kinase. One approach is to generate a construct similar to the Pfleger group that would express IvaA and IvaB. The expressed proteins could be utilized in our activity assay to see if they would also catalyze the transformation from 4-hydroxyacyl-CoA to 3-hydroxy-acyl-CoA. If it is capable of affecting this transformation, this would lend credence to the theory that these proteins serve as a bacterial homologue of our unknown kinase.

The second approach would be to directly express ACAD10 and utilize this to find any proteins which have a strong interaction with ACAD10. This could be done by

generating antibodies specific to ACAD10 and running a co-immunoprecipitation to pull down any strongly interacting proteins which may be serving as a mammalian analogue of lvaB.

5.3 Future works: AMM

The future potential for studies involving AMM is high. As a possible neurotransmitter, it would be necessary to delve deeper into its role in biological systems. It would be important to find out if the molecule exists during periods of low β-alanine concentration. One could also run perfusion studies with labeled AMM to discover the catabolic and anabolic pathways with which it is involved. It would also seem beneficial to test AMM for the ability to activate/inhibit any common neurotransmitter receptors. These are just a few directions of many that this research can take. However, in order to begin any of these studies, one major task must be completed. This task is to find a way to analyze AMM concentration directly rather than relative to a standard.

In order to achieve a more accurate determination of the concentration of AMM, one must prevent decarboxylation during analysis. I have begun work on a number of methods that could be utilized to derivatize AMM in order to stabilize the molecule for analysis. Once this is complete, a new GC/MS or LC/MS/MS method must be generated to look for the AMM and N-acetyl AMM derivatives. Once a reliable method is found, the *in vivo* study can be redone to accurately determine concentrations.

5.4 References

1. Rand, J. M. *et al.* A metabolic pathway for catabolizing levulinic acid in bacteria. *Nat. Microbiol.* **2,** 1624–1634 (2017).

Bibliography

Agostinho, P., A. Cunha, R., & Oliveira, C. (2010). Neuroinflammation, Oxidative Stress and the Pathogenesis of Alzheimers Disease. *Current Pharmaceutical Design*, *16*(25), 2766–2778.

Alary, J., Guéraud, F., & Cravedi, J.-P. (2003). Fate of 4-hydroxynonenal in vivo: disposition and metabolic pathways. *Molecular Aspects of Medicine*, *24*(4–5), 177–187.

Anavi, S., Ni, Z., Tirosh, O., & Fedorova, M. (2015). Steatosis-induced proteins adducts with lipid peroxidation products and nuclear electrophilic stress in hepatocytes. *Redox Biology*, *4*, 158–168.

Ando, T., Rasmussen, K., Nyhan, W. L., & Hull, D. (1972). 3-Hydroxypropionate: Significance of -Oxidation of Propionate in Patients with Propionic Acidemia and Methylmalonic Acidemia. *Proceedings of the National Academy of Sciences*, *69*(10), 2807–2811.

Aston, F. W. (1927). Bakerian Lecture.— A new mass-spectrograph and the whole number rule. *Proceedings of the Royal Society of London. Series A, Containing Papers of a Mathematical and Physical Character*, *115*(772), 487–514.

Baguet, A., Reyngoudt, H., Pottier, A., Everaert, I., Callens, S., Achten, E., & Derave, W. (2009). Carnosine loading and washout in human skeletal muscles. *Journal of Applied Physiology*, *106*(3), 837–842.

Bajpai, A. (2014). Oxidative Stress and Major Depression. *JOURNAL OF CLINICAL AND DIAGNOSTIC RESEARCH*.

Baldwin, J. E., & Krebs, H. (1981). The evolution of metabolic cycles. *Nature*, *291*(5814), 381–382.

Barrera, G., Pizzimenti, S., Ciamporcero, E. S., Daga, M., Ullio, C., Arcaro, A., Cetrangolo, G. P., Ferretti, C., Dianzani, C., Lepore, A., & Gentile, F. (2015). Role of 4-Hydroxynonenal-Protein Adducts in Human Diseases. *Antioxidants & Redox Signaling*, *22*(18), 1681–1702.

Bellinger, P. M., & Minahan, C. L. (2016). Performance effects of acute β -alanine induced paresthesia in competitive cyclists. *European Journal of Sport Science*, *16*(1), 88–95.

Blancquaert, L., Everaert, I., & Derave, W. (2015). Beta-alanine supplementation, muscle carnosine and exercise performance. *Current Opinion in Clinical Nutrition and Metabolic Care*, *18*(1), 63–70.

Boiteau, R., Hoyt, D., Nicora, C., Kinmonth-Schultz, H., Ward, J., & Bingol, K. (2018). Structure Elucidation of Unknown Metabolites in Metabolomics by Combined NMR and MS/MS Prediction. *Metabolites*, *8*(1), 8.

Borras, E., Cheng, A., Wun, T., Reese, K. L., Frank, M., Schivo, M., & Davis, C. E. (2019). Detecting opioid metabolites in exhaled breath condensate (EBC). *Journal of Breath Research*, *13*(4), 046014.

Boscolo-Berto, R., Viel, G., Montagnese, S., Raduazzo, D. I., Ferrara, S. D., & Dauvilliers, Y. (2012). Narcolepsy and effectiveness of gamma-hydroxybutyrate (GHB): A systematic review and meta-analysis of randomized controlled trials. *Sleep Medicine Reviews*, *16*(5), 431–443.

Boyle, J. (2008). Molecular biology of the cell, 5th edition by B. Alberts, A. Johnson, J. Lewis, M. Raff, K. Roberts, and P. Walter. In *Biochemistry and Molecular Biology Education*.

Broekaert, D., & Fendt, S.-M. (2019). Measuring In Vivo Tissue Metabolism Using 13C Glucose Infusions in Mice. In *Methods in Molecular Biology* (pp. 67–82).

Bruce, S. J., Jonsson, P., Antti, H., Cloarec, O., Trygg, J., Marklund, S. L., & Moritz, T. (2008). Evaluation of a protocol for metabolic profiling studies on human blood plasma by combined ultra-performance liquid chromatography/mass spectrometry: From extraction to data analysis. *Analytical Biochemistry*, *372*(2), 237–249.

Buescher, J. M., Antoniewicz, M. R., Boros, L. G., Burgess, S. C., Brunengraber, H., Clish, C. B., DeBerardinis, R. J., Feron, O., Frezza, C., Ghesquiere, B., Gottlieb, E., Hiller, K., Jones, R. G., Kamphorst, J. J., Kibbey, R. G., Kimmelman, A. C., Locasale, J. W., Lunt, S. Y., Maddocks, O. D. K., … Fendt, S.-M. (2015). A roadmap for interpreting 13 C metabolite labeling patterns from cells. *Current Opinion in Biotechnology*, *34*, 189–201.

Buizza, L., Prandelli, C., Bonini, S. A., Delbarba, A., Cenini, G., Lanni, C., Buoso, E., Racchi, M., Govoni, S., Memo, M., & Uberti, D. (2013). Conformational altered p53 affects neuronal function: relevance for the response to toxic insult and growth-associated protein 43 expression. *Cell Death & Disease*, *4*(2), e484–e484.

Burr, GO. Burr, M. (1930). On the nature and role of the fatty acids essential in nutrition. *Biol. Chem.*, *86*, 587–621.

Caputo, F., Vignoli, T., Maremmani, I., Bernardi, M., & Zoli, G. (2009). Gamma Hydroxybutyric Acid (GHB) for the Treatment of Alcohol Dependence: A Review. *International Journal of Environmental Research and Public Health*, *6*(6), 1917–1929.

Catch, J. R., Elliott, D. F., Hey, D. H., & Jones, E. R. H. (1948). 66. Halogenated ketones. Part I. The bromination of acetone and methyl ethyl ketone. *Journal of the Chemical Society (Resumed)*, 272–275.

Chelikani, P., Fita, I., & Loewen, P. C. (2004). Diversity of structures and properties among catalases. *Cellular and Molecular Life Sciences (CMLS)*, *61*(2), 192–208.

Corey, E. J., & Myers, A. G. (1985). Total synthesis of (.+-.)-antheridium-inducing factor

(AAn) of the Fern Anemia phyllitidis. Clarification of stereochemistry. *Journal of the American Chemical Society*, *107*(19), 5574–5576.

Csala, M., Kardon, T., Legeza, B., Lizák, B., Mandl, J., Margittai, É., Puskás, F., Száraz, P., Szelényi, P., & Bánhegyi, G. (2015). On the role of 4-hydroxynonenal in health and disease. *Biochimica et Biophysica Acta (BBA) - Molecular Basis of Disease*, *1852*(5), 826–838.

De Bruyn, T., Augustijns, P. F., & Annaert, P. P. (2016). Hepatic Clearance Prediction of Nine Human Immunodeficiency Virus Protease Inhibitors in Rat. *Journal of Pharmaceutical Sciences*, *105*(2), 846–853.

Deckelbaum, R. J., & Torrejon, C. (2012). The Omega-3 Fatty Acid Nutritional Landscape: Health Benefits and Sources. *The Journal of Nutrition*, *142*(3), 587S–591S.

Décombaz, J., Beaumont, M., Vuichoud, J., Bouisset, F., & Stellingwerff, T. (2012). Effect of slow-release β-alanine tablets on absorption kinetics and paresthesia. *Amino Acids*, *43*(1), 67–76.

Evans, D. A., Trenkle, W. C., Zhang, J., & Burch, J. D. (2005). Synthesis and Confirmation of the Absolute Stereochemistry of the (−)-Aflastatin A C 9 −C 27 Degradation Polyol. *Organic Letters*, *7*(15), 3335–3338.

Faubert, B., Li, K. Y., Cai, L., Hensley, C. T., Kim, J., Zacharias, L. G., Yang, C., Do, Q. N., Doucette, S., Burguete, D., Li, H., Huet, G., Yuan, Q., Wigal, T., Butt, Y., Ni, M., Torrealba, J., Oliver, D., Lenkinski, R. E., … DeBerardinis, R. J. (2017). Lactate Metabolism in Human Lung Tumors. *Cell*, *171*(2), 358–371.

Fernández-García, J., Altea-Manzano, P., Pranzini, E., & Fendt, S.-M. (2020). Stable Isotopes for Tracing Mammalian-Cell Metabolism In Vivo. *Trends in Biochemical Sciences*, *45*(3), 185–201.

Fischer, E. (1881). Ueber das Caffeïn. *Berichte Der Deutschen Chemischen Gesellschaft*, *14*(1), 637–644.

Fischer, E. (1898). Ueber das Purin und seine Methylderivate. *Berichte Der Deutschen Chemischen Gesellschaft*, *31*(3), 2550–2574.

Foster, G. ., Schoenheimer, R., & Rittenberg, D. (1938). Deuterium as an indicator in the study of intermediary metabolism. XIV. Biological formation of deuteroamino acids. *Journal of Biological Chemistry*, *125*, 13–22. https://www.jbc.org/content/125/1/13.full.pdf

Foster, G. L., Keston, A. S., Schoenheimer, R., & Rittenberg, D. (1938). Deuterium as an indicator in the study of intermediary metabolism XII. The action of proteolytic enzymes on peptides in heavy water. *Journal of Biological Chemistry*, *124*, 159–161.

Fridovich, I. (1997). Superoxide Anion Radical ($O^{\cdot-}_2$), Superoxide Dismutases, and Related Matters. *Journal of Biological Chemistry*, *272*(30), 18515–18517.

Furber, M., & Mander, L. N. (1988). Synthesis and confirmation of structure of the antheridium-inducing factor from the fern Anemia mexicana. *Journal of the American Chemical Society*, *110*(12), 4084–4085.

Goldstein, S., Lind, J., & Merényi, G. (2005). Chemistry of peroxynitrites as compared to peroxynitrates. In *Chemical Reviews*.

Gorrini, C., Harris, I. S., & Mak, T. W. (2013). Modulation of oxidative stress as an anticancer strategy. *Nature Reviews Drug Discovery*, *12*(12), 931–947.

Griffin, J. L. (2006). Understanding mouse models of disease through metabolomics. *Current Opinion in Chemical Biology*, *10*(4), 309–315.

Gu, Q., Spinelli, J. J., Dummer, T. B. J., McDonald, T. E., Moore, S. C., & Murphy, R. A. (2018). Metabolic profiling of adherence to diet, physical activity and body size recommendations for cancer prevention. *Scientific Reports*, *8*(1), 16293.

Halliwell, B., & Chirico, S. (1993). Lipid peroxidation: its mechanism, measurement, and significance. *The American Journal of Clinical Nutrition*, *57*(5), 715S–725S.

Harris, R. C., Tallon, M. J., Dunnett, M., Boobis, L., Coakley, J., Kim, H. J., Fallowfield, J. L., Hill, C. A., Sale, C., & Wise, J. A. (2006). The absorption of orally supplied β-alanine and its effect on muscle carnosine synthesis in human vastus lateralis. *Amino Acids*, *30*(3), 279–289.

Harrison, D., Griendling, K. K., Landmesser, U., Hornig, B., & Drexler, H. (2003). Role of oxidative stress in atherosclerosis. *The American Journal of Cardiology*, *91*(3), 7–11.

Huang-Minlon. (1946). A Simple Modification of the Wolff-Kishner Reduction. *Journal of the American Chemical Society*, *68*(12), 2487–2488.

Hudson, R. F., & Chopard, P. A. (1963). The Preparation of Chloromethyl Vinyl Ketones. *Journal of Organic Chemistry*, *28*, 2446–2447.

Ishikawa, T., Esterbauer, H., & Sies, H. (1986). Role of cardiac glutathione transferase and of the glutathione S-conjugate export system in biotransformation of 4-hydroxynonenal in the heart. *The Journal of Biological Chemistry*, *261*(4), 1576–1581. http://www.ncbi.nlm.nih.gov/pubmed/3753704

Ji, C., Kozak, K. R., & Marnett, L. J. (2001). IκB Kinase, a Molecular Target for Inhibition by 4-Hydroxy-2-nonenal. *Journal of Biological Chemistry*, *276*(21), 18223–18228.

Johnson, J. A., & Rocke, A. J. (1995). The Quiet Revolution: Hermann Kolbe and the Science of Organic Chemistry. *The American Historical Review*, *100*(1), 177.

Kaufman, E. E., & Nelson, T. (1991). An overview of ?-hydroxybutyrate catabolism: The role of the cytosolic NADP+-dependent oxidoreductase EC 1.1.1.19 and of a mitochondrial hydroxyacid-oxoacid transhydrogenase in the initial, rate-limiting

step in this pathway. *Neurochemical Research*, *16*(9), 965–974.

Kaufman, E. E., Nelson, T., Miller, D., & Stadlan, N. (1988). Oxidation of ?-Hydroxybutyrate to Succinic Semialdehyde by a Mitochondrial Pyridine Nucleotide-Independent Enzyme. *Journal of Neurochemistry*, *51*(4), 1079–1084.

Kharasch, E. D., Regina, K. J., Blood, J., & Friedel, C. (2015). Methadone Pharmacogenetics. *Anesthesiology*, *123*(5), 1142–1153.

Kim, S.-H., Kelly, P. B., & Clifford, A. J. (2010). Calculating Radiation Exposures during Use of 14 C-Labeled Nutrients, Food Components, and Biopharmaceuticals To Quantify Metabolic Behavior in Humans. *Journal of Agricultural and Food Chemistry*, *58*(8), 4632–4637.

Kind, T., Tsugawa, H., Cajka, T., Ma, Y., Lai, Z., Mehta, S. S., Wohlgemuth, G., Barupal, D. K., Showalter, M. R., Arita, M., & Fiehn, O. (2018). Identification of small molecules using accurate mass MS/MS search. *Mass Spectrometry Reviews*, *37*(4), 513–532.

Kinne-Saffran, E., & Kinne, R. K. H. (1999). Vitalism and synthesis of urea. *American Journal of Nephrology*, *19*(2), 290–294.

Knights, K. M., Stresser, D. M., Miners, J. O., & Crespi, C. L. (2016). In vitro drug metabolism using liver microsomes. *Current Protocols in Pharmacology*.

Kruiswijk, F., Labuschagne, C. F., & Vousden, K. H. (2015). p53 in survival, death and metabolic health: a lifeguard with a licence to kill. *Nature Reviews Molecular Cell Biology*, *16*(7), 393–405.

Kurzer, F., & Sanderson, P. M. (1956). Urea in the history of organic chemistry: Isolation from natural sources. *Journal of Chemical Education*, *33*(9), 452.

Lane, A. N., Fan, T. W. M., & Higashi, R. M. (2008). Stable isotope-assisted metabolomics in cancer research. *IUBMB Life*, *60*(2), 124–129.

Lapolla, A., Fedele, D., Seraglia, R., & Traldi, P. (2006). The role of mass spectrometry in the study of non-enzymatic protein glycation in diabetes: An update. *Mass Spectrometry Reviews*, *25*(5), 775–797.

Li, Q., Sadhukhan, S., Berthiaume, J. M., Ibarra, R. A., Tang, H., Deng, S., Hamilton, E., Nagy, L. E., Tochtrop, G. P., & Zhang, G.-F. (2013). 4-Hydroxy-2(E)-nonenal (HNE) catabolism and formation of HNE adducts are modulated by β oxidation of fatty acids in the isolated rat heart. *Free Radical Biology and Medicine*, *58*, 35–44.

Li, X., Fang, P., Mai, J., Choi, E. T., Wang, H., & Yang, X. (2013). Targeting mitochondrial reactive oxygen species as novel therapy for inflammatory diseases and cancers. *Journal of Hematology & Oncology*, *6*(1), 19.

Lin, D., Zhang, J., & Sayre, L. M. (2007). Synthesis of six epoxyketooctadecenoic acid (EKODE) isomers, their generation from nonenzymatic oxidation of linoleic acid,

and their reactivity with imidazole nucleophiles. *Journal of Organic Chemistry*, *72*(25), 9471–9480.

Lincoln, B. C., Rosiers, C. Des, & Brunengraber, H. (1987). Metabolism of S-3-hydroxybutyrate in the perfused rat liver. *Archives of Biochemistry and Biophysics*, *259*(1), 149–156.

Łuczaj, W., Gęgotek, A., & Skrzydlewska, E. (2017). Antioxidants and HNE in redox homeostasis. *Free Radical Biology and Medicine*, *111*, 87–101.

Luque-Garcia, J. L., & Neubert, T. A. (2007). Sample preparation for serum/plasma profiling and biomarker identification by mass spectrometry. *Journal of Chromatography A*, *1153*(1–2), 259–276.

Macieira, S., Zhang, J., Velarde, M., Buckel, W., & Messerschmidt, A. (2009). Crystal structure of 4-hydroxybutyrate CoA-transferase from Clostridium aminobutyricum. *Biological Chemistry*, *390*(12).

Mali, V. R., & Palaniyandi, S. S. (2014). Regulation and therapeutic strategies of 4-hydroxy-2-nonenal metabolism in heart disease. *Free Radical Research*, *48*(3), 251–263.

Mamelak, M. (1989). Gammahydroxybutyrate: An endogenous regulator of energy metabolism. *Neuroscience & Biobehavioral Reviews*, *13*(4), 187–198.

Moselhy, H. F., Reid, R. G., Yousef, S., & Boyle, S. P. (2013). A specific, accurate, and sensitive measure of total plasma malondialdehyde by HPLC. *Journal of Lipid Research*, *54*(3), 852–858.

Naviaux, R., Naviaux, J., Li, K., Wang, L., Monk, J., Bright, A., Koslik, H., Ritchie, J., & Golomb, B. (2019). Metabolic features of Gulf War illness. *PLoS ONE*, *14*(7).

Nier, A. O., & Gulbransen, E. A. (1939). Variations in the Relative Abundance of the Carbon Isotopes. *Journal of the American Chemical Society*, *61*(3), 697–698.

Nyhan, W., Barshop, B., & Al-Aqeel, A. (2011). Propionic acidemia. In *Atlas of Inherited Metabolic Diseases 3E* (pp. 8–18). CRC Press.

Papackova, Z., & Cahova, M. (2015). Fatty Acid Signaling: The New Function of Intracellular Lipases. *International Journal of Molecular Sciences*, *16*(2), 3831–3855.

Picou, D., & Taylor-Roberts, T. (1969). The measurement of total protein synthesis and catabolism and nitrogen turnover in infants in different nutritional states and receiving different amounts of dietary protein. *Clinical Science*, *36*(2), 283–296. http://www.ncbi.nlm.nih.gov/pubmed/5772104

Playdon, M. C., Moore, S. C., Derkach, A., Reedy, J., Subar, A. F., Sampson, J. N., Albanes, D., Gu, F., Kontto, J., Lassale, C., Liao, L. M., Männistö, S., Mondul, A. M., Weinstein, S. J., Irwin, M. L., Mayne, S. T., & Stolzenberg-Solomon, R. (2017).

Identifying biomarkers of dietary patterns by using metabolomics. *The American Journal of Clinical Nutrition*, *105*(2), 450–465.

Qin, Z., Hu, D., Han, S., Reaney, S. H., Di Monte, D. A., & Fink, A. L. (2007). Effect of 4-Hydroxy-2-nonenal Modification on α-Synuclein Aggregation. *Journal of Biological Chemistry*, *282*(8), 5862–5870.

Ramberg, P. J. (2014). The Death of Vitalism and The Birth of Organic Chemistry: Wohler's Urea Synthesis and the Disciplinary Identity of Organic Chemistry. *Ambix*, *47*, 170–195.

Rand, J. M., Pisithkul, T., Clark, R. L., Thiede, J. M., Mehrer, C. R., Agnew, D. E., Campbell, C. E., Markley, A. L., Price, M. N., Ray, J., Wetmore, K. M., Suh, Y., Arkin, A. P., Deutschbauer, A. M., Amador-Noguez, D., & Pfleger, B. F. (2017). A metabolic pathway for catabolizing levulinic acid in bacteria. *Nature Microbiology*, *2*(12), 1624–1634.

Reuter, S., Gupta, S. C., Chaturvedi, M. M., & Aggarwal, B. B. (2010). Oxidative stress, inflammation, and cancer: How are they linked? *Free Radical Biology and Medicine*, *49*(11), 1603–1616.

Robberecht, H., De Bruyne, T., & Hermans, N. (2017). Effect of various diets on biomarkers of the metabolic syndrome. *International Journal of Food Sciences and Nutrition*, *68*(5), 627–641.

Roe, C. R., Sweetman, L., Roe, D. S., David, F., & Brunengraber, H. (2002). Treatment of cardiomyopathy and rhabdomyolysis in long-chain fat oxidation disorders using an anaplerotic odd-chain triglyceride. *Journal of Clinical Investigation*, *110*(2), 259–269.

Römisch-Margl, W., Prehn, C., Bogumil, R., Röhring, C., Suhre, K., & Adamski, J. (2012). Procedure for tissue sample preparation and metabolite extraction for high-throughput targeted metabolomics. *Metabolomics*, *8*(1), 133–142.

Sadhukhan, S., Han, Y., Zhang, G. F., Brunengraber, H., & Tochtrop, G. P. (2010). Using isotopic tools to dissect and quantitate parallel metabolic pathways. *Journal of the American Chemical Society*, *132*(18), 6309–6311.

Sadhukhan, S., Zhang, G.-F., & Tochtrop, G. P. (2014). Modular Isotopomer Synthesis of γ-Hydroxybutyric Acid for a Quantitative Analysis of Metabolic Fates. *ACS Chemical Biology*, *9*(8), 1706–1711.

Sayre, L. M., Lin, D., Yuan, Q., Zhu, X., & Tang, X. (2006). Protein Adducts Generated from Products of Lipid Oxidation: Focus on HNE and ONE. *Drug Metabolism Reviews*, *38*(4), 651–675.

Sayre, L. M., Zelasko, D. A., Harris, P. L., Perry, G., Salomon, R. G., & Smith, M. A. (1997). 4-Hydroxynonenal-derived advanced lipid peroxidation end products are increased in Alzheimer's disease. *Journal of Neurochemistry*, *68*(5), 2092–2097.

Schoenheimer, R., & Rittenberg, D. (1935a). Deuterium as an Indicator in the Study of Intermediary Metabolism. III The Role of the Fat Tissues. *Journal of Biological Chemistry*, *111*, 175–181. http://www.degruyter.com/view/books/harvard.9780674366701/harvard.9780674366701.c124/harvard.9780674366701.c124.xml

Schoenheimer, R., & Rittenberg, D. (1935b). Deuterium as an indicator in the study of intermediary metabolism. *Science*, *82*(2120), 156–157x.

Schoenheimer, R., & Rittenberg, D. (1936). Deuterium as an indicator in the study of intermediary metabolism. VI. Synthesis and destruction of fatty acids in the organism. *Journal of Biological Chemistry*, *114*, 381–396. https://www.jbc.org/content/114/2/381.full.pdf

Schoenheimer, R., & Rittenberg, D. (1937). Deuterium as an indicator in the study of intermediary metabolism XI. Further studies on the biological uptake of deuterium into organic substances, with special reference to fat and cholesterol formation. *The Journal of Biological Chemistry*, *121*, 235–253. https://www.jbc.org/content/121/1/235.full.pdf

Serrano, E., Navarro, R., Soler, T., Carbó, J. J., Liedós, A., & Urriolabeitia, E. P. (2009). Experimental and computational study of the bonding properties of mixed bis-ylides of phosphorus and sulfur. *Inorganic Chemistry*, *48*(14), 6823–6834.

Singh, S. P., Chen, T., Chen, L., Mei, N., McLain, E., Samokyszyn, V., Thaden, J. J., Moore, M. M., & Zimniak, P. (2005). Mutagenic Effects of 4-Hydroxynonenal Triacetate, a Chemically Protected Form of the Lipid Peroxidation Product 4-Hydroxynonenal, as Assayed in L5178Y/ Tk + / – Mouse Lymphoma Cells. *Journal of Pharmacology and Experimental Therapeutics*, *313*(2), 855–861.

Singh, U., & Jialal, I. (2006). Oxidative stress and atherosclerosis. *Pathophysiology*, *13*(3), 129–142.

Skrzydlewska, Elżbieta; Agnieszka, G. (2019). Biological effect of protein modifications by lipid peroxidation products. *Chemistry and Physics of Lipids*, *221*, 46–52.

Slauch, J. M. (2011). How does the oxidative burst of macrophages kill bacteria? Still an open question. *Molecular Microbiology*, *80*(3), 580–583.

Sofia, M., Maniscalco, M., de Laurentiis, G., Paris, D., Melck, D., & Motta, A. (2011). Exploring Airway Diseases by NMR-Based Metabonomics: A Review of Application to Exhaled Breath Condensate. *Journal of Biomedicine and Biotechnology*, *2011*, 1–7.

Stocker, R., & Keaney, J. F. (2004). Role of Oxidative Modifications in Atherosclerosis. *Physiological Reviews*, *84*(4), 1381–1478.

Su, B., Wang, X., Nunomura, A., Moreira, P., Lee, H. -go., Perry, G., Smith, M., & Zhu, X. (2008). Oxidative Stress Signaling in Alzheimers Disease. *Current Alzheimer*

Research, *5*(6), 525–532.

Sudhakar Reddy, G., Arjunreddy Mallampudi, N., Lakshmi, J. K., & Mohapatra, D. K. (2018). Total Synthesis of Cryptorigidifoliol K: Confirmation of Structure and Absolute Configuration. *Asian Journal of Organic Chemistry*, *7*(12), 2504–2510.

Sun, M., Deng, Y., Batyreva, E., Sha, W., & Salomon, R. G. (2002). Novel bioactive phospholipids: Practical total syntheses of products from the oxidation of arachidonic and linoleic esters of 2-lysophosphatidylcholine. *Journal of Organic Chemistry*, *67*, 3575–3584.

Tiedje, K. E., Stevens, K., Barnes, S., & Weaver, D. F. (2010). β-Alanine as a small molecule neurotransmitter. *Neurochemistry International*, *57*(3), 177–188.

Uchida, K. (2003). 4-Hydroxy-2-nonenal: a product and mediator of oxidative stress. *Progress in Lipid Research*, *42*(4), 318–343.

Urey, H. C., Huffman, J. R., Thode, H. G., & Fox, M. (1937). Concentration of N 15 by Chemical Methods. *The Journal of Chemical Physics*, *5*(11), 856–868.

Urey, H. C., Pegram, G. B., & Huffman, J. R. (1936). The Concentration of the Oxygen Isotopes. *The Journal of Chemical Physics*, *4*(9), 623–623.

Valko, M., Leibfritz, D., Moncol, J., Cronin, M. T. D., Mazur, M., & Telser, J. (2007). Free radicals and antioxidants in normal physiological functions and human disease. *The International Journal of Biochemistry & Cell Biology*, *39*(1), 44–84.

Walker, G. S., & O'Connell, T. N. (2008). Comparison of LC-NMR and conventional NMR for structure elucidation in drug metabolism studies. *Expert Opinion on Drug Metabolism & Toxicology*, *4*(10), 1295–1305.

Wilkinson, D. J. (2018). Historical and contemporary stable isotope tracer approaches to studying mammalian protein metabolism. *Mass Spectrometry Reviews*, *37*(1), 57–80.

Wilson, K., Tochtrop, G. P., Brunengraber, H., Zhang, G., Hess, J. P., Zhang, M., Chapman, K. A., & Cline, G. (2017). Inter-relations between 3-hydroxypropionate and propionate metabolism in rat liver: relevance to disorders of propionyl-CoA metabolism. *American Journal of Physiology-Endocrinology and Metabolism*, *313*(4), E413–E428.

Wong, C. G. T., Chan, K. F. Y., Gibson, K. M., & Snead, O. C. (2004). ??-Hydroxybutyric Acid. *Toxicological Reviews*, *23*(1), 3–20.

Zhang, G.-F., Kombu, R. S., Kasumov, T., Han, Y., Sadhukhan, S., Zhang, J., Sayre, L. M., Ray, D., Gibson, K. M., Anderson, V. A., Tochtrop, G. P., & Brunengraber, H. (2009). Catabolism of 4-Hydroxyacids and 4-Hydroxynonenal via 4-Hydroxy-4-phosphoacyl-CoAs. *Journal of Biological Chemistry*, *284*(48), 33521–33534.

Zhang, G.-F., Sadhukhan, S., Ibarra, R. A., Lauden, S. M., Chuang, C.-Y., Sushailo, S., Chatterjee, P., Anderson, V. E., Tochtrop, G. P., & Brunengraber, H. (2012).

Metabolism of γ-hydroxybutyrate in perfused rat livers. *Biochemical Journal*, *444*(2), 333–341.

Zhou, L., & Nilsson, A. (2001). Sources of eicosanoid precursor fatty acid pools in tissues. *Journal of Lipid Research*, *42*(10), 1521–1542. http://www.ncbi.nlm.nih.gov/pubmed/11590208

Zhu, X., Tang, X., Anderson, V. E., & Sayre, L. M. (2009). Mass Spectrometric Characterization of Protein Modification by the Products of Nonenzymatic Oxidation of Linoleic Acid. *Chemical Research in Toxicology*, *22*(8), 1386–1397.

Zukunft, S., Prehn, C., Röhring, C., Möller, G., Hrabě de Angelis, M., Adamski, J., & Tokarz, J. (2018). High-throughput extraction and quantification method for targeted metabolomics in murine tissues. *Metabolomics*, *14*(1), 18.